

Assessment of Bone Condition using Acoustic Emission and Acousto-Ultrasonic Technique

THESIS

Submitted in partial fulfilment
of the requirements for the degree of

DOCTOR OF PHILOSOPHY

by

SHARAD SHRIVASTAVA

Under the Supervision of

Prof. RAVI PRAKASH



**BIRLA INSTITUTE OF TECHNOLOGY AND SCIENCE
PILANI - 333 031 (RAJASTHAN) INDIA**

2010



BIRLA INSTITUTE OF TECHNOLOGY AND SCIENCE
PILANI – 333 031 (RAJASTHAN) INDIA

CERTIFICATE

This is to certify that the thesis entitled “**Assessment of Bone Condition using Acoustic Emission and Acousto-Ultrasonic Technique**” and submitted by **Sharad Shrivastava**, ID.No. **2007PHXF016P** for award of Ph.D. Degree of the Institute, embodies original work done by him under my supervision.

PROF. RAVI PRAKASH

**Vice Chancellor,
Jaypee University of Information Technology, Solan, (H.P.)**

Date: 13/12/2010

ACKNOWLEDGEMENTS

I am short of words to thank my respected supervisor Professor Ravi Prakash, Vice-Chancellor, Jaypee University of Information Technology, Solan (H.P.) & Former Dean, Research and Consultancy Division BITS, Pilani without whose guidance and active interest, the thesis would have never attained such an accomplishment. He not only motivated me constantly but also gave appropriate suggestions at the time of the need.

I am immensely thankful to Prof. B N Jain, Vice-Chancellor BITS Pilani, Prof. G Raghurama, Director, BITS-Pilani Campus; Prof. R K Mittal, Director, BITS-Pilani, Dubai Campus; Prof. R N Saha, Deputy Director (Administration, Research & Educational Development) BITS, Pilani for providing me this opportunity to pursue the on-campus Ph.D. of the Institute. I express my gratitude to Prof. Ashis Kumar Das, Dean, Research & Consultancy Division BITS, Pilani for his constant official support, encouragement and making the organization of my research work through the past months easy.

My sincere thanks to Prof. Manisankar Dasgupta, Head of Mechanical Engineering Department and Dr. R Mahesh, Unit Chief, Community Welfare & Societal Development and Professor in Pharmacy Department, BITS, Pilani for their kind suggestions, moral support and assistance.

I thank Dr. Hemant R Jadhav, Mr. Dinesh Kumar, Dr. Monica Sharma, Mr. Gunjan Soni, Mr. Amit Singh and Ms. Sunita Bansal, nucleus members of R&C Division, BITS, Pilani, without whose cooperation and guidance it would not have been possible for me to pursue such goal oriented research during each of the past few semesters.

I also express my gratitude to the office staff of RCD whose secretarial assistance helped me in submitting the various evaluation documents in time and give pre-submission seminar smoothly.

I thank my Doctoral Advisory Committee (DAC) members, Dr. Hemant R Jadhav and Dr. Manisankar Dasgupta, who spared their valuable time to go through my

draft thesis and were audience to my pre-submission seminar in order to provide several valuable suggestions that immensely helped in improving the quality of my Ph.D. Thesis report.

I express my sincere thanks to Dr. Sushil Yadav, In-charge of Central Animal Facility, BITS Pilani for his valuable cooperation. I would like to thank Prof. Rambabu Kodali, former Head of Mechanical Engineering Department for his valuable suggestions during my research work.

I would also like to thanks Mr. Santosh Kumar Saini, ARC Division, BITS, Pilani for his help in Compilation of Thesis. I also express my thanks to all the persons who have been directly or indirectly attachment with me during the thesis work.

Finally, thanks must go to my family. My sincere thanks to my great guiding parents for making all my dreams come true. Their love, support, motivation and all physical help have been immeasurable. My special loving thanks to my wife Kanchan and lovely daughter Kavya for all the sacrifices they have gone through these years for the successful completion of my thesis.

Dated: 13/12/2010



Sharad Shrivastava

Place: BITS, Pilani

ABSTRACT

The assessment of bone condition by non-destructive/non-invasive techniques is useful for diagnosis of metabolic diseases such as osteoporosis and in evaluation of fracture healing process. Recent investigations pointed out the drawbacks of the currently used methods such as the radiographic technique and the manual assessment of stability for the assessment of *in vivo* bone condition. Therefore there is a definite need for an additional non-invasive technique to assess the *in vivo* bone condition, particularly the mechanical integrity of bone.

Many investigators attempted various techniques such as mechanical impedance, natural frequency, vibration analysis, stress wave propagation and the ultrasonic techniques for the assessment of *in vivo* bone condition. Yet none of the above techniques have been found to be suitable for wide spread clinical use. Since the bone is a natural composite material and also as the acoustic emission (AE) and acousto-ultrasonic (AU) technique have already proved their usefulness in non-destructive evaluation of composite materials, these techniques have been chosen from the available non-destructive testing techniques. In present research work the application of acoustic emission and acousto-ultrasonic techniques for the assessment of bone condition has been studied.

The thesis is divided in to seven chapters. Since in this research study two separate techniques are used for their possible clinical applications, the materials and methods, results and discussions are all given separately under each heading and are presented as different chapters (Chapters 3-6).

Chapter 1 introduces the problem i.e. the assessment of bone condition and its clinical diagnosis. The limitations of the currently used techniques are also presented. The aim of the present work is also given at the end of this chapter.

Chapter 2 gives the literature review in the field of Biomechanical measurements in bone and the assessment of bone condition by different diagnostic techniques. The literature review gives more emphasis on the work done in the area of

acoustic emission technique. Not much work has been done using acousto-ultrasonic technique in the field of medical sciences. The application of AE and AU techniques for the non-destructive evaluation of composite materials and also the details about the investigations made previously with these techniques in the field of biomechanical measurements of bones are given in this chapter. The scope of the present work is discussed at the end of this chapter.

Chapter 3 describes the acoustic emission characteristic of bones. The study of acoustic emission response from *in vitro* bone is given. The experimental set up used for acoustic emission monitoring to facilitate the accurate determination of time of occurrence of initial AE is discussed.

Chapter 4 discusses the linear location technique for locating the fracture in bones. The *in vitro* study has been carried out for the same. The GUI (Guided User Interface) software has been developed for the linear location of the fracture in the bones.

A study was made about the acousto-ultrasonic technique to study about its reproducibility and sensitivity. The results of this study and the methods by which better sensitivity can be achieved are discussed in Chapter 5. The details about the development of modified acousto-ultrasonic technique and also the MATLAB coding developed to process the acousto-ultrasonic signals is discussed in this chapter. The validity of using the acousto-ultrasonic technique for assessing the *in vivo* bone condition is proved by the *in vitro* studies carried out with both dry and fresh animal bones. The MATLAB coding developed for the AU signals is mentioned in appendix **C**.

Chapter 6 discusses the application of AU technique for monitoring the fracture healing process. The results of the experimental work are given. The acousto-ultrasonic measurements and the radiological examination are presented with discussion. The advantages and limitation of using AU technique for the present purpose is also discussed in this chapter.

Chapter 7 discusses the overall conclusion and future scope of the present study.

***Dedicated to my Parents,
Wife & Daughter***

TABLE OF CONTENTS

ACKNOWLEDGEMENT	i
ABSTRACT	iii
TABLE OF CONTENTS	vi
LIST OF FIGURES	ix
LIST OF TABLES	xiii
GLOSSARY OF TERMS	xiv
CHAPTER 1 INTRODUCTION	1-4
CHAPTER 2 LITERATURE REVIEW	5-42
CHAPTER 3 ACOUSTIC EMISSION CHARACTERISTICS OF <i>IN VITRO</i> BONE	43-59
3.1 INTRODUCTION	43
3.2 MATERIALS AND METHODS	44
3.2.1 Preservation of Fresh Bone for Testing	44
3.2.2 Selecting the Type of Loading	44
3.2.3 Acoustic Emission Monitoring	44
3.3 RESULTS AND DISCUSSION	46
3.3.1 AE Characteristic of Dry Bones	46
3.3.2 AE Characteristic of Fresh Bones	53
3.4 CONCLUSION	57
References	58
CHAPTER 4 LOCATION OF FRACTURE BY ACOUSTIC EMISSION TECHNIQUE	60-72
4.1 INTRODUCTION	60
4.2 AE Source Location Techniques	61
4.2.1 Linear Location Technique	61
4.2.2 Zonal Location Technique	63
4.3 MATERIALS AND METHODS	63
4.3.1 Calculation of Wave Velocity	64

4.3.2	Linear Location of Fracture Using GUI Software	65
4.3.3	Linear Location of Fracture using AE 2-Channel Set Up	66
4.4	RESULTS AND DISCUSSION	67
4.5	CONCLUSION	70
	References	72
CHAPTER 5	ASSESSMENT OF <i>IN VITRO</i> BONE CONDITION BY ACOUSTO-ULTRASONIC TECHNIQUE	73-96
5.1	INTRODUCTION	73
5.2	A CRITICAL ASSESSMENT OF ACOUSTO-ULTRASONIC TECHNIQUE	74
5.2.1	Modified Acousto-Ultrasonic Technique	74
5.2.2	Reproducibility of the Acousto-Ultrasonic Technique	75
5.2.2.1	Materials and Methods	76
5.2.2.2	Results and Discussions	77
5.2.2.3	Conclusions	78
5.2.3	Sensitivity of the Acousto-Ultrasonic Technique	78
5.2.3.1	Materials and Methods	79
5.2.3.2	Results and Discussions	80
5.2.3.3	Conclusions	82
5.3	<i>IN VITRO</i> ANALYSIS BY ACOUSTO-ULTRASONIC TECHNIQUE	82
5.3.1	Materials and Methods	82
5.3.2	Results and Discussions	83
5.3.2.1	Acousto-Ultrasonic Measurements on Composite Specimens	83
5.3.2.2	Acousto-Ultrasonic Measurements on Dry Bones	84
5.3.2.3	Acousto-ultrasonic measurements on Fresh Bones	90
5.3.2.4	Conclusions	94
	References	95

CHAPTER 6	MONITORING THE FRACTURE HEALING PROCESS BY ACOUSTO-ULTRASONIC TECHNIQUE	97-127
6.1	INTRODUCTION	97
6.2	EXPERIMENTAL STUDY	99
6.2.1	Creating Closed Fracture	99
6.2.2	Procedure for Creating Surgical Fracture	100
6.2.2.1	Pre-Requirements	100
6.2.2.2	Procedure	101
6.2.2.3	Post Surgical Treatment	106
6.3	ACOUSTO-ULTRASONIC MEASUREMENT	107
6.4	RESULTS AND DISCUSSION	109
6.5	CONCLUSION	124
	References	126
CHAPTER 7	OVERALL CONCLUSIONS AND FUTURE SCOPE OF WORK	128-131
7.1	ACOUSTIC EMISSION STUDY	128
7.2	ACOUSTO-ULTRASONIC STUDY	129
7.3	SCOPE FOR FURTHER WORK	130
Appendix A	Fracture location using AE technique	A1-A4
Appendix B	Acousto-Ultrasonic Signal Processing	B1-B3
Appendix C	GUI Software for calculating different parameters of AU signals	C1-C12
Appendix D	GUI Software for monitoring the fracture healing process	D1-D14

List of Publications

Brief Biography of the Supervisor

Brief Biography of the Candidate

LIST OF FIGURES

FIGURE No.	TITLE	Page No.
2.1	Detection of acoustic emission event by remote piezoelectric transducers.	15
2.2	Signal waveform for one acoustic emission event.	15
2.3	Stress vs. strain and acoustic emission counts vs. strain curves for one of the control specimens	17
2.4	Stress vs. strain and acoustic emission counts vs. strain curves for one of the decalcified specimens	17
2.5	Stress-strain curves for the three test groups constructed from the mean values in table 2.1. Error bars are shown for ultimate stress values	18
2.6	Acoustic emissions from healthy knee joint cartilage deformation after the sudden change from a two leg stand to a one leg stand.	23
2.7	Frequency response of the intact femur A	24
2.8	Frequency response of the cut femur	25
2.9	Schematic of AU Technique	27
2.10	Principle of AU Technique	27
3.1	Acoustic Emission Equipment	44
3.2	Schematic Diagram for Acoustic emission set up	45
3.3	Acoustic Emission Response of Dry Bones (S.R. = 5 mm/minute)	47
3.4	Acoustic Emission Response of Dry Bones (S.R. = 15 mm/minute)	48
3.5	AE characteristic of Dry bone sample-1 (S.R.= 5 mm/minute)	48
3.6	AE characteristic of Dry bone sample-3 (S.R.= 5 mm/minute)	49
3.7	AE characteristic of Dry bone sample-4 (S.R.= 5 mm/minute)	49
3.8	AE characteristic of Dry bone sample-2 (S.R.= 15 mm/minute)	50
3.9	AE characteristic of Dry bone sample-3 (S.R.= 15 mm/minute)	50
3.10	AE characteristic of Dry bone sample-4 (S.R.= 15 mm/minute)	51
3.11	Amplitude Distribution of AE counts (S R.= 5 mm/minute)	52

FIGURE No.	TITLE	Page No.
3.12	Amplitude Distribution of AE counts (S.R.= 15 mm/minute)	52
3.13	Acoustic Emission Response of Fresh Bones (S.R. = 5 mm/minute)	53
3.14	Acoustic Emission Response of Fresh Bones (S.R. = 15 mm/minute)	54
3.15	AE characteristic of fresh bone sample-1(S.R.= 5mm/minute)	54
3.16	AE characteristic of fresh bone sample-2 (S.R.= 5 mm/minute)	55
3.17	AE characteristic of fresh bone sample-5 (S.R.= 15 mm/minute)	55
4.1	Linear source location	62
4.2	Linear Source Location measured from the mid point	62
4.3	Schematic diagram for acoustic emission set up	64
4.4	Linear location of fracture by AE-2 Channel set up (Distance between sensors = 5 cm)	68
4.5	Linear location of fracture by GUI software (Distance between sensors = 5 cm)	68
4.6	Linear location of fracture by AE-2 Channel set up (Distance between sensors = 6.5 cm)	69
4.7	Linear location of fracture by GUI software (Distance between sensors = 6.5 cm)	69
5.1	Schematic diagram of Acousto-Ultrasonic Unit	75
5.2	Positioning of Transducers on GFRP Specimen for AU Measurements	76
5.3	Reproducibility of SWF in Acousto-ultrasonic Measurements	78
5.4	GFRP Specimen with small indentation at the centre	79
5.5	SWF of Good Area and Bad Area at different Threshold values	80
5.6	AU measurements with 380 mV threshold setting	81
5.7	SWF of Good Area and Bad Area at different Gate width Values (Threshold 380 mV)	81
5.8	Change in the value of SWF (Composite rod specimens)	83


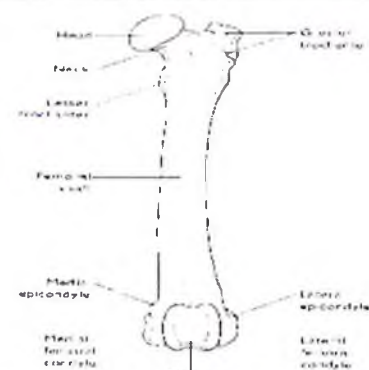
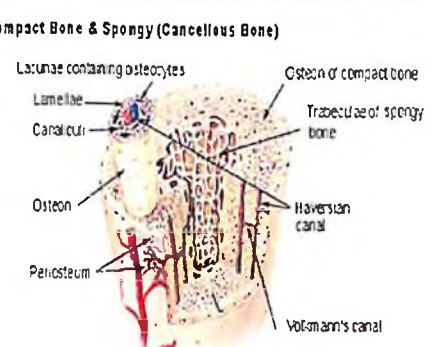
FIGURE No.	TITLE	Page No.
5.9	Change in the value of the SWF with the depth of cut for composite specimens	84
5.10	A-waveform for normal dry bone (sample1)	85
5.11	A-waveform for fractured dry bone (sample1)	85
5.12	Change in the value of SWF (In Dry Bone)	86
5.13	Change in the value of peak amplitude (In Dry Bone)	87
5.14	Change in the value of the SWF with the depth of crack for dry bone	88
5.15	Relation between SWF and Flexural Strength of Dry Bones	89
5.16	Relation between Peak amplitude and Failure Load of Dry Bones	89
5.17	A-waveform for normal fresh bone (sample1)	90
5.18	A-waveform for fractured fresh bone (sample1)	91
5.19	Change in the value of SWF (In Fresh Bovine Bone)	91
5.20	Change in the value of Peak amplitude (In Fresh Bone)	92
5.21	Change in the value of SWF with the depth of crack in fresh bone	93
6.1	The axial transmission technique used for the ultrasonic evaluation of fracture healing in long bones	98
6.2	Removing of hairs form right tibia of Rabbit	102
6.3	Hair removed from the rabbit right limb	102
6.4	Rabbit wrapped in green cloth for surgery	103
6.5	Injecting local anaesthesia on the right limb	103
6.6	Photograph of giving vertical incision to remove the soft tissues	104
6.7	Photograph of surgical fracture	104
6.8	Measurement of depth of fracture	105
6.9	Suturing of soft tissues after surgery	105
6.10	Rabbit's right limb immobilised with Plaster of Paris	106

FIGURE No.	TITLE	Page No.
6.11	Experimental set up for Acousto-ultrasonic measurement on rabbits	108
6.12	Acousto-ultrasonic parameters calculated for rabbit No.4 just after surgery	111
6.13	Acousto-ultrasonic measurements for rabbit No.4 just after the surgery	112
6.14	X-ray of Rabbit No.4 just after the surgery	112
6.15	Acousto-ultrasonic measurements for rabbit No.4 at fourth week	113
6.16	X-ray of rabbit No.4 at Fourth week	113
6.17	Acousto-ultrasonic measurements for rabbit No.4 at eighth week	114
6.18	X-ray of rabbit No.4 after eighth week	114
6.19	Acousto-ultrasonic measurements for rabbit No.4 at twelfth week	115
6.20	X-ray of rabbit No.4 at twelfth week	115
6.21	Acousto-ultrasonic measurements for rabbit No. 6 just after the surgery	116
6.22	X-ray of rabbit No.6 just after the surgery	116
6.23	Acousto-ultrasonic measurements for rabbit No.6 at fourth week	117
6.24	X-ray of rabbit No.6 at fourth week	117
6.25	Acousto-ultrasonic measurements for rabbit No.6 at eighth week	118
6.26	X-ray of rabbit No. 6 at eighth week	118
6.27	Acousto-ultrasonic measurements for rabbit No.6 at twelfth week	119
6.28	X-ray of rabbit No.6 at twelfth week	119
6.29	Acousto-ultrasonic measurements for rabbit No.7 just after surgery	120
6.30	Acousto-ultrasonic measurements for rabbit No.7 at fourth week	121
6.31	X-ray of rabbit No.7 at fourth week	121
6.32	Acousto-ultrasonic measurements for rabbit No.7 at eighth week	122
6.33	X-ray of rabbit No.7 at eighth week	122
6.34	Acousto-ultrasonic measurements for rabbit No.7 at twelfth week	123
6.35	X-Ray of rabbit No.7 at twelfth week	123
6.36	Healing Index values for Rabbit 10, 11 and 13	124

LIST OF TABLES

TABLE No.	TITLE	Page No.
2.1	Mechanical properties of decalcified and partially deproteinized bovine bones	18
2.2	The predictive capability of acoustic emissions expressed in terms of the specimen's fatigue life	21
2.3	A statistically significant effect of time on these mechanical properties was detected. Within a row, values with differing letters are significantly different from each other ($P < 0:05$).	22
3.1	Ultimate load of Dry Bones under different strain rates	51
3.2	Percentage of Ultimate Load at which initial AE occurred for dry bones	52
3.3	Ultimate loads of Fresh Bones under different strain rates	56
3.4	Percentage of Ultimate Load at which initial AE occurred for fresh bones	56
4.1	Summary of results obtained from the software	70
5.1	Input Settings for testing Reproducibility of AU measurements	77
5.2	Gate width values for testing the sensitivity of AU measurements	80
5.3	Acousto-Ultrasonic measurements from Composite specimens	84
5.4	Acousto-Ultrasonic measurements from dry bone specimens	86
5.5	Acousto-Ultrasonic measurements from dry bone specimens	87
5.6	Change in the value of the peak amplitude with the depth of crack for dry bone	88
5.7	Acousto-Ultrasonic measurements from Fresh bone specimens	92
5.8	Acousto-Ultrasonic measurements from Fresh bone specimens	92
5.9	Change in the value of the peak amplitude with the depth of crack for fresh bone	93

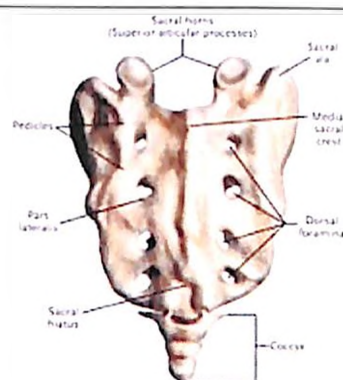
GLOSSARY OF TERMS

<i>In vitro</i>	Refers to an experiment conducted in the laboratory
<i>In vivo</i>	Refers to an experiment conducted in the body
Osteoporosis	Thinning of the bones with reduction in bone mass due to depletion of calcium and bone protein
Diaphyseal	Pertaining to or affecting the shaft of a long bone (diaphysis).
	
Osteology	The branch of anatomy that deals with the structure and function of bones.
Femur	The long bone of the thigh, and the longest and strongest bone in the human body, situated between the pelvis and the knee and articulating with the hipbone and with the tibia and patella. Also called <i>thighbone</i> .
	
Cancellous bone	Cancellous bone, synonymous with trabecular bone or spongy bone, is one of the two types of osseous tissue that form bones.
	<p>Compact Bone & Spongy (Cancellous Bone)</p> 
Osteons	A central canal containing blood capillaries and the concentric osseous lamellae around it occurring in compact bone.
Bovine bone	Relating to, or resembling a ruminant mammal of the genus <i>Bos</i> , such as an ox, cow, or buffalo
Canine	Refer to dog
Haversian System	Compact bone is very hard and dense. It consists of microscopic cylindrical structures oriented parallel to the long axis of a bone. The cylindrical, column-like structures are the

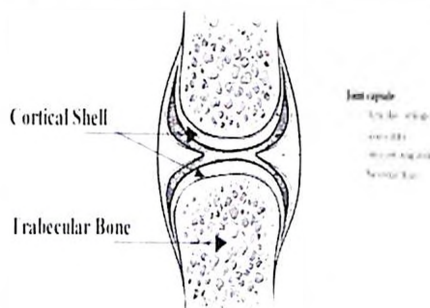
Haversian systems and are laid down in concentric rings called lamellae. Each of these systems is in turn interconnected to other systems to provide a continuous network of blood vessels and nerves. Trabecular bone comprises the majority of interior long bone tissue, in addition to that of the hip and vertebrae. It is also called "spongy" or "cancellous" bone because of its soft, spongy texture. Cortical bone, however, is dense and very hard. It is the second of the two types of bone and forms bone surfaces. Periosteum is the fibrous membrane of connective tissue that snugly covers all bones, but it does not cover articular surfaces (where bones come in contact with each other). The articular surfaces are covered with cartilage, which prevents bones from rubbing together. The periosteum also contains attachment sites for muscles, ligaments, and tendons. For adults, the periosteum is responsible for forming new bone as a result of injury or infection. And in children, the periosteum is critical to new bone formation, as well as configuring the shape of bone. A Volkmann's canal is one which allows the transmission of blood vessels (or capillaries) from the periosteum into the bone. A nutrient artery is an artery which supplies the medullary cavities of long bones.

Callus The hard bony tissue that develops around the ends of a fractured bone during healing.

Sacrum Triangular bone made up of five fused vertebrae and forming the posterior section of the pelvis.



Trabecular bone Small, often microscopic, tissue element in the form of a small beam, strut or rod, generally having a mechanical function, and usually but not necessarily composed of dense collagenous tissue.



Resorption The absorption of the bone by large multi-nucleated cells called osteoclasts

Osteopenia

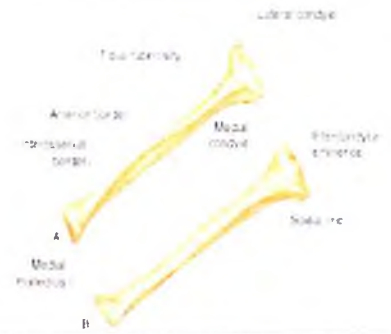
Osteopenia is a condition where bone mineral density is lower than normal. It is considered by many doctors to be a precursor to osteoporosis. However, not every person diagnosed with osteopenia will develop osteoporosis.

Valgus

Characterized by an abnormal outward turning of a bone, especially of the hip, knee, or foot; occasionally used to indicate an inward turning.

Tibia

The inner and larger bone of the leg below the knee. It articulates with the femur and head of the fibula above and with the talus below.



CHAPTER 1

INTRODUCTION

1.1 INTRODUCTION

Bone is primary structural element of human body. It serves to protect vital internal organs and permits skeletal motions necessary for survival. The anatomy of human beings is quite well known but the strength and mechanical properties of bones have not been investigated thoroughly. Assessment of *in vivo* bone condition is one of the research areas, which have attracted many biomedical engineers and clinical orthopaedicians in recent times. The development of techniques for the assessment of bone condition is more desirable in clinical orthopaedics.

In broad sense, the assessment of bone condition includes the following problems of clinical orthopaedicians:

1. Monitoring the fracture healing process including determination of mechanical strength and assessing the degree of fracture healing.
2. Detecting the delayed or non-union in long bone fractures.
3. Non-invasive measurements of physical properties such as bone density and bone mineral content.
4. Evaluating the mechanical performance (such as bending stiffness) of the long bones (non-invasively).
5. Diagnosis of osteoporosis.

Presently the radiological examination is widely used for the assessment of *in vivo* bone condition ^[1-2]. In some clinical problems such as diagnosis of the point of clinical union of fracture, the manual assessment of stability is also used along with the radiological examination. However for many applications the radiographic technique was found to be suffered from low sensitivity. For instance, for the evaluation of osteoporosis it requires a minimum loss of 30% or more of bone mineral content before an unequivocal Roentgen logical diagnosis can be made ^[3]. Other quantitative techniques such as single or dual photon

absorptiometry, neutron activation analysis, Compton scattering, quantitative computed tomography are available, but they are expensive and most of them involve exposure to radiation. Thus large scale screening for osteoporosis is difficult to carry out with the available techniques.

Monitoring the fracture healing process is another area where the currently used techniques failed to give satisfactory results. Uncertainty regarding the significance of the radiographic and clinical findings may result in unnecessarily long immobilization periods which can produce discomfort and inconvenience for the patients, as well as possible joint stiffness and even permanent loss of motion especially in the elderly.

In the case of patients returning to strenuous work or professional sport, the accurate definition of mechanical integrity of the healed fracture is very important. The normal clinical and radiological methods of assessment are inaccurate for defining the mechanical integrity of healing bone. That means in our present state of knowledge these patients may either be placed at the risk of re-fracture, or be prevented from taking part in normal activities for many months longer than necessary. It should also be noted that it will be a devastating event for a person to sustain a fracture after perhaps a long and difficult period of treatment.

In certain long bone shaft fractures the healing process is modified by the method of treatment so that the clinical assessment of mechanical integrity is impossible and the interpretation of radiographs may be difficult. Diaphyseal fractures treated by "rigid" internal fixation always posed this problem, because the fracture cannot be tested mechanically and the external callus formation is not seen on radiographs. Hence newer methods are needed to assess the mechanical integrity of fracture healing in such circumstances. Otherwise unreliable and unsafe rehabilitation programme may get prescribed.

Mechanical impedance, natural frequency, vibration analysis, stress wave propagation, ultrasonic-measurements, impact response technique, electrical potential measurements and mechanical tissue response analysis are some of the

techniques, which have been attempted by different investigators for the assessment of *in vivo* bone condition in the past^[4-6].

Despite the efforts of many investigators there is still no technique which could be widely accepted for assessing bone quality *in vivo*. For any method to have success in clinical application, it should be non-invasive in nature, simple to operate and painless to patients.

1.2 MOTIVATION

The structure of bone is very much similar to engineering composite materials and is therefore advantageous to use a non-destructive testing technique, which has already proved its usefulness in the field of composite materials testing. Acoustic emission (AE) technique and Acousto-ultrasonic (AU) technique have been used very successfully for the non-destructive evaluation of composites. The proven applications of these techniques in similar situations such as predicting the mechanical performance of composite structures, assessing the residual life of structural component etc. make these two techniques more suitable for the present study i.e. the assessment of bone condition.

1.3 OBJECTIVES OF THE PRESENT STUDY

(A) Acoustic Emission Study

1. To investigate the acoustic emission characteristics of dry and fresh bones under suitable loading conditions and at different strain rates.
2. To explore the application of acoustic emission technique in locating the fracture in dry bones.

(B) Acousto – Ultrasonic Study

1. To carry out *in vitro* studies with dry and fresh bones with simulated fractures/cracks.
2. To carry out an experimental study with rabbits to see the application of Acousto-ultrasonic as a non-invasive method for monitoring the fracture healing process.

References

1. Lachmann, E., Whelan, M. (1936) The Roentgen Diagnosis of Osteoporosis and its Limitations, *Radiology*, 26, pp.165-177.
2. Lachmann, E. (1955) Osteoporosis: The Potentialities and Limitations of its Roentgenologic Diagnosis, *Amer.J. Roentgenology*, 74, pp.712-715.
3. Chen, I.I.H., and Saha. S, (1987) Wave Propagation Characteristics in Long Bones to Diagnose Osteoporosis, *J.Biomech*, 20:5, pp.523-527.
4. Wong, F.Y., Pal, S. and Saha, S. (1983) The Assessment of In vivo Bone Condition in Humans by Impact Response Measurement, *J.Biomech*, 16:10, pp.849-856.
5. Guzelsu, N. and Saha, S. (1981) Electromechanical Wave Propagation in Long Bones. *J.Biomech*, 14, pp.19-33.
6. Anast, G.T., Fields, M.S and Siegel (1958) .Ultrasonic Technique for the Evaluation of Bone Fracture, *Amer. J. Physical. Med*, 37, pp.157-159.

CHAPTER 2

LITERATURE REVIEW

2.1 INTRODUCTION

The 206 named bones of skeleton constitutes 18% of the adult human body weight, only skin and fat (25%) and muscles (43%) being greater^[1]. In order to support and protect internal organs some other functions of bones are storage places for calcium, regulators of the calcium/phosphorus ratio in the blood, and producers of red blood cells. In biological terms bone is described as a connective tissue and in mechanical terms bone is a composite material with several distinct solid and fluid phases ^[1].

The mechanical properties of bone perhaps have been more extensively investigated than those of any other biological tissue materials. Although our understanding of the mechanical properties and fracture behavior of bone is continuously improving, as yet it is far from complete. As pointed by Hayes ^[2] while fundamental research is needed on many aspects of the mechanical response of the bone, applications of the techniques of analytical and experimental mechanics in this area are made complicated by the fact that bone is highly complex living material.

The initial work in the field of bone biomechanics can be traced back to the 17th century when “attempts to express biological findings in physical terms ^[3]” were made by the scholars at that time. This philosophical background of the aspect was intensified in the age of determinism which lasted until the middle of the 19th century. One of the main aspects of the research work in that time was to relate the architecture of bone and its mechanical functions. In the year 1832, Bourgerie in his work on anatomy raised the question of relation between architecture and mechanical functions of bone ^[4]. In his book on osteology, Ward ^[5] compared the proximal end of the human femur with a crane and he mentioned the compressive and tensile stresses evoked in the bone by loading. In the year 1867, a more detailed analysis of the structure of cancellous bone and its

mathematical significance was given by Meyer^[6] in association with the famous mathematician Culmann.

The industrial revolution took place in the second half of the 19th century. It had an impact on the research works on bone also. New developments were made in the field of material testing and the new methods were developed for mechanical measurements. For a while, these methods were used to determine the *in vitro* mechanical properties of bone. The bones were tested under various loading conditions and the ultimate strength of bone was determined by many investigators.

The first biomechanical measurements were made by Wertheim in 1847^[7], who had measured the bone strength and its elasticity. He concluded that there was no correlation between the tensile strength and the age. Rauber^[8] in the year 1876 made first systematic investigation of the material properties of bone. He designed his own equipment and carefully prepared his specimens of compact and cancellous bone, which he tested in tension, compression, shear and torsion. Most of the external factors quite familiar in bone biomechanics today were first observed by Rauber: the influence of humidity and temperature on strength and elasticity, the response of bone to prolonged loading with bending tests, and the anisotropic behavior of bone.

Carothers et al.^[9] determined the ultimate tensile strength of samples from the femoral diaphysis of embalmed cadavers and found its average value as 22,000 lb./in². Evans and Lebow^[10, 11] studied about the regional differences in the physical properties of the human femur. They tested human cortical samples and concluded that the middle third of the shaft not only had the greatest tensile strength, modulus of elasticity and hardness but also the greatest percentage elongation under tension. Dehydrated wet samples showed a greater elongation than did dry bones from the same region. They also compared the tensile strength of tibia and fibula and concluded that tibia had the greatest average tensile strength and the fibula had the greatest percentage elongation under strain.

Burstein et al. ^[12] investigated the aging of bone tissue. They determined the mechanical properties of machined specimens from human femurs and tibia in tension, torsion and compression for a population ranging in age from 21 to 86 years. No significant differences were found between the mechanical properties of male and female specimens. Tibial specimens had greater ultimate strength, stiffness and ultimate strain than femoral specimens. They found that there was consistent decrease with age for all mechanical properties except the plastic modulus in the femoral but not in the tibial specimens.

Sierpowska et al. ^[13] investigated the interrelationships of electrical and dielectric properties with mechanical characteristics of human trabecular bone. In their study, electrical and dielectric properties, i.e. permittivity, conductivity, phase angle, loss factor, specific impedance and dissipation factor of human trabecular bone samples ($n = 26$, harvested from the distal femur and proximal tibia) were characterized in a wide frequency range (50 Hz–5 MHz). Mechanical properties, i.e. Young's modulus, ultimate strength, yield stress, yield strain and resilience of the samples ($n = 20$) were determined by using destructive compressive testing. Subsequently, measurements of electrical and dielectric properties were repeated after mechanical testing. The measurements were also repeated for the control samples ($n = 6$) that were not mechanically tested. Electrical, dielectric or mechanical properties showed no significant differences between the intact femoral and tibial samples. The electrical and dielectric parameters as well as the linear correlations between the dielectric and electrical parameters with mechanical parameters were strongly frequency dependent. At the frequency of 1.2 MHz, the relative permittivity showed the strongest linear correlations with the Young's modulus ($r = 0.71$, $p < 0.01$, $n = 20$) and ultimate strength ($r = 0.73$, $p < 0.01$, $n = 20$). Permittivity and dissipation factor showed statistically significant changes after mechanical testing. Their results suggest that the measurements of low frequency electrical and dielectric properties may provide information on the mechanical status of trabecular bone and, possibly, may even help to diagnose bone micro damage.

Nyman et al. ^[14] examined about the progressive mechanical behaviour of human cortical bone in tension for two age groups (The middle aged group had

bone from 4 female donors of 53, 54, 54, and 56 years and from 5 male donors of 49, 51, 51, 52, and 55 years, while the elderly group had bone from 4 female donors of 84, 88, 88, and 90 years and from 4 male donors of 72, 76, 79, and 87 years.). The elastic modulus, maximum stress, permanent strain, stress relaxation, viscoelastic time constant, plastic strain energy, elastic release strain energy, and hysteresis energy were determined at incremental strains of each loading cycle. Experimental results showed that elderly bone failed at much lower strains compared to middle aged bone, but little age-related differences were observed in the mechanical behaviour of bone until the premature failure of elderly bone. Energy dissipation and permanent strain appeared to linearly increase with increasing strain, while non-linear changes occurred in the modulus loss and stress relaxation/time constant with increasing strain. They suggested that two distinct stages may exist in the progressive deformation of bone. In Stage I, rapid damage accumulation and increased involvement of collagen in load bearing appeared to dominate the mechanical behaviour of bone with limited energy dissipation (<20% of total energy dissipated), whereas Stage II is dominated by continuous plastic deformation, accompanied by major energy dissipation through all three pathways till failure. They concluded that damaging mechanisms in bone vary with deformation and age affects the post-yield mechanisms causing a significant decline in the capacity of aged bone to dissipate energy.

Mc Elhaney^[15] from his study on the strain rate dependence of the mechanical properties of bone showed that both the compressive strength and modulus of longitudinally oriented compact bone specimens were significantly increased by increasing the strain rate. A critical strain rate for bone has been claimed in compression^[15], torsion^[16] and tension^[17]. However Wright and Hayes^[18] found no critical strain rate in tensile tests of bovine bone over a wide strain-rate range.

In the last few decades attempts were made to use the newly developed/improved non-destructive testing techniques to find the mechanical properties of *in vivo* and *in vitro* bones. Those include finding the elastic constants using ultrasonic techniques^[19-22] and finding the mechanical strength of bone specimens by X-ray computed tomography.

Non-invasive evaluation of *in vivo* mechanical properties of bone is of obvious importance to orthopaedics. Vibration analysis, stress wave propagation, ultrasonic-measurements e.t.c. are some of the techniques, which have been attempted by different investigators for the assessment of *in vivo* bone condition in the past.

Vibration technique:

A vibration technique for non-destructive testing has been used for hundreds probably thousands of years, yet the subject is still in its infancy. Vibration techniques have been extensively used for non-destructive evaluation of engineering materials. Since it was truly non-invasive and also free from radiation exposure, many investigators readily used this technique for the assessment of *in vivo* bone condition.

Holi and Radhakrishnan ^[23] in their study carried out quantitative assessment of osteoporosis by impulse response test on the tibial bone of 42 women subjects. The stress waves were generated in the tibial bone by the impact of impulse force hammer and were monitored by accelerometers and were analyzed in the frequency domain. It was found that the natural frequency of stress wave signal was significantly decreased in osteopenia and osteoporosis subjects, indicating decrease in mechanical strength of bone and bone mineral mass. Li et al. ^[24] used the concept of vibration for the diagnosis of loosening of total hip prosthesis. They used the concept from the expectation that a vibrating force would cause a loose implant to undergo independent movement within a bone cavity, thereby generating its own vibration 'signature', whereas securely fitted prosthesis would remain rigid.

Stress wave propagation methods were used by different investigators for the diagnosis of osteoporosis and to monitor the rate of fracture healing ^[25-28]. The application of stress wave propagation technique for monitoring the fracture healing process is described by Saha and Pelker ^[29]. In their study stress waves were generated in fresh and embalmed human femurs and tibias by a longitudinal impact of a steel ball on one end of the bone. The waves were

monitored by bonded semiconductor strain gauges and also by a skeleton traction pin inserted in the bone and placed in a magnetic field.

Naggar et al. ^[30] suggested an analytical solution of electromechanical wave propagation in a long bone. Nagatani et al. ^[31] performed a numerical and experimental study on the wave attenuation in bone. In cancellous bone, longitudinal waves often separate into fast and slow waves depending on the alignment of bone trabeculae in the propagation path. They studied the generation process of fast wave by numerical solution using elastic finite - difference time - domain method and experimental measurements. Simulation and experimental results showed that the attenuation of fast wave was always higher in the early state of propagation, and they gradually decreased as the wave propagated in bone. This phenomenon is supposed to come from the complicated propagating paths of fast waves in cancellous bone.

Hsia et al. ^[32] studied the effect of wave field due to microstructure of bones. The work contributed to some extent of the understanding of ultrasound propagation in the biological effects of human tissue.

Ultrasonic technique:

Claes and Willie ^[33] reviewed the enhancement of bone regeneration by ultrasound. LIPUS (low intensity pulsed ultrasound) treatment led to increased callus area and accelerated returns of bone strength following fracture. They came to the conclusion that despite clinical and experimental studies demonstrating the enhancing effects of LIPUS on bone regeneration, the biophysical mechanics involved in the complex fracture healing process remains unclear and requires further research.

Malizos et al. ^[34] studied application of low-intensity ultrasound for the enhancement and monitoring of fracture healing process in sheep. Hijazy et al. presented the results of the stimulated interaction of ultrasonic waves with a featured tibia ^[35]. The human body is modeled as a four layer medium: skin, fasciae with fat, muscle & bone. Each of these layers is characterized by its acoustic impedance. These impedances influence the incident, transmitted & reflected ultrasonic waves. They developed a mathematical model to describe

these interactions and used the model to quantify the bone healing process. Boonen and Nicholson ^[36] discussed briefly the fundamentals of ultrasound measurement of bone, role of ultrasound in bone quality assessment and hip fracture prediction.

Nowicki et al. ^[37] described a novel approach to estimate broadband ultrasound attenuation in human bone structure *in vivo* using coded excitation. They concluded that acoustic peak pressure amplitude probing the tissue decreases markedly. Qin et al. ^[38] initiated a new modality of quantitative ultrasound by developing a scanning confocal acoustic diagnostic technology particularly for identifying the strength of trabecular bone. They found that yield and ultimate strength (the best indications of true fracture risk) were better correlated than elastic modulus (simply a measure of stiffness). Also they reported that ultrasound values were best correlated with overall parameters such as structural model index which is again the best indicator of global quality of bone.

Protopappas and Fotiadis ^[39] investigated the propagation of guided ultrasonic waves through intact and healing bones. They presented two-dimensional simulation of wave propagation in a bone for callus bones. They demonstrated that the dispersion of lamb waves was influenced by the presence of callus and concluded that the use of guided waves can enhance the monitoring capabilities of ultrasonic evaluation. Evans and Tavakoli ^[40] studied ultrasonic attenuation and velocity in bones. They measured both the velocity and attenuation in a number of samples of cancellous bone and tested their mechanical properties for obtaining a correlation between these parameters and bone density.

Lasaygues et al. ^[41] discussed *in vitro* quantitative imaging of human femur using ultrasonic tomography. Malizos et al. ^[42] gave an overview of low-intensity pulsed ultrasound for bone healing. They discussed about trans-cutaneous application of ultrasound in management of fresh fracture, the trans-osseous application of the LIUS for the enhancement of callus formation and monitoring of callus formation. They also gave their view about treatment of nonunion and distraction osteogenesis by measuring intensity of ultrasound. Based on the assumption that the process of bone healing in bones of the extremities and maxillofacial

skeleton is essentially same, the potential of ultrasound to simulate the maxillofacial bone healing was investigated by Schortinghuis et al. [43].

Rawool et al. [44] used power Doppler sonography for assessing the changes in vascularity during treatment of fractured sites with low intensity ultrasound. Gray scale sonography was performed to evaluate the fracture site. Power dropper sonography was also used to assess the flow pattern of sound waves at the fracture site and surrounding soft tissue. Dodd et al. [45] performed the measurements on bovine cortical bone samples at 200 kHz using an axial transmission technique to investigate the factors that determine how ultrasonic waves propagate across a simulated fracture. The peak amplitude of the first arrival signal was studied. For small fracture gaps, it was found that the change in amplitude was sensitive to the presence of fracture.

However, in all these studies, the intervening soft tissues, whose quantity and quality changes with individual to individual, affected the results. Furthermore some methods were not really non-invasive in nature and some were not practical for widespread clinical use because of low reliability and complicated instrumentation. For a successful clinical application of any technique, the method should be non-invasive in nature, simple to operate and painless to patients.

The structure of bone is very much similar to engineering composite materials and is therefore advantageous to use a non-destructive testing technique, which has already proved its usefulness in the field of composite materials testing. Acoustic emission (AE) technique has been used very successfully for the non-destructive evaluation of composites. The relationship between AE response and mechanical behavior in composite materials has been extensively studied in the past [46].

2.2 ACOUSTIC EMISSION TECHNIQUE

Acoustic Emission (AE) in simple terms is defined as a transient elastic wave generated as an outcome of a material deformation [47-48]. This stress wave propagates through the solid due to the energy released during the

deformation process. The amount of acoustic energy released depends primarily on the size and the speed of the local deformation process.

Acoustic activity may be observed both in highly elastic as well as brittle materials. The classical sources of acoustic emissions are defect-related deformational processes such as crack nucleation/growth and plastic deformation. Its unique ability to passively record events at their moment of occurrence is definitely the main reason for this technique to come in to the forefront of structural monitoring. This advantageous quality permits monitoring during loading ^[49]. The technique can also be characterized as dynamic and volumetric since it is well adapted for remote monitoring of active defects on varied structures.

The AE technique has been studied for about 60 years ^[50] and numerous advantages and disadvantages have been observed, of which a few are listed in the following paragraphs.

The advantages of the technique may be summarized as:

1. The only non-destructive method that enables passive and global monitoring of active defects.
2. Use of multiple sensors can aid in locating the source of acoustic emissions.
3. Measurements can be done in real time.
4. Detailed analysis of the signals allows for differentiation between genuine damage associated signals and background noise.

The AE technique is the sound produced by materials as they fail. A familiar example is the audible cracking noise from wood. Almost all engineering materials generate acoustic emissions but unlike wood, the sound is too faint to be heard without sensitive electronic gadgets. Acoustic emission waves can be detected by means of remote piezoelectric sensors and their source can be located by timing the wave arrival at several sensors. Thus AE provides a unique method of recognizing when and where deformation is taking place as a structure is stressed.

The first systematic investigations of AE phenomenon was made in 1950 by Joseph Kaiser^[51] at the technical university of Munich. In his investigations, the noise emitted by the deformation of materials was examined by means of electronic equipment capable of detecting inaudible ultrasonic signals. Kaiser, while working with polycrystalline specimens concluded that acoustic vibrations originate in grain boundary interfaces and was believed to be associated with the interaction induced between interfaces by applied stresses. He noted that, for a given materials, characteristics spectra of frequency and amplitude existed. One of the important observations made in his study was that irreversible processes were involved with AE phenomenon; an effect later came to be known as Kaiser Effect. The universality of the AE phenomenon, as recognized by Kaiser, leads to a very wide range of applicability. AE has been recorded from hundreds of materials - metals, composites, ceramics, plastics, glasses, building materials, biological materials *in vitro* and *in vivo* as well as from multi material structures and joints between different materials^[52]. Compared to other NDT techniques which rely on extraneous energy for the evaluation of defect; AE enjoys the unique feature that the defect makes its own signal.

2.2.1 Acoustic Emission Detection and Signal Processing

Figure 2.1^[53] shows the method of detection of acoustic emission events by remote piezoelectric transducers. Here, an AE source generates an expanding spherical wave packet losing intensity at a rate of r^{-2} . When this wave reaches the body boundary, a surface wave packet is created, either Rayleigh or Lamb wave type depending on the thickness. This method is mainly used for flaw monitoring in inaccessible areas. The individual signal has a short duration at the source and a corresponding broad spectrum which typically extends from zero frequency to many Mega Hertz. The form of the signal at the point of detection is a damped oscillation, developed in the structure according to known principles of acoustic wave propagation. Figure 2.2^[53] shows the signal waveform of one acoustic emission event and different parameters normally measured to characterize the acoustic emission source.

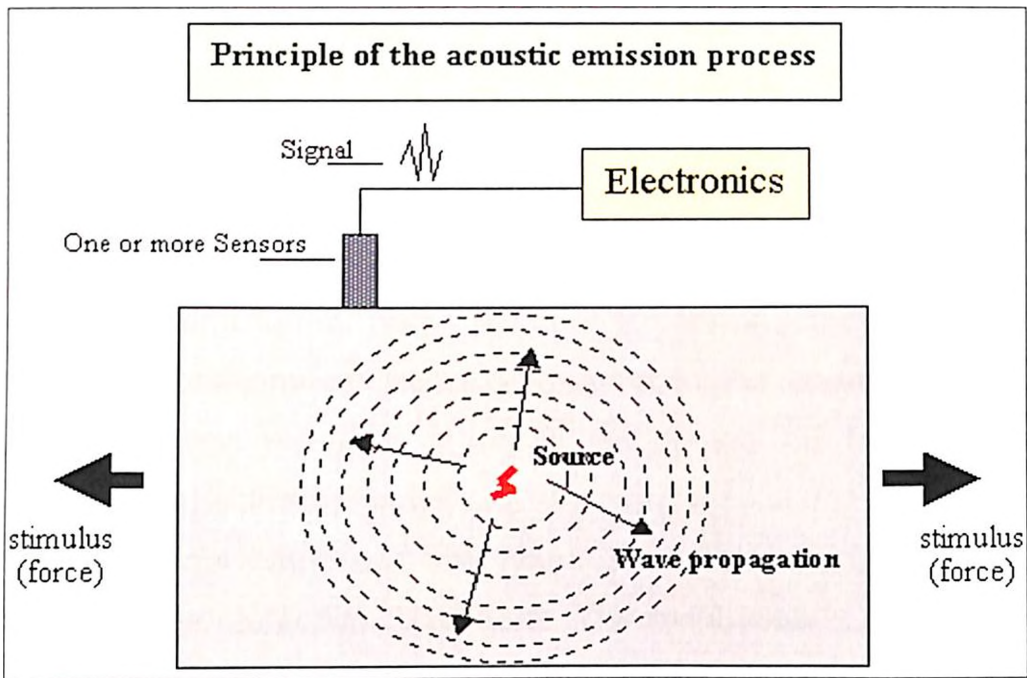


Figure 2.1 Detection of acoustic emission event by remote piezoelectric transducers [Source: Ref. 53]

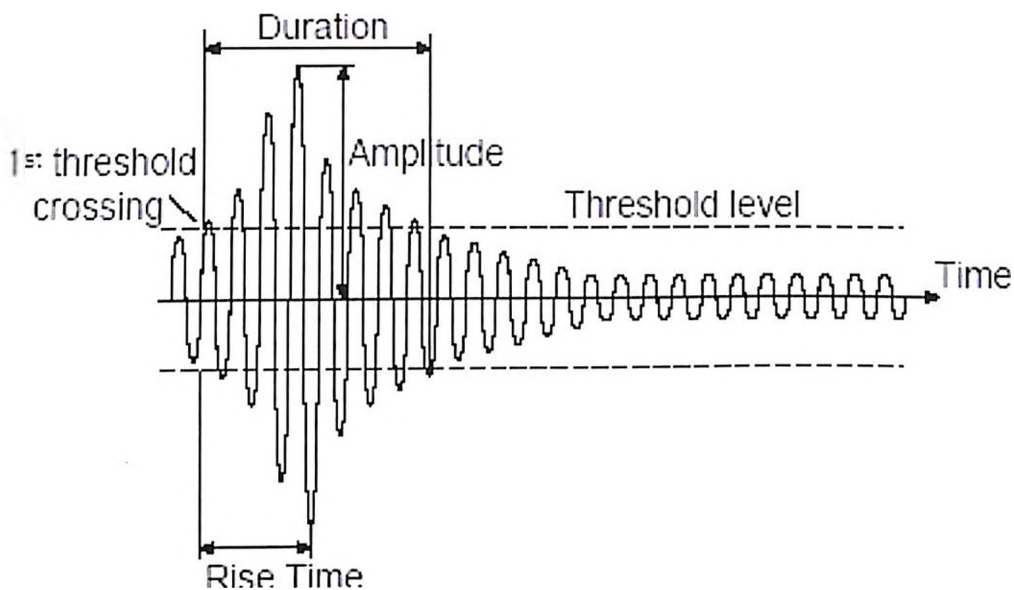


Figure 2.2 Signal waveform for one acoustic emission event [Source: Ref. 53]

2.3 ACOUSTIC EMISSION IN BONE

Hanagud et al. ^[54] using bovine femora first demonstrated detectable acoustic emissions from bone. His work made the way for other investigators to use the AE technique for characterization of bone and also to explore the possibilities of using it as a tool for clinical orthopaedicians to detect bone abnormalities ^[54-58]. Knet et al. ^[55] have shown that the character of the fracture surface depends on

the orientation of the load relative to the direction of the osteons, the rate of loading and the geometrical shape of the actual sample. They concluded that the most promising approach in testing the internal state of a bone is acoustic emission, sometimes also known as the method of stress-wave emission. This approach involves recording of deformation noise in the material due to the development and further propagation of structural defects. These defects may include dislocations or cracks appearing in the course of loading. In another investigation Hanagud et al. ^[59] conducted AE tests on carefully prepared bone specimens subjected to bending loads. Their specimen included femur from cattle and cadavers. They compared the AE patterns from 60 perfect and defective specimens. The result clearly indicated that the development of an effective early diagnostic tool for osteoporosis was possible using AE technique.

Thomas et al. ^[60] studied the acoustic emissions from fresh bovine femora and its clinical applications. They employed a more sophisticated set up of AE technique by including both amplitude and pulse width distribution to investigate whole fresh bovine femora which were loaded in compression and bending. They found that both the amplitude distribution and pulse width distribution results of fresh bone had clearly shown characteristic spectra which could be used for the early detection of bone abnormalities such as fracture and osteoporosis.

Yoon et al. ^[61] studied the AE fresh bovine animal bones. Bones from several different species of animals and different kinds in the same species were tested to obtain AE parameters. Their results indicated that the AE amplitude distributions of all the bones are similar, somewhat independent of the species of animals and kind in the same species materials such as metals, ceramics and plastics.

Netz ^[62] monitored the AE response of canine femora in torsion at 6 degrees per second. His work demonstrated that the AE events occur in the non-linear plastic portion of the load deflection curve. Wright et al. ^[63] monitored the permanent deformation of compact bone using AE technique. Uniaxial tension tests were performed on standardized specimens of bovine harvesian bone to examine the contributions of mineral and collagen to permanent deformation in bone and to monitor the damage mechanisms occurring in permanent deformation using AE

technique. Their results were consistent with a two-phase model for bone in which the mineral behaves as an elastic – perfectly plastic material when bound to the collagen fiber matrix. The AE events occurred just prior to the yield point and continued during yielding. Significant AE counts occurred again just prior to fracture. No emissions occurred in the elastic region and few occurred in the major portion of plastic region between yield and fracture. To monitor micro cracks in the specimen they used AE and plotted graphs. Figure [2.3, 2.4] ^[63] show stress vs. strain and cumulative acoustic emission counts vs. strain curves for one of the control specimens and decalcified specimens. These graphs indicate the similarity between the acoustic emission data of the bones prior to fracture. Figure 2.5^[55] shows stress strain plots based on the mean values from Table 2.1^[63].

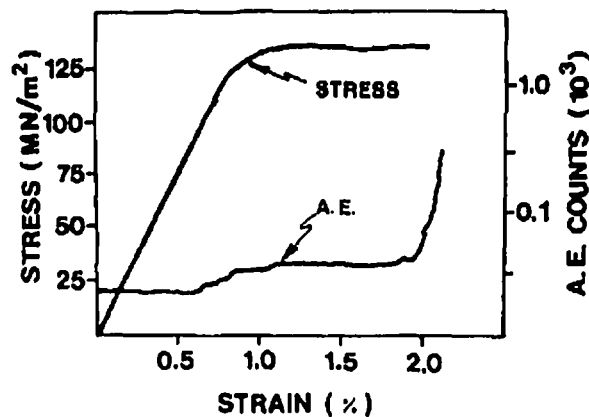


Figure 2.3 Stress vs. strain and acoustic emission counts vs. strain curves for one of the control specimens [Source: Ref.63]

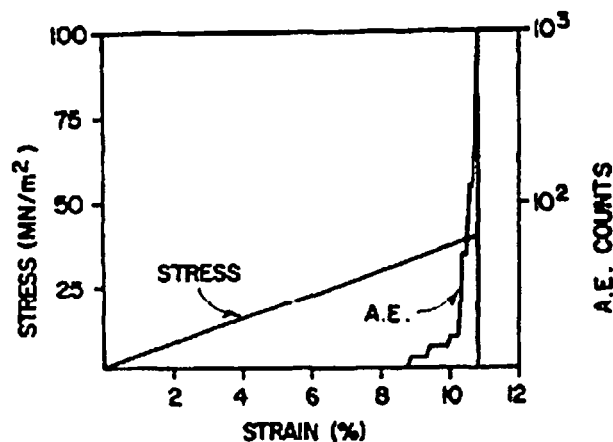


Figure 2.4 Stress vs. strain and acoustic emission counts vs. strain curves for one of the decalcified specimens [Source: Ref.63]

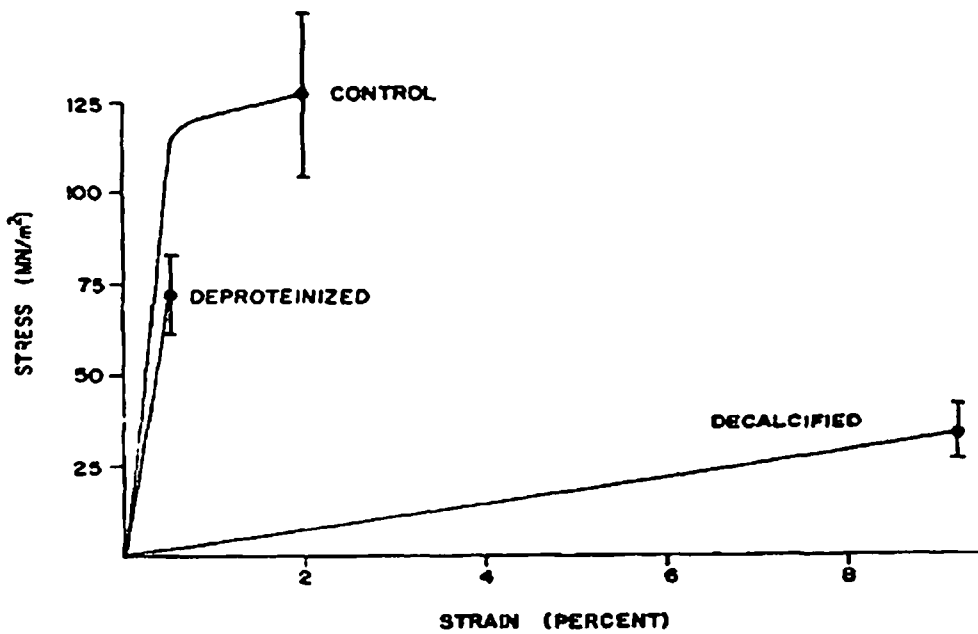


Figure 2.5 Stress-strain curves for the three test groups constructed from the mean values in table 2.1. Error bars are shown for ultimate stress values [Source: Ref.63]

Table 2.1 Mechanical properties of decalcified and partially deproteinized bovine bones [Source: Ref.63]

	control	decalcified	Deproteinized
No of specimens	7	11	10
Yield stress (MNm ⁻²)	118(9.8)	-	-
Yield strain (%)	0.544(0.150)	-	-
Ultimate stress(MNm ⁻²)	128(15.6)	34(7.5)	71(11.5)
Ultimate strain (%)	2.02(0.924)	9.247(1.524)	0.956(0.342)
Elastic modulus (GNm ⁻²)	20.6(2.76)	0.37(0.05)	11.3(3.15)
Plastic modulus (GNm ⁻²)	0.66(0.357)	-	-

*All above mentioned data given as mean (standard deviation)

It is an established fact that the ultimate tensile strength of bone is dependent on the applied strain rate. Based on these Fischer et al.^[64] studied the effect of using two different strain rates on the AE in bones. In their work bovine cortical bone was milled in to standard tensile specimens which were tested at two different strain rates while being monitored with AE equipment. They found that the amplitude distribution of the AE events in bone is dependent on strain rate. Greater number of events occurred with the slower strain rate but the events were of lower amplitude than those emitted during the more rapid strain rate. Here also the initial AE occurred well in to the plastic region of the stress-strain curve near the point of fracture of the tensile specimens.

The work done till this time has demonstrated that the safe use of AE technique for the non-destructive testing of bone is impossible because the AE events occurred only after plastic deformation occurred.

Later on Nicholls and Berg^[65] studied the AE properties of callus bones. In their work, rabbits with 45 degree midshaft oblique osteotomies were strained in shear while monitoring for AE events. Each fracture remained essentially quiet until over 50% of load to failure was applied. They suggested that since callus formation during fracture healing plays important role in the healing process, the AE from callus may have clinical applications. In most of the AE studies of bone the bone has been tested without the surrounding soft tissues. But in the case of clinical applications of AE, one cannot separate the bone from soft tissues and hence the tests should be performed with soft tissues. Hanagud et al.^[66] studied these phenomena. They used freshly dissected rabbit tibia and femur with soft tissues. Tests were conducted through bending load. They found that the soft tissues of 2 to 9 mm thickness did not affect the bone's AE response.

A study of bone-tissue samples by Marten et al.^[67] used acoustic emission to study the mechanical behavior of femoral bones in bending loading. Ono^[68] provided an insight about the fundamental theories and equations related to acoustic emission. Stromsoe et al.^[69], worked on bending strength of femur using non invasive bone mineral assessment.

Lentle^[70] used acoustic emission to monitor osteoporosis. He devised a method for *in vivo* diagnosis of patients using AE technique, which could also predict the severity of osteoporosis.

Acoustic emission has been used to predict changes in mechanical properties due to fatigue^[71-73]. Kevin et al.^[75] developed an acoustical technique for the measurement of structural symmetry of hip joints. Since, these techniques depend very much on the intensity and quality of sounds emitted from the joints under investigation. They developed an acoustical technique for the measurement of relative acoustic transmission across both hips of the test subjects while they were subjected to an external vibratory force applied at the sacrum. The merit of this approach was that it allows direct comparison of the sound signals transmitted across both hips regardless of the measure of the input vibratory force. Simultaneously, other acoustic techniques like scanning acoustic microscopy^[71, 72] acoustic mapping^[78, 79] has been used to predict and study mechanical properties of tissues and bone.

A review by Browne et al.^[81] on acoustic emission's capability to monitor bone degradation and bone fatigue provided us information with latest developments in this field. Ozan^[80] worked on a hypothesis that an increase in micro damage activity during repeated loading of bone will signal the approaching stress fracture. Interception with the training regime prior to the incidence of the fracture as signaled by acoustic emissions would reduce the time necessary for recuperation. Acoustic emission was used for real time monitoring of micro cracks. He used acoustic emission technique to predict the failure of cortical bone. Table 2.2 indicates the predictive capability of acoustic emissions expressed in terms of the specimen's fatigue life^[80].

Table 2.2 The predictive capability of acoustic emissions expressed in terms of the specimen's fatigue life [Source: Ref.80]

	Maximum stress (MPa)	N_F Fatigue life [cycles]	N_P Fracture onset via AE [cycles]	Predictive Capability [% of fatigue life]
Specimen 1	55	26363	22580	85%
Specimen 2	61	35020	33382	95%
Specimen 3	66	4737	2989	63%
Specimen 4	71	600	402	67%

Information was collected on all acoustic events, regardless of whether they originated from micro damage or somewhere else and then signals originating from the micro damage were isolated. The rest of the irrelevant signals were filtered out based on their average frequency, duration, amplitude, and intensity. With the non-micro damage signals removed from the data, we were able to determine the number acoustic events related to bone damage as well as the time at which they occurred. Fracture healing and prediction of healing time of fractures were increasingly being studied. Hirasawa et al.^[74] used AE technique to predict mechanical properties of fractures. They focused on how AE signals can help a surgeon to remove the external fixators in the sense that AE signals can be used to monitor healing of bones. Table 2.3^[74] indicates a statistically significant effect of time on these mechanical properties.

Table 2.3 A statistically significant effect of time on these mechanical properties was detected. Within a row, values with differing letters are significantly different from each other ($P < 0.05$) [Source: Ref.74]

Mechanical properties	Weeks after surgery			
	4(n=8)	4(n=8)	4(n=9)	4(n=9)
Tensile strength (N/mm ²)	36±21a	130±60b	220±32c	510±95d
Tensile stiffness(N/mm)	0.47±0.18a	1.3±6b	1.8±6b	3.0±2c
Maximum strain (%)	10±3a	3.7±3b	1.6±0.4b	1.8±0.3b
AE initiation load (N)	21±15a	71±3b	150±62c	330±31d
Std. tensile strength(N/mm ²)	0.12±0.6a	0.33±0.2b	0.55±0.1c	0.82±0.03d
Std. tensile stiffness(N/mm)	0.028±0.02a	0.57±0.3b	0.82±0.3b,c	1.0±0.06c
Std. maximum strain	5.6±1.4a	2.2±1b	0.90±0.2b	0.86±0.1b

Singh ^[84] reviewed an acoustic imaging technique known as acoustic stress wave propagation technique which was used for bone examination.

Watanabe et al. ^[85] developed a non-destructive method for monitoring fracture healing process using acoustic emission technique. Experimentally produced fractures of the rat femur were tested in tension and in torsion at 4, 6, 8 and 12 weeks after fracture. AE signals were monitored during these mechanical tests. The values for load and torque at the initiation of the AE signal were defined as new mechanical parameters. Tensile strength, tensile stiffness, and torsional stiffness were found to increase with time.

In 2004, R.P. Franke et al. ^[82] used acoustic emission for *in vivo* diagnosis of the knee joint. For the assessment of the tribological knee function and by the probability of fracture of the femur an adapted Acoustic Emission

Measurement System named Bone Diagnostic System (BONDIAS) was developed. This system makes the *in vivo* analysis of the medical status possible. Different mechanisms of cracking were accompanied by different acoustic emission from human femora. An acoustic emission signal typical of crack initiation is shown in Figure 2.6 ^[82]. This Figure is indicative of the acoustic emission from healthy knee joint cartilage after a sudden change from a two leg stand to a one leg stand. It is characterized by a very short rise time and an exponential decrease of the amplitudes. From the medical point of view such mechanical loads are regarded as non destructive although there is already crack initiation in the interface of the compact and the trabecular system of the bone. These micro cracks seem to be essential for the physiological bone remodeling. For the description of the development of bone strength over time it is necessary to assess both the threshold of crack initiation and the conditions for crack propagation. The sudden change in amplitude indicates high thickness of the cartilage layer.

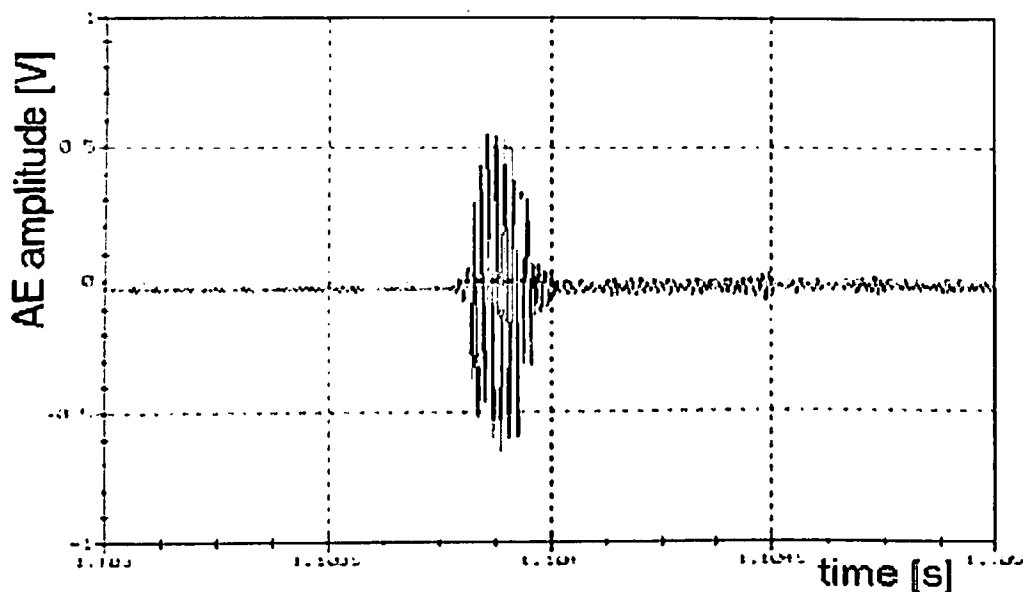


Figure 2.6 Acoustic emissions from healthy knee joint cartilage deformation after the sudden change from a two leg stand to a one leg stand [Source: Ref.82]

Tatarinov et al.^[83] proposed multiple acoustic wave method for assessing long bones. The method was based on measurement of ultrasound velocity at different ratio of wavelength to the bone thickness and taking into account both bulk and guided waves. They assessed the changes in both the material

properties related to porosity and mineralization as well as the cortical thickness influenced by resorption from inner layers, which are equally important in diagnosis of osteoporosis and osteopenia.

In 2006, Alizad et al. [86] studied the change in resonant frequencies of a bone due to change in its physical properties caused due to a fracture. Experiments were conducted on rat femurs and resonance frequencies of intact, fractured, and bonded (simulating healed) bones were measured. These experiments demonstrated that changes in the resonance frequency indicated bone fracture and healing. The fractured bone exhibits a lower resonance frequency than the intact bone and the resonance frequency of the bonded bone approaches that of the intact bone. The graphs are indicative of the result Figure [2.7, 2.8] [86] that the frequency response of a cut femur is less than the intact femur.

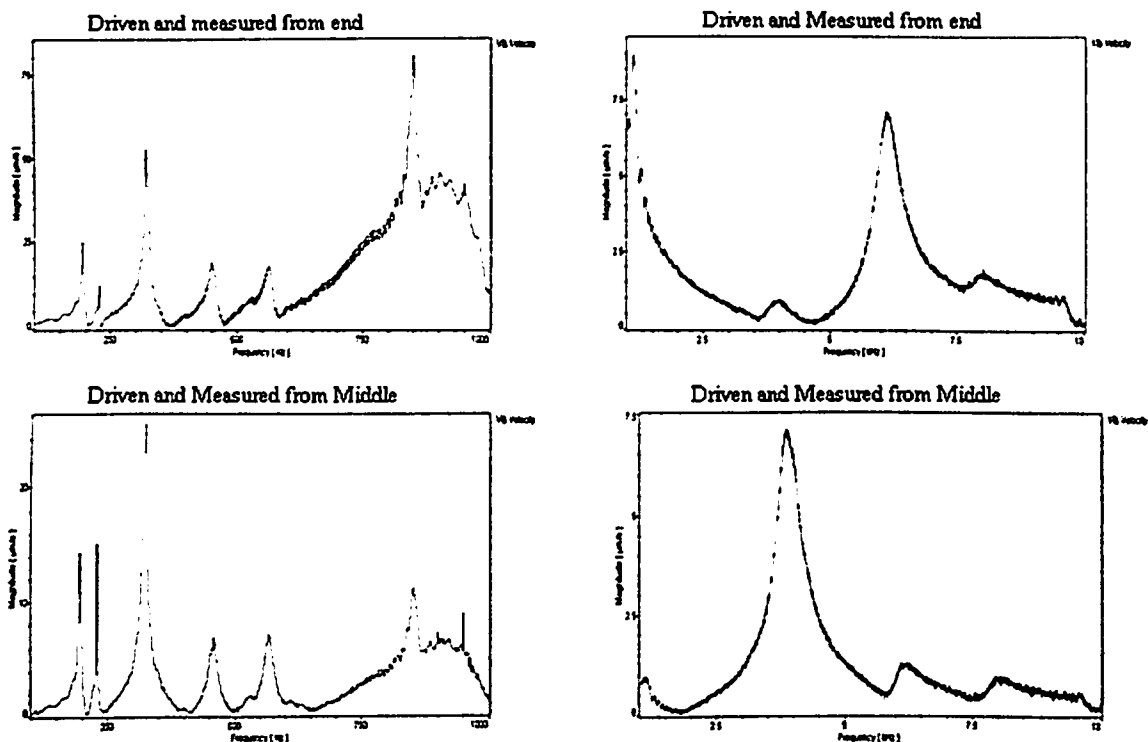


Figure 2.7 Frequency response of the intact femur A. The plots show the motion of the intact femur vs. frequency. These Fig plots indicate peaks at 925 Hz, 4.2 kHz, and 8.1 kHz. Peaks of motion below 700 Hz were explored and found not to be related to the femur. Top left: Driven and measured at the end of the femur at frequency range of 100 Hz to 1000 Hz. Top right: Driven and measured at the end of the bone at 1 kHz-10 kHz. Bottom left: Driven and measured at bone midpoint at 100 Hz-1000 Hz. Bottom right: Driven and measured at bone midpoint at 1 kHz-10 kHz [Source: Ref.86]

In 2008, Bose et al.^[87] studied the effect of valgus bending and shear loading on knee joint. They used acoustic sensors to determine the failure timing of soft tissues attached to femur and tibia. The failure timing was determined based on the knee injury mechanism due to valgus loading. At the estimated time injury, the corresponding values of $\alpha_{\text{valgus_fail}}$, $d_{\text{shear_fail}}$, $M_{\text{valgus_fail}}$, and $V_{\text{shear_fail}}$ were designated as the failure parameters of the knee. Elmar et al.^[88] did stiffness analysis of tibia implant system under cyclic loading. Elmar used a bio-mechanical system integrated with acoustic emission sensors at the screw head. 3 sequences of loading were used to determine when the locking screws break. Data was obtained from the acoustic sensors onto a data acquisition board and were processed using a acoustic emission software. This acquired data was used to determine as to which screw is bearing the load and as to when does the screw break.

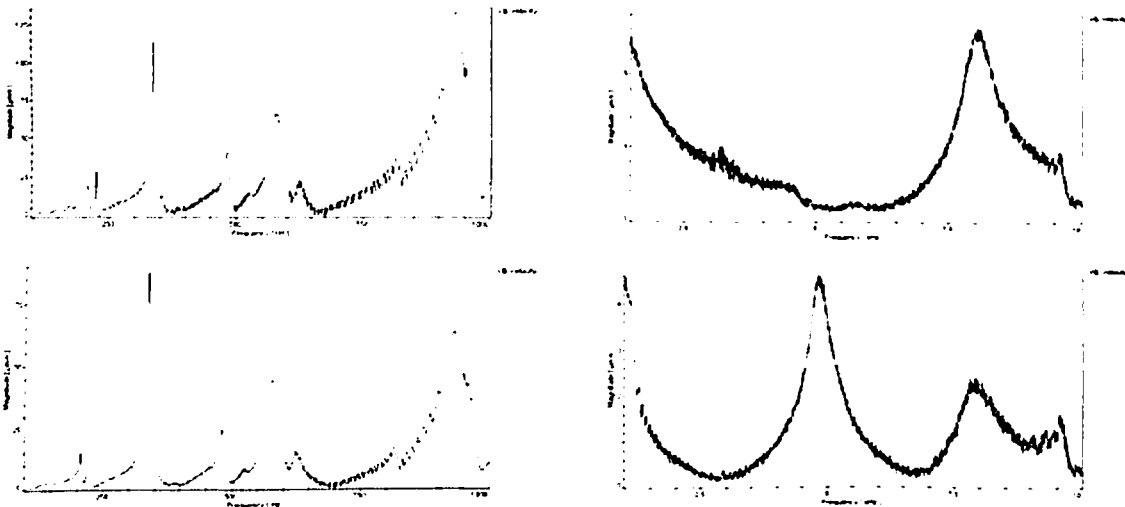


Figure 2.8 Frequency response of the cut femur [Source: Ref.86]

Almost all the studies related to acoustic emission in bone indicated that the initial acoustic emission occurs only in the plastic region and just prior to yield. That means the use of acoustic emission technique for clinical application cannot be considered as safe technique. The occurrence of acoustic emission during the fracture suggests that if proper loading conditions could be used, definitely it could be used to locate the fracture in bones.

2.4 ACOUSTO-ULTRASONIC TECHNIQUE

The basic idea for Acousto-ultrasonic (AU) approach came from the work of Egle and Brown ^[89], who investigated stress wave simulation by using various excitation methods. Vary and his colleagues ^[90-92] advanced the technique by using ultrasonically simulated stress waves and acoustic emission analysis method to evaluate defect states and mechanical properties ^[90-91]. Acousto-ultrasonic technique is still in developmental stage. Though initial work was done in late seventies, major improvements and applications of advanced digital signal processing technique were made only in the last few years ^[92]. Acousto-Ultrasonic technique denotes the combination of certain aspects of acoustic emission (AE) and ultrasonic materials characterization methodology. Unlike AE, Acousto-Ultrasonic technique is not concerned with flaw location and characterization; instead it deals primarily with the assessment of integrated effect of diffused defect states; and population of sub critical flaws. Unlike the acoustic emission technique, this technique is truly non-destructive, wherein only application of low intensively pulses are made and that too only for few seconds to get proper evaluation of the specimen. Due to its truly non-destructive nature and also its ability to evaluate the mechanical performance of materials under test, makes this technique far more suitable for the non-invasive assessment of bone condition. Figure 2.9 and Figure 2.10 shows the schematic diagram of acousto-ultrasonic set up and the principle of the technique respectively ^[93]. In this technique discrete ultrasonic pulses are injected in to the material using an ultrasonic pulsar and the ultrasound is allowed to interact with the material. Due to this interaction of ultrasound with the internal features of the material, the resultant waveform provides a modulated signal characterizing the material quality. An acoustic emission sensor is then used to pick up this resultant waveform. The signal thus obtained is suitably processed to provide the measure of the quality of the material under test.

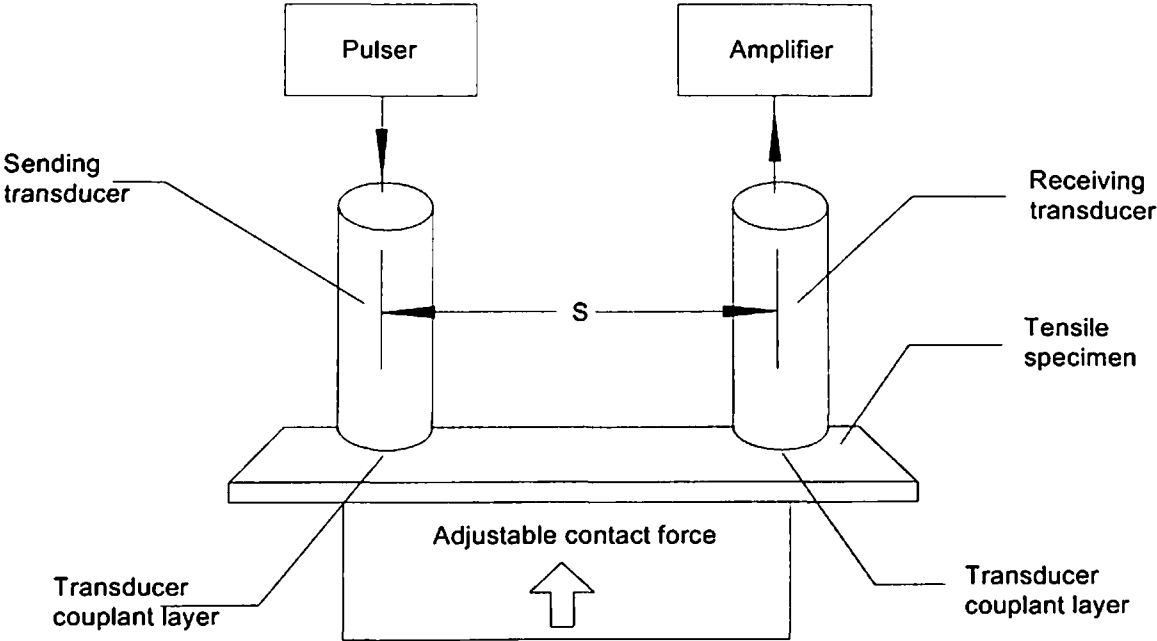


Figure 2.9 Schematic of AU Technique [Source: Ref.93]

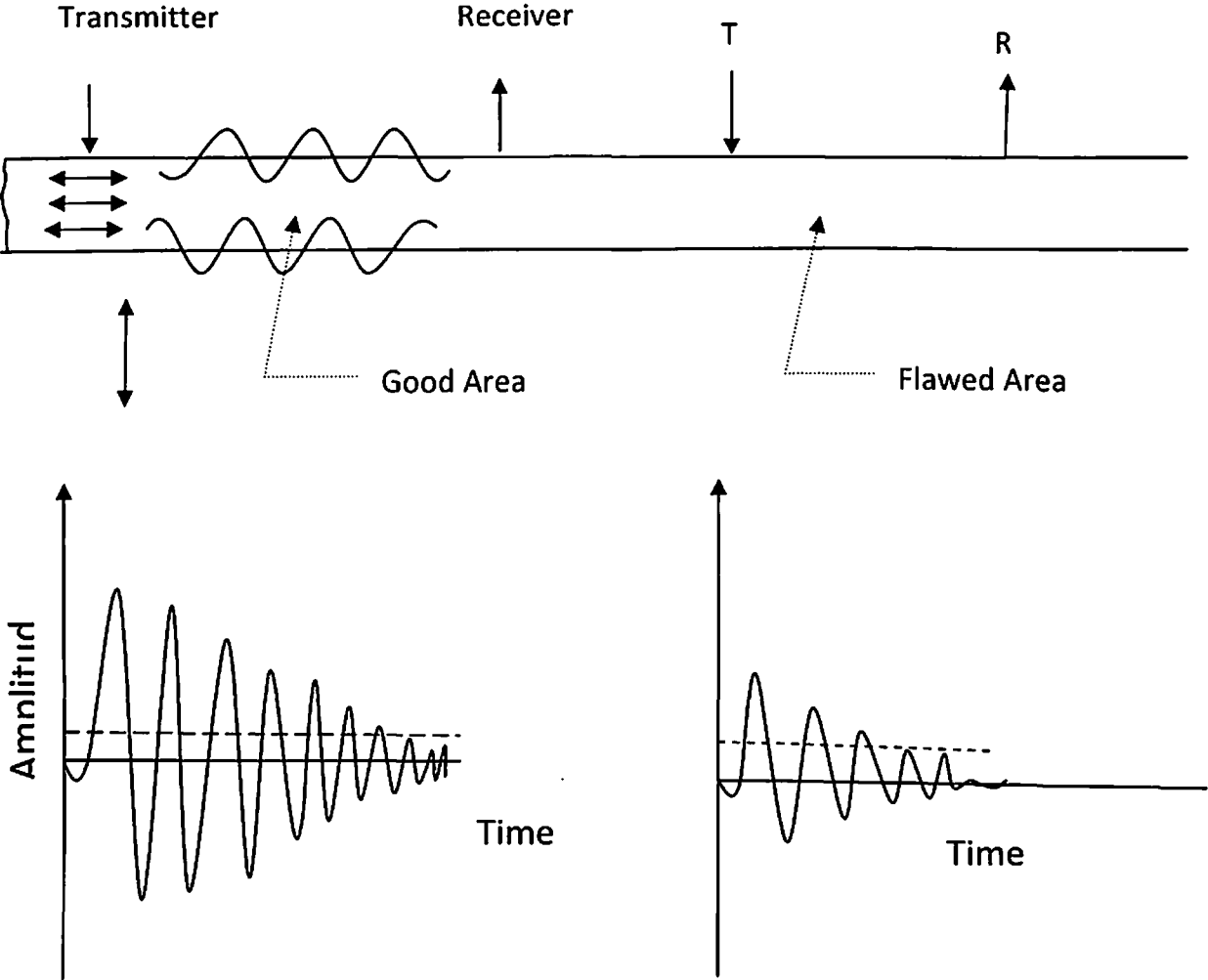


Figure 2.10 Principle of AU Technique [Source: Ref.93]

It is important to recognize the difference between the AU method and pitchcatch ultrasonics. In pitch-catch ultrasonics, the path of the wave is traceable. In acousto-ultrasonics, however, the introduction of the pulse into the specimen yields mixed modes of propagation whose paths are difficult to trace throughout the specimen ^[94]. These mixed modes of propagation ultimately result in the disturbance of the surface at the point of detection. This approach is based on how well the stress wave energy can propagate through a material and how it interacts with the microstructure. The underlying principle of AU is that if the stress wave energy is not efficiently distributed through the material, then the applied load is more likely to promote cracking in the inefficient regions of the material than in regions with more efficient energy transmission. Therefore, if the stress waves are efficiently transmitted, more efficient strain energy transfer will occur, which is associated with an increased mechanical strength ^[92,95].

Another basis for this approach is the assessment of the specimen as a whole while it is in its relaxed state. In normal AE testing, it is necessary to apply a load to the specimen in order for it to generate the necessary stress waves for detection. In AU, the stress waves are stimulated with the ultrasound signal. Also, often in AE or ultrasound, the results of the evaluation are specific to the area of the specimen where the flaw exists. With AU, its concentration is on assessing the serviceability of the specimen, rather than characterizing the flaw.

2.4.1 Acousto-Ultrasonic Signal Measurement

The analysis of the waveform is primarily done using acoustic emission (AE) technology. One method for quantifying the waveform detected by the receiving (or AE) transducer is using what is referred to as the *stress wave factor* (SWF). The SWF is a measure of the stress wave energy that propagates through the specimen. This SWF is used to quantify the AU signal in terms of the material's mechanical properties. In general, if the SWF is high, less attenuation has occurred and the material has efficiently transmitted the stress wave energy.

Often, better stress distribution, or stress wave energy transfer, relates to an increase in strength and fracture resistance.

2.4.2 Stress Wave Factor Measurements (SWF)

The SWF can be defined in more than one way, depending on the application, specimen, and material characteristic being explored. Some common ways come directly from AE methods: ring down count, peak voltage, and energy^[92, 96].

The ring down count is the product of the repetition rate of the ultrasonic pulser, the reset time in the receiver, and the count, the number of oscillations which exceed a preset threshold voltage:

$$E_{SWF} = (R)(T)(C) \quad (2.1)$$

The peak voltage method of quantifying the SWF relies on the peak value of an energy envelope created from the waveform.

The energy method is similar to the peak voltage in that the energy envelope waveform is subjected to a spectral analysis and the SWF is assigned the peak value of the spectrum^[92, 96]. Although ring down counting is the most common method for measuring an acoustic emission signal^[93], the difficulty with this method is that the AU signal changes as the defect in the material grows. Therefore, it becomes much more difficult to make an accurate mathematical model of the signal and consequently more difficult to directly relate the ring down counts to the energy of the signal.

Sundaresan and Henneke^[93] discuss other methods for quantifying and measuring the content of the energy in an AU signal. One particular method involves a measurement of the RMS voltage. There are studies which show the correlation between the frequency spectrum of the waveform and the moments of the AU signal as described in equation

$$M_r = \int_0^{\infty} S(f) f^r df \quad (2.2)$$

where, M_r is the zeroth moment, $S(f)$ is the power spectral density, and f is the frequency. An integration of the Fast Fourier Transform of the frequency spectrum of the AU signal of these moments yields a correlation between the

zeroth moment and the level of damage to the material. It is also shown that the RMS voltage measurement was equivalent to the zeroth moment of the AU signal [97-98]. This indicates that by measuring the RMS voltage, it is an assessment of the amount of damage to a material.

Acousto-ultrasonic technique has already been used successfully in the past for evaluating the properties of composites, woods etc. [99-102]

2.5 SCOPE OF THE PRESENT WORK

1. Many investigations carried out in the field "Assessment of bone condition" are mainly *in vitro* studies. For any method which is going to be used in clinical practice, a thorough experimental study with animals and/or a clinical study with human volunteers are very much essential.
2. Much work has been done with vibration techniques. However, the cost considerations of the specialized hardware and the discomfort to the patient (by the way of excitation) are some of the points which go against it.
3. Ultrasonic techniques have been attempted by different investigators for the assessment of the bone condition *in vitro/ in vivo* but the lack of possible theory to explain the wave interactions *in vivo* and also the difficulty experienced in establishing good reproducibility indicate that much work needs to be done before using this technique for clinical applications.
4. Stress wave propagation has also been used by many investigators for the assessment of *in vivo* bone condition. Again, most of these investigators have done only *in vitro* studies and have not included animal experimentation.
5. In the case of Acoustic Emission Technique, a few researchers have used this technique for *in vitro* as well as *in vivo* characterization of bone. However, the clinical application of the technique was not fully

investigated. The time of occurrence of initial AE and the AE response of bone under different loading conditions at different strain rates are not well established. So the current study is focused on finding the exact time of occurrence of initial AE with respect to the stress/strain curve and the AE behavior under a suitable loading condition at different strain rates.

6. The AE technique has been used for the location of crack in pressure vessels, pipes etc. The technique has also been used to locate the fracture in bones to some extent, but still the accuracy of location is in question. In the present study an *in vitro* study on dry bones has been carried out to locate the fracture in bones.
7. Acousto-ultrasonic technique is still in developmental stage. Many investigators have successfully used it for non-destructive evaluation of composites. Though this technique has many advantages such as being truly non-destructive in nature, its ability to predict the mechanical performance of the component under test; its reproducibility is however not so good. Also the sensitivity and other aspects of the technique is operator dependent and one has to carry out many standardization procedures before actually performing the real experiment. Due to these problems, this technique was found to be unsuccessful when it is performed outside the laboratory by actual users. So this technique should be modified to make it suitable for clinical application. In this work we planned to do a separate study on the reproducibility and sensitivity of the technique and suggest a method to improve them. A modified acousto-ultrasonic technique was developed with the help of much sophisticated instrumentation set up and digital signal processing techniques. This modified technique was ultimately used for the assessment of bone condition *in vitro* and *in vivo*.

In the case of assessment of bone condition, till now there was only one or two attempts made with acousto-ultrasonic technique. These studies were also as *in vitro* studies. So it is planned to do an extensive *in vitro* study first to see the validity of using the AU technique for the present application under simulated conditions. In the *in vitro* study both dry and fresh animal bones were used. In the *in vivo* study the use of AU technique for monitoring the fracture healing process was investigated. An experimental study using rabbits was carried out for this purpose.

References

1. Evans, F.G. (1982) Bones and Bones, Trans. of ASME, J. Biomechanical Engg., 104:1, pp.1-5.
2. Hayes, W.C. (1978) Biomechanical Measurements of Bone, In. CRC Handbook on Engg. In Medicine and Biology, Section B. Instruments and Measurements, Feinberg, B.N. and Fleming, D.G.(eds.) CRC Press, Florida, I, pp.333-372.
3. Singer, C.J. (1959) A Short History of Scientific Ideas to 1900, Oxford University Press, New York.
4. Bourguery, J.M. (1832) Traite Complet de l' Anatomie de l' Homme. I. Osteologie, Paris.
5. Ward, F.O. (1838) Outlines of Human Osteology, London, 370.
6. Meyer, G.H. (1867) Die Architektur der Spongiosa. Arch. Anat. Physiol. Wiss. Med., 34, pp.615-628.
7. Wertheim, M.G. (1847) Memoire sur l' elasticite et al. cohesion des principeaux tissues du corps humaine. Annals. Chim. Phys., 21, pp.385-414.
8. Rauber, A.A. (1876) Ueber Elastizitat und Festigkeit der Knochen. Wilhelm Engelmann, Leipzig.
9. Carothers, C.O., Smith, F.C. and Calabrisi, P.(1949) The Elasticity and Strength of Some Long Bones of the Human Body, Nav. Med. Res. Inst. Rept. NM 001056.02.13.
10. Evans, F.G. and Lebow, M. (1951) Regional Differences in Some of the Physical Properties of the Human Femur, J. Appl.Physiol., 3, 563-572.
11. Evans, F.G. and Lebow, M. (1952) The Strength of Human Bone as Revealed by Engineering Techniques, Am. J. Surg., 83, pp. 326.
12. Burstein, A.H., Reilly, D.T. and Marten, M.(1975) Aging of Bone Tissue: Mechanical Properties, J. Bone J. Surg, 58, pp.82-86.

13. Sierpowska, J., Hakulinen, M.A., Toyras, J., Day, J.S., Weinans, H., Jurvelin, J.S. and Lappalainen, R. (2005) Prediction of Mechanical properties of Human trabecular bone by electrical measurements, *Physiol. Meas.*, 26, pp.S119-S131.
14. Nyman, J.S., Roy, A., Reyes, M.J. and Wang, X. (2009) Progressive Mechanical Behaviour of Human Cortical Bone in Tension for Two Age Groups, *J.Biomed. Mater. Res A.*, 89:2, 521-529.
15. Mc Elhaney, J.H. (1966) Dynamic Response of Bone and Muscle Tissue, *J. Appl. Physiol.*, 21, pp.1231-1236.
16. Panjabi, M.M., White, A.A., and Southwick, W.O. (1973) Mechanical Properties of Bone as a Function of Rate of Deformation, *J.Bone. Surg*, 55(A), 322-330.
17. Crowinshield, R.D. and Pope, M.H. (1974) The Response of Compact Bone in Tension at Various Strain Rates, *Ann. Biomed. Engg*, 2, pp.217-225.
18. Wright, T.M. and Hayes, W.C. (1976) Tensile Testing of Bone over a Wide Range of Strain Rates: Effects of Strain Rate, Microstructure and Density, *Med. Biol. Engg.* 14, pp.671-680.
19. Lang, S.B. (1970) Ultrasonic Method for Measuring Elastic Coefficients of Bone and Results on Fresh and Dried Bovine Bones, *IEEE Trans. Biomed.Engg.*, 17, pp.101-105.
20. Yoon, H.S. and Katz, J.L. (1976) Ultrasonic Wave Propagation in Human Cortical Bone. I. Theoretical Considerations for Hexagonal Symmetry, *J.Biomechanics*, 9, pp.407-412.
21. Yoon, H.S. and Katz, J.L. (1976) Ultrasonic Wave Propagation in Human Cortical Bone.II. Measurements of Elastic Properties and Micro hardness, *J.Biomechanics*, 9, pp.459-464.
22. Ashman, R.B., Corin, J.D. and Turner, (1987) C.H. Elastic Properties of Cancellous Bone: Measurement by an Ultrasonic Technique, *J.Biomech*, 20:10.pp.979-986.

23. Holi, M.S., Radhakrishnan, S. (2003) In vivo assessment of osteoporosis in women by impulse response technique, TENCON, pp.1395-1398.
24. Li, P.L.S., Jones N.B., Gregg, P.J. (1995) Loosening of total hip anthroplasty, diagnosis by vibration analysis, Journal of Bone and Joint Surgery, 77, pp.640-644.
25. Guzelsu, N. and Saha, S. (1981) Electromechanical wave propagation in long bones. J.Biomechanics, 14, pp.19-33.
26. Guzelsu, N. and Saha, S. (1983) Diagnostic Capacity of flexural waves in wet bones. Biomechanics Symposium Woo, S.L.Y. and Mates, R.E. (eds.), pp. 197-200. ASME, New York.
27. Guzelsu, N. and Saha, S. (1984) Electromechanical behavior of wet bone. Part II: Wave propagation. J. Biomech. Engg, 106, pp. 262-271.
28. Pelker, R.R. and Saha, S. (1983) Stress wave propagation in bone. J.Biomechanics, 16, pp-481-489.
29. Saha, S. and Pelker, R.R. (1976) Measurement of fracture Healing by the use of stress waves. 22nd Annual ORS, New Orleans, Louisiana.
30. El-Naggar, A.M., Abd-Alla, A.M. and Mahmoud, S.R. (2001) Analytical solutions of electro-mechanical wave propagation in long bones, Applied Mathematics and Computation, 119, pp.77-98.
31. Nagatani, Y., Mizuno, K., Saeki, T., Matsukawa, M., Sakaguchi, T. and Hosoi, .H. (2008) Numerical and experimental study on the wave attenuation in bone—FDTD simulation of ultrasound propagation in cancellous bone, Ultrasonics, 48, pp.607-612.
32. Hsia, S.Y., Chiu, S.M. and Cheng, J.W. (2008) Wave propagation at the human muscle-compact bone interface. Theoret, Appl. Mech, 33:3, pp.223-243.
33. Claes, L., Willie, B. (2007).The enhancement of bone regeneration by ultrasound- Review. Journal of Progress in Biophysics and Molecular Biology, 93, pp.384-398.

34. Malizos, K.N., Athanasios, A., Protopappas, V.C., Fotiadis, D.I.(2006) Transosseous application of low-intensity ultrasound for the enhancement and monitoring of fracture healing process in a sheep osteotomy model, *Journal of Bone* ,38, pp.530-539.
35. Hijazy, A., Al-Smoudi, H., Swedan, M., Qaddoum, N., Al-Nashash, H., Ramesh, K.G.(2006) Quantitative monitoring of bone healing process using ultrasound, *Journal of Franklin Institute.*, 343, pp. 495-500.
36. Boonen, S., Nicholson, P.(1998) Assessment of femoral bone fragility and fracture risk by ultrasonic measurements at the calcaneus, *Age and Ageing*, 27, pp. 231-237.
37. Nowicki, A., Litniewski, J., Secomski, W., Lewin, P.A., Trots, I.(2003) Estimation of ultrasonic attenuation in a bone using coded excitation, *Journal of Ultrasonics.*, 41, pp.615-621
38. Qin, Y., Mitra, E., Lin, W., Xia, Y., Rubin, C. (2003) Non-invasive assessment of bone strength and density using scanning ultrasound, *Proceedings of Summer Bioengineering Conference*, June 25-29, Florida, pp.373-374.
39. Protopappas, V.C., Fotiadis, D.I. (2005) Two-dimensional simulation of guided ultrasound wave propagation in healing long bones, *IEEE Ultrasonic Symposium*, 2, pp. 842-845.
40. Evans, J.A., Tavakoli, M.B. (1990) Ultrasonic attenuation and velocity in bone. *Journal of Physics in Medicine and Biology*, 35, pp.1387-1396.
41. Lasaygues, P., Ouedraogo, E., Lefebvre, J.P., Gindre, M., Talmant, M., Laugier, P. (2005) Progress towards in vitro quantitative imaging of human femur using compound quantitative ultrasonic tomography, *Journal of Physics in Medicine and Biology.*, 50, pp.2633-2649.
42. Malizos, K.N., Hantes, M.E., Protopappas, V.C., Papachristos, A.(2006) Low intensity pulsed ultrasound for bone healing-an overview, *International Journal of Care Injured*. 37, pp. S56-S62.

43. Schortinghuis, J., Stegenga, B., Raghoobar, G.M., Debont, L.G.M. (2003) Ultrasonic stimulation of maxillofacial bone healing, *Crit Rev Oral Bio Med.*, 14, pp.63-74.
44. Rawool, N.R., Goldberg, B.B., Flemming, F., Winda, A.A., Hume, E. (2003) Power doppler assessment of vascular changes during fracture treatment with low intensity ultrasound, *Journal of Ultrasound Medicine.*, 22, pp.145-153.
45. Dodd, S.P., Cunningham, J.L., Miles, A.W., Gheduzzi, S., Humphrey, V.F.(2007) An in vitro study of ultrasound signal loss across simple fractures in cortical bone mimics and bovine cortical bone samples, *Journal of Bone.*, 40, pp.656-661.
46. Prakash, R. (1980) Non destructive testing of composites, *Composites*, 10, pp. 217-224.
47. Arrington, M., (1987) Acoustic emissions, Non-destructive testing of fiber reinforced composites, ed. J. Summerscales, Elsevier, London, pp. 25-63.
48. Sarfarazi, M.P., (1992) Acoustic emissions and damage constitutive characteristics of Paper, Institute of paper science and technology, Project 3571.
49. Grosse, C. U, (2002), NDT.net - Editorial: Special Issue on Acoustic Emission. Grosse, C., Reinhardt, H., Dahm, T., Localization and classification of fracture types in concrete with quantitative acoustic emission measurement techniques.
50. American Society of Nondestructive testing (ASNT) (2005): Non Destructive Handbook – Acoustic emission testing, pp.6.
51. Kaiser, J. (1950) Untersuchungen uber das auftreten gereausen beim Zugersuch. Ph.D. Thesis, Technische Hutshule, Munich.
52. Pollock, A.A. (1979) An Introduction to Acoustic Emission and a Practical Example, *J.Environmental Sciences*, March/April, pp1-4.
53. Radhakrishnan, S. (1992) The assessment of bone condition by acoustic emission and acousto-ultrasonic techniques. Ph.D. Thesis, Banaras Hindu University.

54. Hanagud, S., Clinton, R. G. and Lopez, J.P. (1973) Acoustic emission in bone substance, Proceedings of Biomechanics Symposium of the American Society of Mechanical Engineers, pp.74, ASME, New York.
55. Knet-s,L.V., Krauya, U.E. and Vilks,Y.K. (1975) Acoustic Emission in Human Bone Tissue upon Lengthwise Stretching, Mekh.Polim, 4, pp.685-690.
56. Kruya, U.E. and Lyakh, Y.A. (1978) Acoustic Emission in Human Bone Tissue. Mekh.Polim, 1, pp.109-112.
57. Peters, A. (1982) Acoustic Emission Technique and Fracture Healing, Med. Biol.Engng. Comput, 20, pp.8.
58. Wright, T.M. and Carr, J.M. (1983) Soft Tissue Attenuation of Acoustic Emission Pulses. Trans. Of ASME J. Biomech. Engg, 105:1, pp.21-23.
59. Hanagud. S., Hannon, G. T. and Clinton, R. G. (1974) Acoustic emission and diagnosis of osteoporosis, Proceedings of Ultrasonics Sym., pp. 77-80.
60. Thomas, R.A., Yoon, H.S. and Katz, J.L. (1977) Acoustic Emission from Fresh Bovine Femora, Proceedings of Ultrasonics Symp. IEEE Cat.No. TICH12G4-ISU, pp.237-240.
61. Yoon, H.S., Caraco, B.R. and Katz, J.L. (1980) Further Studies on the Acoustic Emission of Fresh Animal Bone, IEEE Trans. Sonics, Ultrasonic, SU-27, pp.160.
62. Netz, P. (1979) The Diaphyseal Bone under Torgue, Acta Orthop.Scand.Suppl. 176, pp.1-31.
63. Wright, T.M., Booburgh, F. and Burstein, A.H. (1981) Permanent Deformation of Compact Bone Monitored by Acoustic Emission, J.Biomech, 14, pp. 405-409.
64. Fischer, R.A., Arms, S.W., Pope, M.H. and Seligson, D. (1986) Analysis of the Effect of using Two Different Strain Rates on the Acoustic Emission in Bone, J.Biomech, 19:2 , pp. 119-127.
65. Nicholls, P.J. and Berg, E. (1981) Acoustic Emission Properties of Callus, Med. Biol. Engg. Comput, 19, pp. 416-418.

66. Hanagud, S., Clinton, R. G., Chouinard, M. D., Berg, E. and Nicholls, P. J. Soft (1977) Tissues and Acoustic Emission Based Diagnostic Tools, Ultrasonics Symposium Proceedings, IEEE CAT. No. 77CH1264-ISU, pp.242-245.
67. Martens, M., van Audekercke, R., de Meester, P., Mulier, J.C. (1986) Mechanical Behaviour of Femoral Bones in Bending Loading, Journal of Biomechanics, 19:6, pp.443-454.
68. Ono, K. (1979) Fundamentals of Acoustic Emission, Los Angeles (CA), UCLA, pp.167-207.
69. Stromsoe, K., Hoiseth, A., Alho, A., Kok, W.L. (1995) Bending Strength of the Femur in Relation to Non-invasive Bone Mineral Assessment, Journal of Biomechanics 28:7, pp.857-861.
70. Lentle, B. CC (1999) Diagnosis of Osteoporosis Using Acoustic Emission, The University of British Columbia, Patent no A61B8/08.
71. Wells, J.G. (1985) Acoustic Emission and Mechanical Properties of Trabecular Bone, Biomaterials, 6, pp.218-24.
72. Leguerney, I., Raum, K., Saied, A., Follet, H., Boivin, G., and Laugier, P. (2003) Evaluation of Human Trabecular Bone Properties by Scanning Acoustic Microscopy, J. Bone Min. Res., 18, pp.S187.
73. Rajachar, RM, Chow, D.L., Curtis, C.E., Weissman, N.A., Kohn, D.H. (1999) Use of Acoustic Emission to Characterize Focal and Diffuse Micro damage in Bone, In: Acoustic Emissions: Standards and Technology Update. West Conshohocken, PA: American Society for Testing and Materials, pp.3-19.
74. Hirasawa, Y., Takai, S., Kim, W. C., Takenaka, N., Yoshino, N., and Watanabe, Y. (2002) Biomechanical Monitoring of Healing Bone Based on Acoustic Emission Technology, Clin. Orthop. Related Res., 402, pp.236–244.
75. Kevin, S. C. K., Xiaolin, H., Jack, C. Y. C., John, H. E. (2003) Acoustic Transmission in Normal Human Hips: Structural Testing of Joint Symmetry, Medical Engineering & Physics, 25:10, pp.811-816.

76. Bumrerraj, S. and Katz, J. L. (2001) Scanning Acoustic Microscopy Study of Human Cortical and Trabecular Bone, *Ann. Biomed. Engg.*, 29, pp.1034-1042.
77. Eckardt, I. and Hein, H. J. (2001) Quantitative Measurements of the Mechanical Properties of Human Bone Tissues by Scanning Acoustic Microscopy, *Ann. Biomed. Engg.*, 29:12, pp.1043-1047.
78. Xia, Y., Lin, W., Mitra, E., Demes, B., Gruber, B., Rubin, C., and Qin, Y. (2003) Performance of a Confocal Acoustic Mapping in Characterization of Trabecular Bone Quality in Human Calcaneus, *J. Bone Min. Res.*, 18, pp.S209.
79. Cardoso, L., Teboul, F., Sedel, L., Oddou, C., and Meunier, (2003) A. In vitro Acoustic Waves Propagation in Human and Bovine Cancellous Bone, *J. Bone Min. Res.*, 18:10, pp.1803-1812.
80. Ozan, A. (2005) Acoustic Emission Based Surveillance System for Prediction of Stress Fractures, Ph.D. Nicholas Wasserman, The University of Toledo Annual report.
81. Browne, M., Roques, A. and Taylor A. The Acoustic Emission Technique in Orthopaedics - a Review, *J. Strain Analysis*, 40: 1, pp.59-79.
82. Franke, R.P., Dörner, P., Schwalbe, H.-J. and Ziegler, B. (2004) Acoustic Emission Measurement System for the Orthopedical Diagnostics of the Human Femur and Knee Joint, University of Ulm, Dept. of Biomaterials, Ulm, Germany, Bad Griessbach, Germany, University of Applied Science Giessen, Giessen, Germany.
83. Tatarinov A., Noune S., Armen S. (2005) Use of Multiple Acoustic Wave Modes for Assessment of Long Bones: Model study, *Journal of Ultrasonics*, 43, pp. 672-680.
84. Singh, V. R. (1989) Acoustical Imaging Techniques for Bone Studies, *Applied Acoustics*, 27, pp.119-128.
85. Watanabe, Y., Takai, S., Arai, Y., Yoshino, N., Hirasawa, Y. (2001) Prediction of Mechanical Properties of Healing Fractures Using Acoustic Emission, *Journal of Orthopedic Research*, 19, pp.548-553.

86. Alizad, A., Walch, M., Greenleaf, J.F., Fatemi, M. (2006) Vibrational characteristics of bone fracture and fracture repair: application to excised rat femur, *Journal of Bio Mech. Engg., Trans ASME*, 128, pp.301-307.
87. Bose, D., Bhalla, K., Costin D. Untaroju, B., Ivarsson, J., Crandall, Jeff R. (2008) Injury Tolerance and Moment response of Knee Joint to combined Valgus Bending and Shear loading, *Journal of BioMech. Engg., Trans ASME*, 130, pp.1-8.
88. Elmar, K. T., Stefan, H., Patrick W., Michael J., Stefanie S.T. and Heinz, R. (2008) Stiffness analysis of tibia implant system cyclical loading, *Material Science and Engineering C 28* , pp 1203-1208.
89. Egle, D.M. and Brown, A.E. (1976) A note on Pseudo Acoustic Emission Sources' *J. Testing and Evaluation*, 4, pp.196-199.
90. Vary, A. and Bowles, K.J. (1977) Ultrasonic Evaluation of the strength of Unidirectional Graphite-Polimide Composite, In *Proceedings of the Eleventh Symposium on Non-destructive testing*, American Society for Nondestructive Testing and Southwest Research Institute, San Antonio, Tex., pp.242-258.
91. Vary, A. and Lark, R.F. (1979) Correlation of fiber composite Tensile Strength with the Ultrasonic Stress Wave factor, *J. Testing and Evaluation*, 7, pp.185-191.
92. Vary, A. (1988) The Acousto-ultrasonic approach. In *Acousto-Ultrasonics Theory and Application*, Duke J.C.Jr. (ed.). Plenum Press, New York, NY, pp.1-22.
93. Sundaresan, M.J. and Henneke II, E.G. (1988) Measurement of energy content in acousto-ultrasonic signals, In *Acousto-Ultrasonics, Theory and Application*, Duke, Jr. J.C. (ed.) Plenum Press, New York, pp. 275-282.
94. Duke, J. C. (1992) *Acousto-Ultrasonics, NDE Testing Techniques*, eds. D. F. Bray and D. McBride, Wiley Interscience, NY.

95. Molina, G. J. and Haddad, Y. M. (1996) Acousto-ultrasonics approach to the characterization of impact properties of a class of engineering materials, *International Journal of Pressure Vessels and Piping*, 67 :3, pp.307-315.
96. Vary, A. (1982) Acousto-Ultrasonic Characterization of Fiber Reinforced Composites, *Materials Evaluation*, 40, pp.650-654.
97. Sundaresan, M. J., E.G. Henneke, II, Reifsnider, K. L. and D. Post, (1987) *Nondestructive Evaluation of Filament Wound Pressure Vessels*, CCMS-87-02, Center for Composite Materials and Structures, Virginia Tech.
98. Sundaresan, M. J., E. G. Henneke, II, and Brosey, W. D. (1991) Acousto-Ultrasonic Investigation of Filament Wound Pressure Vessels, *Materials Evaluation*, 49:5, pp.601-606.
99. Srivastava, V. K. and Prakash, R.(1987) Fatigue life prediction of glass fibre reinforced plastics using the acousto-ultrasonic technique, *Int J. Fatigue*, 9:3, pp.175-178.
100. Liu, T., Kitipornchai, S., Veidt M. (2001) Analysis of acousto-ultrasonic characteristics for contact- type transducers coupled to composite laminated plates", *Int. J. of Mech. Sci.*,43, pp.1441-1456.
101. Beall, F.C. (1989) Monitoring of in situ curing of various wood-bonding adhesives using acousto-ultrasonic transmission, *Int. J. Adhesion and Adhesives*, 9:1, pp.21-25.
102. Andrew, L. G., Gregory, N. M., Laura, M. C. (2006) In situ monitoring of damage in SiC/SiC composites using acousto-ultrasonics, *Composites: Part B* 37, pp.47-53.

CHAPTER 3

ACOUSTIC EMISSION CHARACTERISTICS OF *IN VITRO* BONE

3.1 INTRODUCTION

All the techniques which are going to be used in clinical practice should be thoroughly established with the simulated studies in the laboratory. The results of the *in vitro* tests can be used to see the suitability of a technique. In the case of Acoustic emission technique also, *in vitro* studies have to be done to prove its potentials before using it as a tool for clinical orthopaedicians. Though some investigators carried out *in vitro* studies with bone, many acoustic emission characteristics, such as the time of occurrence of initial AE, the acoustic emission response of bone under various loading conditions and at different strain rates are not clearly established. So in this *in vitro* study the focus was made in finding the exact time of occurrence of initial AE by simultaneously recording the load and AE response with respect to time. In a failure scenario, bone will often have been exposed to high strain rates. Rubin et al. ^[1] concluded that physiological strain rates during walking and running are in the range of 0.005-0.08 s⁻¹ and that this is a realistic range also for humans. Lanyon et al. ^[2] measured strain rates of 0.013 s⁻¹ in Human during running and Burr et al. ^[3] measured strain rates of 0.050 s⁻¹ during sprinting and downhill running. Strain rates during traumatic events clearly depend on the particular circumstances, and it is impossible to specify a single traumatic strain rate.

In this study, the bone was tested under three point bending load at two different strain rates, by keeping in mind that the main purpose of the present study is to assess the potential of AE technique as a tool for clinical orthopaedicians, only whole bones were used in this study for testing. This point was supported by Hayes ^[4] also, who in his paper on Biomechanical measurements in bone reported that the experimental investigation with whole bones best reflects the functional capacity of musculoskeletal components *in vivo*.

3.2 MATERIALS AND METHODS

In vitro study was carried out with both dry bones and wet bones. In the case of dry bones, bovine bones were obtained from the slaughter house and kept for drying in the electric oven at the temperature of 40-50⁰C for 3-4 days. Fresh animal (bovine) bones were also used in the present study.

3.2.1 Preservation of Fresh Bone for Testing

The fresh animal bones obtained from slaughterhouse immediately after sacrificing the animal, were always kept in normal saline to keep the bone moistened. All the studies were carried out on the same day within 2 hours.

3.2.2 Selecting the Type of Loading

Previous investigations on the structural strength of whole bone and AE monitoring from bone, a wide variety of testing configurations were used. Acoustic emissions were monitored when the bone was tested under bending ^[5], Compression ^[7], tension ^[6, 8] and torsion ^[9]. In the present study, the bending load configuration was used for AE monitoring for *in vitro* studies. The present load configuration also satisfied most of the criteria's given by Burstein and Frankel ^[10] for choosing the possible load configuration for biomechanical measurement in whole bones.

3.2.3 Acoustic Emission Monitoring

The instrument used for acoustic emission monitoring is shown in Figure 3.1. Figure 3.2 gives the schematic diagram of the experimental setup.

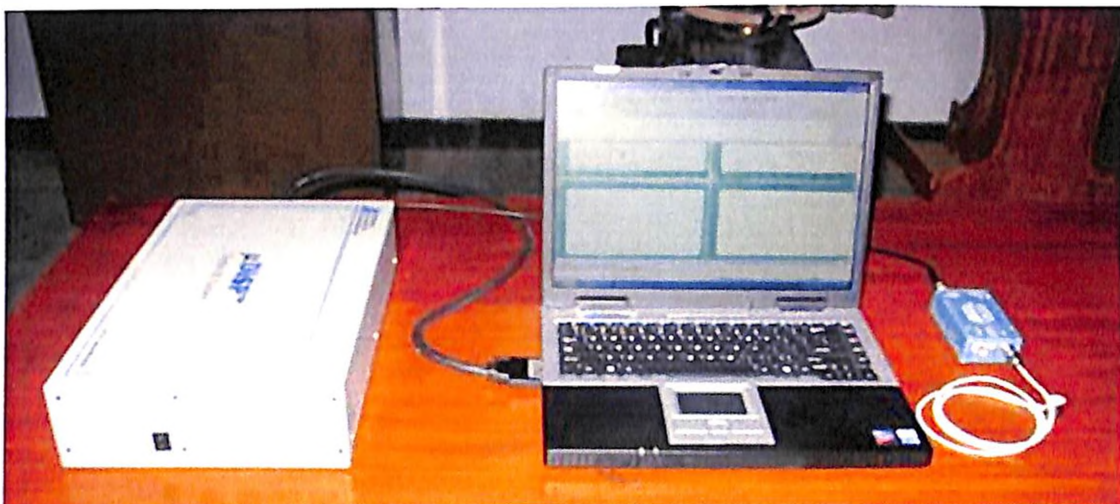


Figure 3.1 Acoustic Emission Equipment

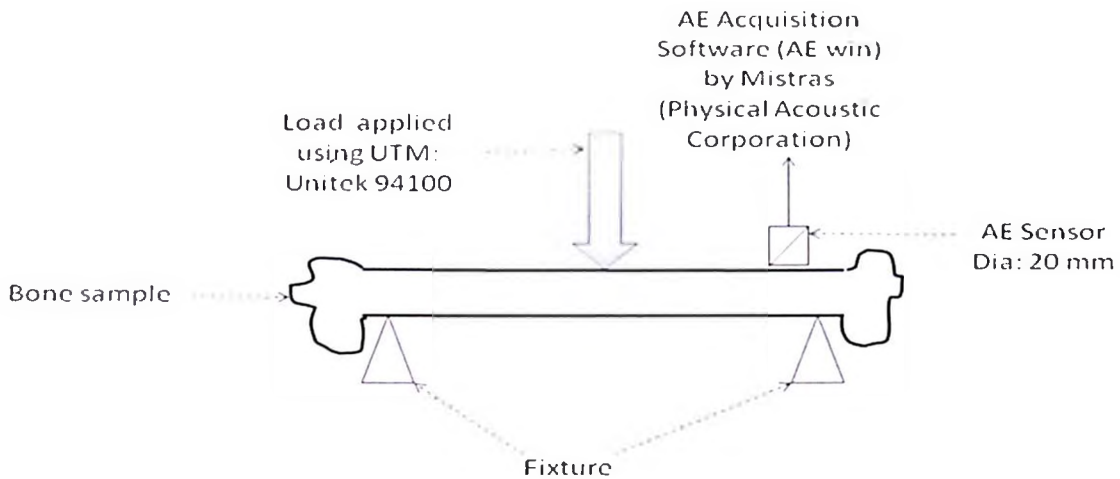


Figure 3.2 Schematic Diagram for Acoustic emission set up

The specimen to be tested was placed in the 3 point bending arrangement of electronic universal testing machine [Unitek 94100]. This electronic testing machine had a controller for the cross head speed (i.e. strain rate) and the applied load was measured by the load cell and displayed in seven segments LED display at the form of D.C. Voltage proportional to the digital display for recording purpose. The acoustic emission signals were picked up from the bone specimen by a miniature acoustic emission sensor R15D-AA51 of Diameter: 20 mm, and frequency response of 3 kHz – 3 MHz. The sensor was attached to the specimen with the help of adhesive tape. The high vacuum grease was used as a couplant between sensor and the specimen. Acoustic emission preamplifier (1220A, Physical Acoustics Corporation, U.S.A.) with the frequency response of 20-1200 KHz and gain of 40dB/60dB was used to amplify the AE signals picked up from the specimen. The preamplifier was powered by the AE-1A Acoustic emission amplifier (PAC, USA). The AE signals thus picked up from the preamplifier was processed using at AET-206 Single Channel Acoustic Emission System. This AE System can process the signal and can give the cumulative number of count or events, count rate or event rate, signal level and also the signal output and the digital counter output for recording purpose. The facility for threshold setting and further post amplification gains was also available with this instrument. This instrument had an excellent facility for rejecting extraneous noise coming from the loading machine by instrument setting called floating threshold. Here the threshold is always added with the signal level so that noise will never be counted as a signal of interest. Throughout this study, the floating threshold setting was used since the loading

machines, even though electronically controlled, was not as sophisticated as a servo-hydraulic testing system such as Instron or MTS Systems (which were always recommended for noise free AE monitoring).

To study the acoustic emission characteristics of dry and wet bones the AE was monitored after selecting the proper instrument settings and the cumulative count at each load level was noted until the plastic deformation occurred. To record the time of occurrence of initial AE, the displacement's reading obtained from the UTM were divided with the strain rate to get the time readings. These time readings were then calibrated with the time of the acoustic emission signal. Both UTM and AE acquisition system were started simultaneously at the start of the test with the AE system in acquire mode. AE sensor of suitable band frequency was placed on one end of the bone and the load was applied at the middle of the bone samples. The simultaneous monitoring of load Vs time from the electronic universal testing and acoustic emission features with respect to time, facilitated the accurate determination of the time of occurrence of initial AE with respect to the load deformation curve.

Bone specimens both dry and fresh (20 in each category) were tested in the three point bending load configuration. The Acoustic emission response was monitored and the load vs. time and cumulative AE counts vs. time were recorded during all the tests. For testing the bones under different strain rate, two cross head speeds of universal testing machine were selected. During the loading under the higher cross head speed (20 mm/minute) it was found that noise level of the UTM was very high and the threshold setting of the AE instrument has been increased to 70dB to eliminate the noise. Due to this high threshold setting only few AE counts were recorded during the very higher cross head speed. So the speed of the cross head (strain rate) was carefully chosen.

3.3 RESULTS AND DISCUSSION

3.3.1 AE Characteristic of Dry Bones

The Acoustic emission response of dry bones (representative specimens 1 to 5) when loaded under 3 point bending in the electronic universal testing machine is

given in Figure 3.3. Here the cumulative AE counts were plotted against the load applied. This AE response corresponds to the strain rate (cross head speed) of 5 mm/minute. It is clear from the Figure 3.3 that AE occurs just during the failure. There is no cumulative count during the initial loadings and just during the failure/deformation a sudden rise of cumulative AE counts has occurred. Figure 3.4 gives the AE response of the dry bones under higher strain rate i.e. 15 mm/minute. Here also the similar response were recorded i.e. there was no sufficient release of AE counts during the elastic region and just before or during the failure sudden burst of AE activity occurred, which can be associated with permanent deformation.

The important aim of this study is to clearly establish the time of occurrence of initial AE with respect to stress-strain curve. The acoustic emission characteristics of dry bones for 3 representative samples for the strain rate of 5mm/minute are shown in Figure 3.5, Figure 3.6 and Figure 3.7. The figures clearly establish the exact time of occurrence of initial AE. Here the significant amount of AE occurs at 70-80% of ultimate load required to make permanent deformation.

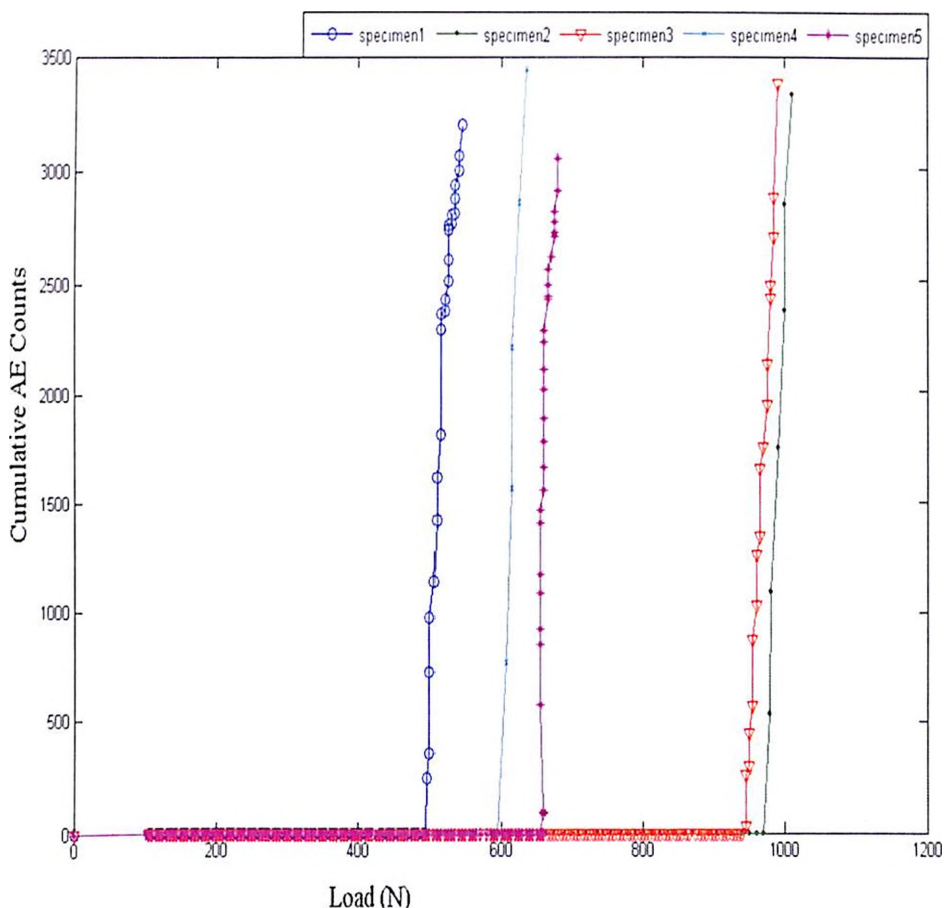


Figure 3.3 Acoustic Emission Response of Dry Bones (S.R. = 5 mm/minute)

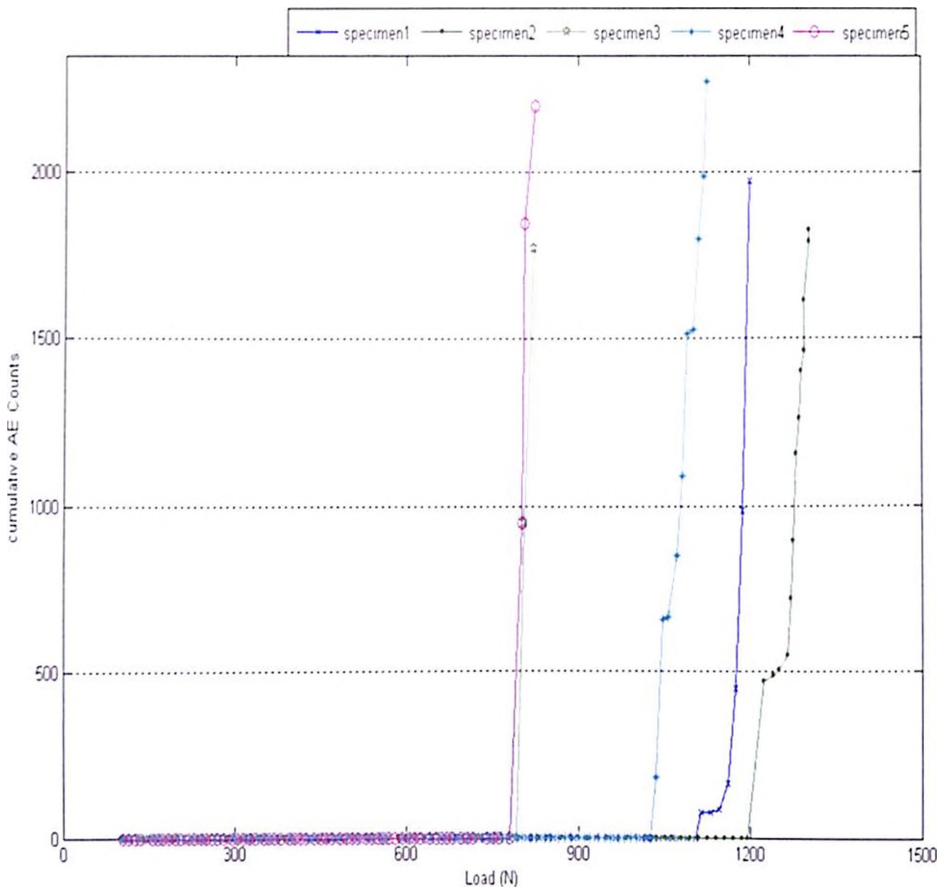


Figure 3.4 Acoustic Emission Response of Dry Bones (S.R. = 15 mm/minute)

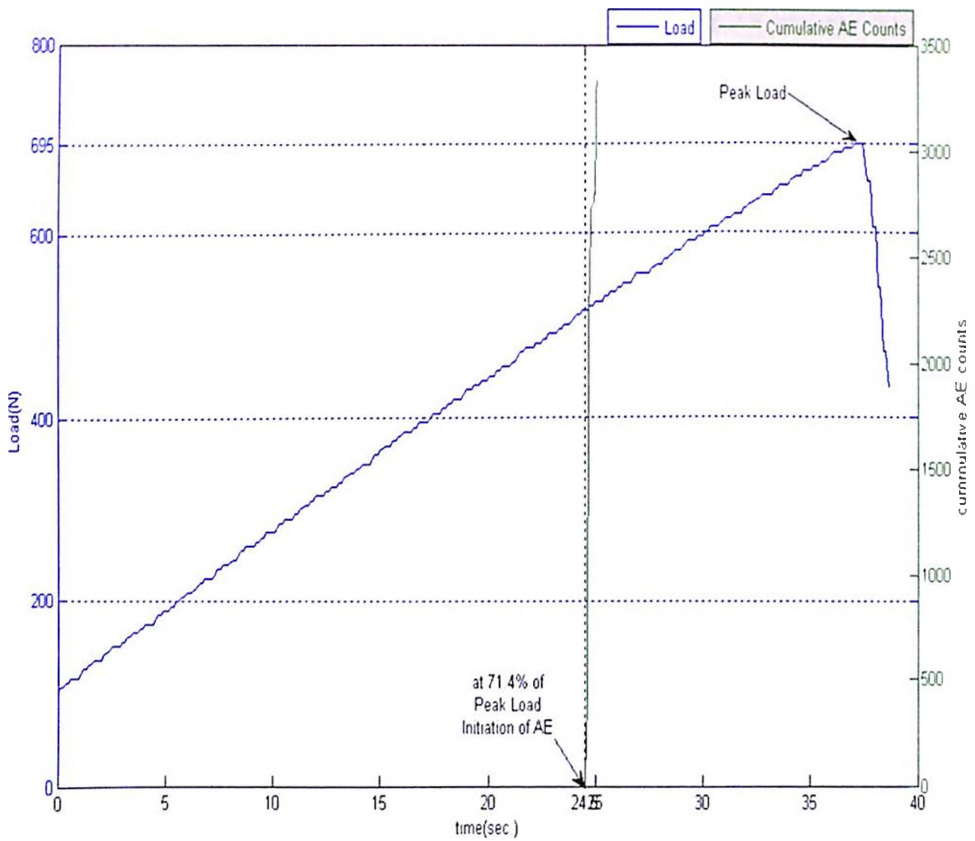


Figure 3.5 AE characteristic of Dry bone sample-1 (S.R.= 5 mm/minute)

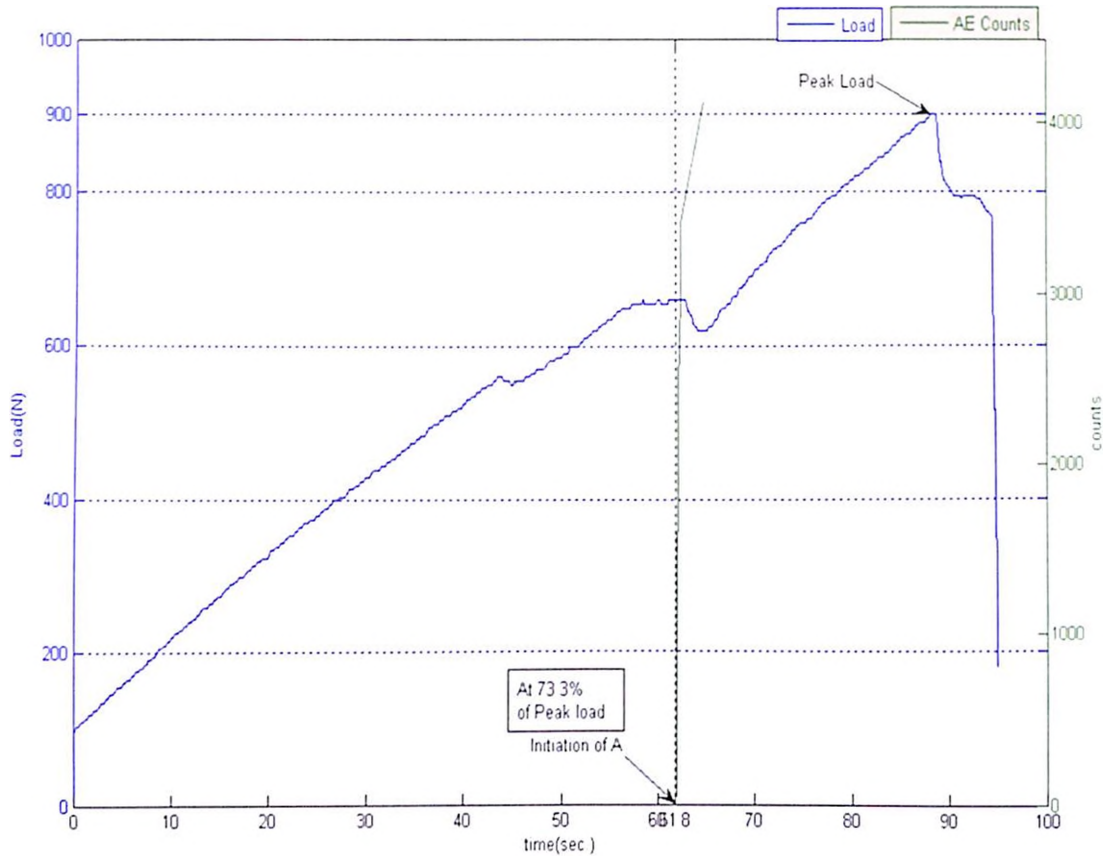


Figure 3.6 AE characteristic of Dry bone sample-3 (S.R.= 5 mm/minute)

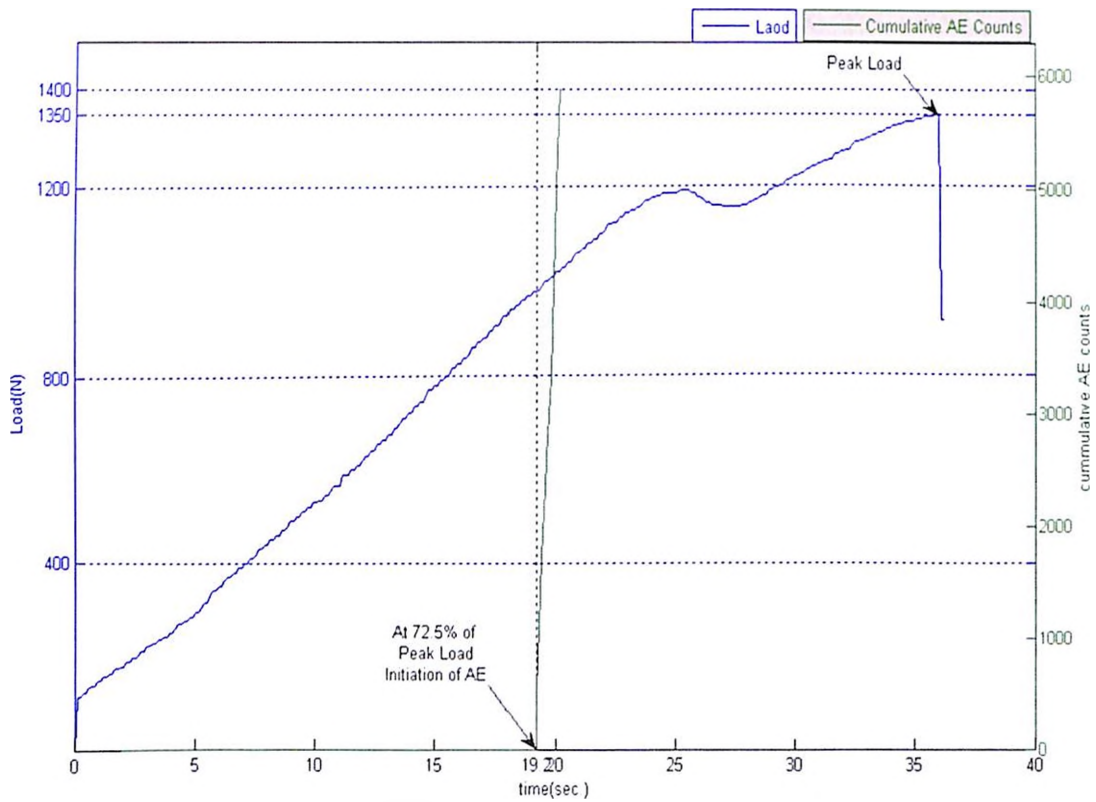


Figure 3.7 AE characteristic of Dry bone sample-4 (S.R.= 5 mm/minute)

To see the effect of higher strain rate on the AE characteristics, the bone was loaded to 3-point bending test at the strain rate of 15 mm/minute. Figure 3.8, Figure 3.9 and Figure 3.10 represents the acoustic emission characteristic of dry bones at this strain rate. Once again, it was found that in the case of higher strain rate also the initial AE occurs just during the plastic deformation in the bone. Here the significant amount of AE occurs before failure at 75-85% of ultimate load required to make permanent deformation.

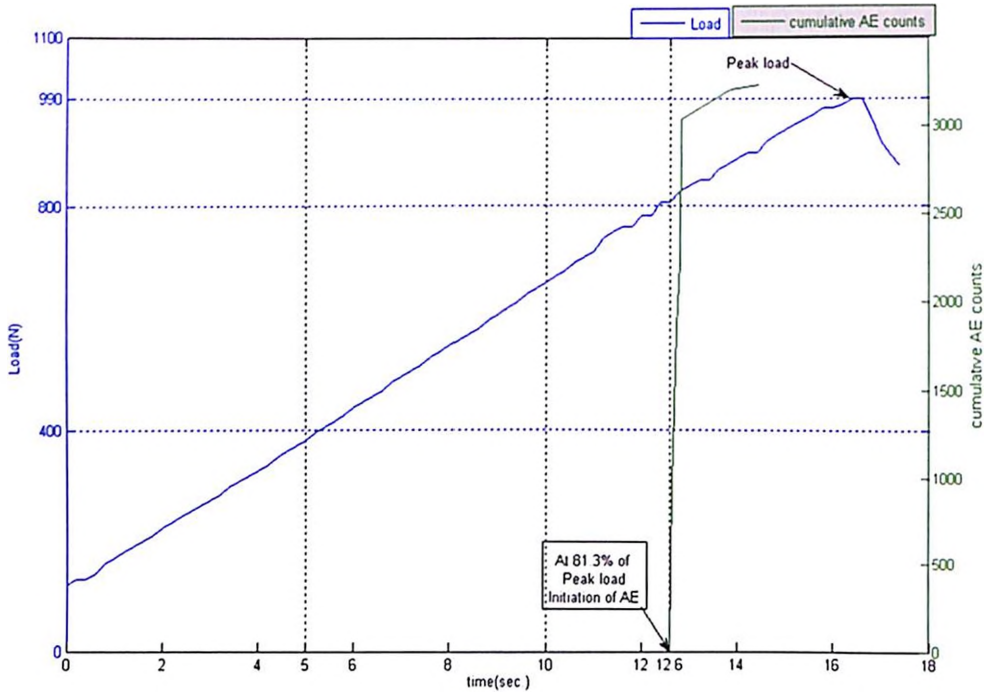


Figure 3.8 AE characteristic of Dry bone sample-2 (S.R.= 15 mm/minute)

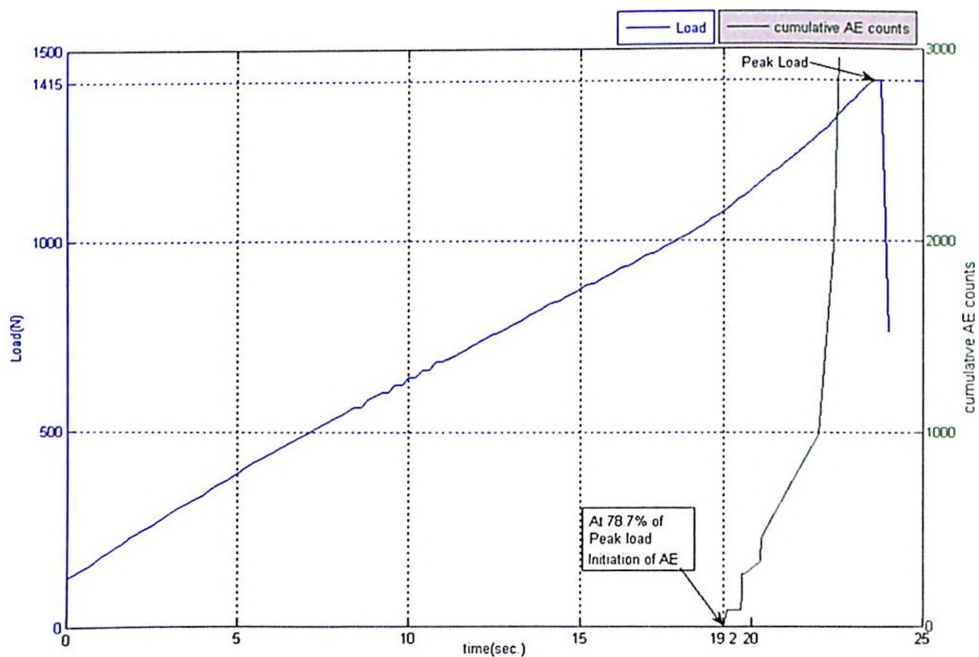


Figure 3.9 AE characteristic of Dry bone sample-3 (S.R.= 15 mm/minute)

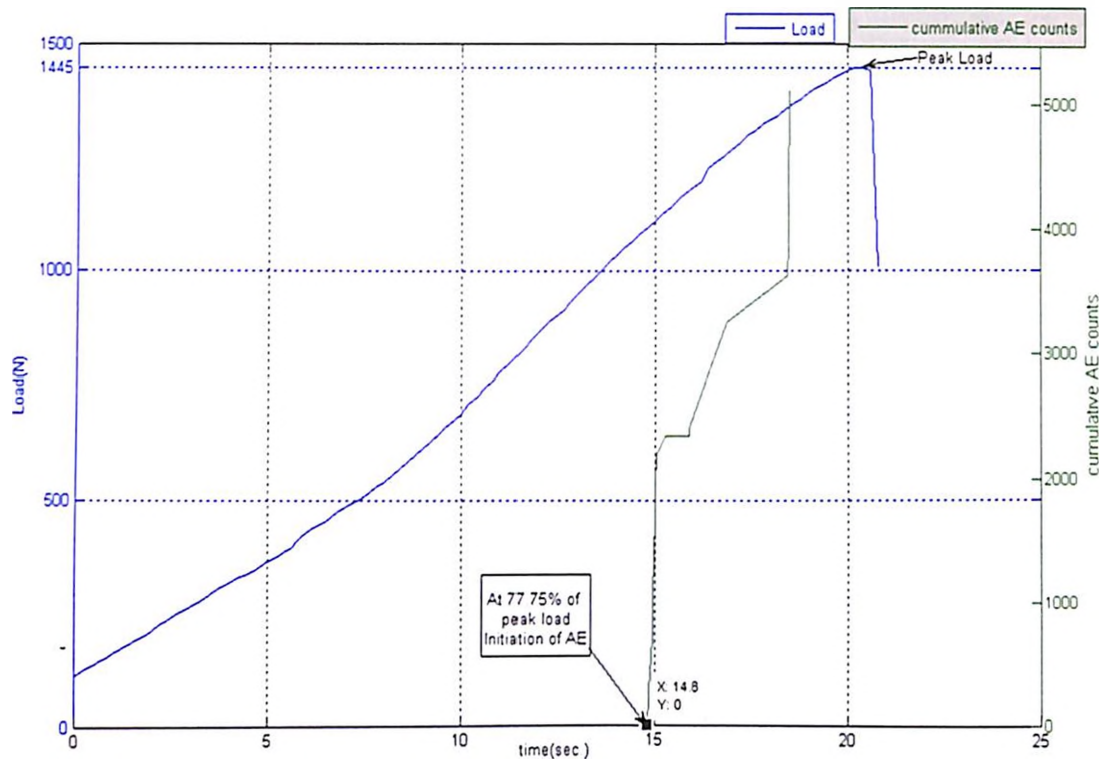


Figure 3.10 AE characteristic of Dry bone sample-4 (S.R.= 15 mm/minute)

Table 3.1 and Table 3.2 summaries the result of the mechanical loading of the whole bones (dry bones) at two strain rates of 5mm/minute and 15mm/minute respectively. In most of the cases, the acoustic emission started at 70-80% of the ultimate load required for the permanent deformation. The effect of the strain rate on the amplitude of the signal is shown in Figure 3.11 and Figure 3.12. The counts of higher amplitude were obtained at the higher strain rate.

Table 3.1 Ultimate load of Dry Bones under different strain rates

Ultimate Load (in N)	Strain Rate		p-value
	5mm/minute	15mm/minute	
Mean	957.50	1291.67	p = 0.04
Standard Deviation	214.54	165.10	

No. of samples (n) =5

Table 3.2 Percentage of Ultimate Load at which initial AE occurred for dry bones

Strain Rate	Mean%	Standard Deviation
5mm/minute	72.7%	0.8514
15mm/minute	80.41%	2.067

No. of samples (*n*) =5

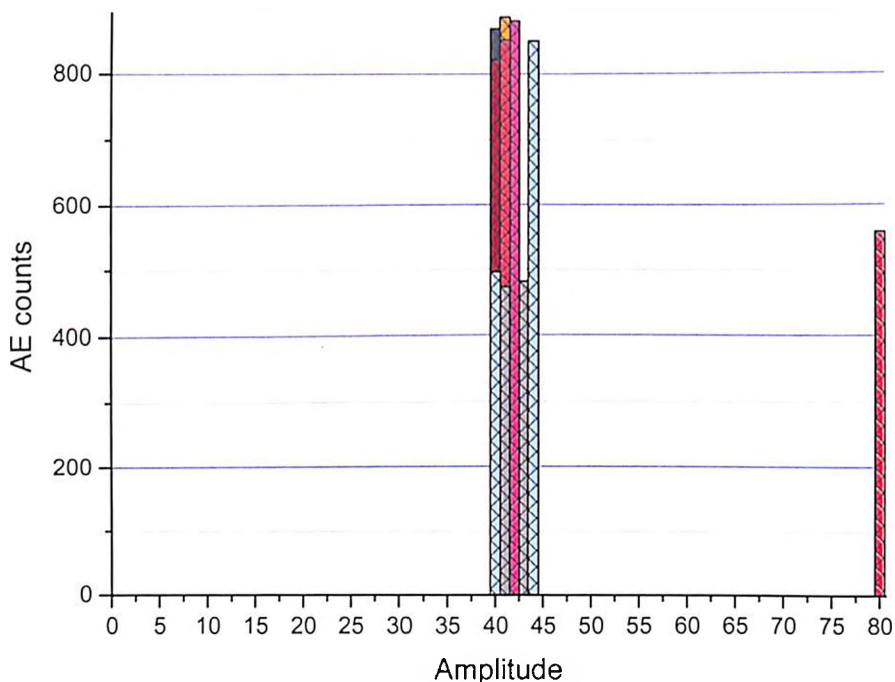


Figure 3.11 Amplitude Distribution of AE counts (S R.= 5 mm/minute)

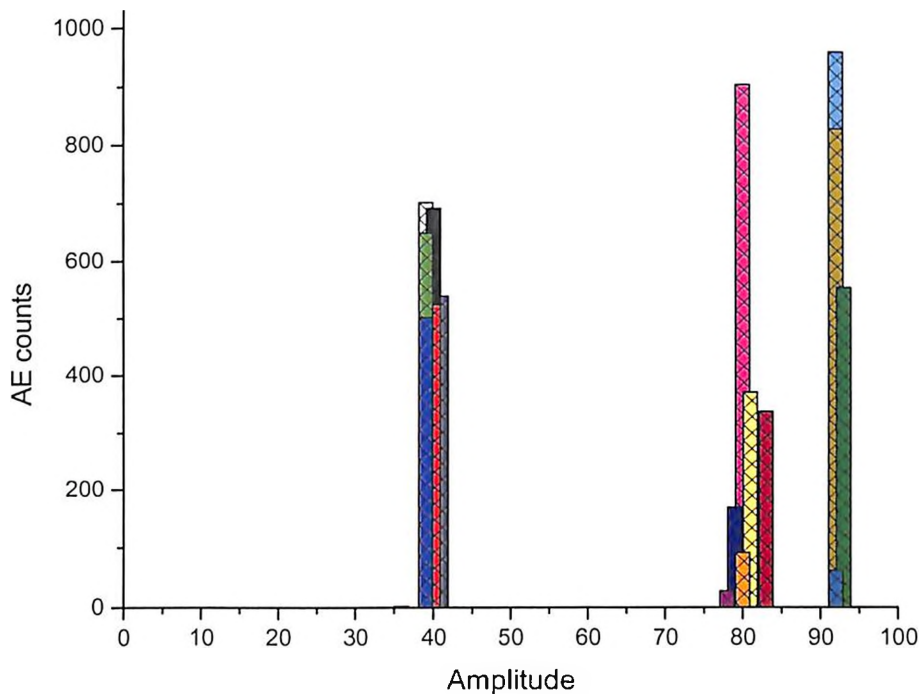


Figure 3.12 Amplitude Distribution of AE counts (S.R.= 15 mm/minute)

3.3.2 AE CHARACTERISTIC OF FRESH BONES

To see the effect of strain rate on the time of occurrence of initial AE in fresh bone, the whole bone specimens were loaded under 3 point bending at a strain rate of 5mm/minute and 15 mm/minute respectively. Figure 3.13 and Figure 3.14 shows the plot between cumulative counts and the load applied. Here also the significant counts occurred during the plastic deformation/fracture stage only. Figure 3.15-3.17 clear gives the idea of initial occurrence of acoustic emission. Here also the significant amount of AE occurs just before failure at 95-98% of ultimate load required to make permanent deformation.

Table 3.3 and Table 3.4 summarize the results of the mechanical loading of the whole bones (fresh bovine). In most of the specimens, the initial AE occurred just before or during the failure (95-98% of ultimate load, which caused the deformation).

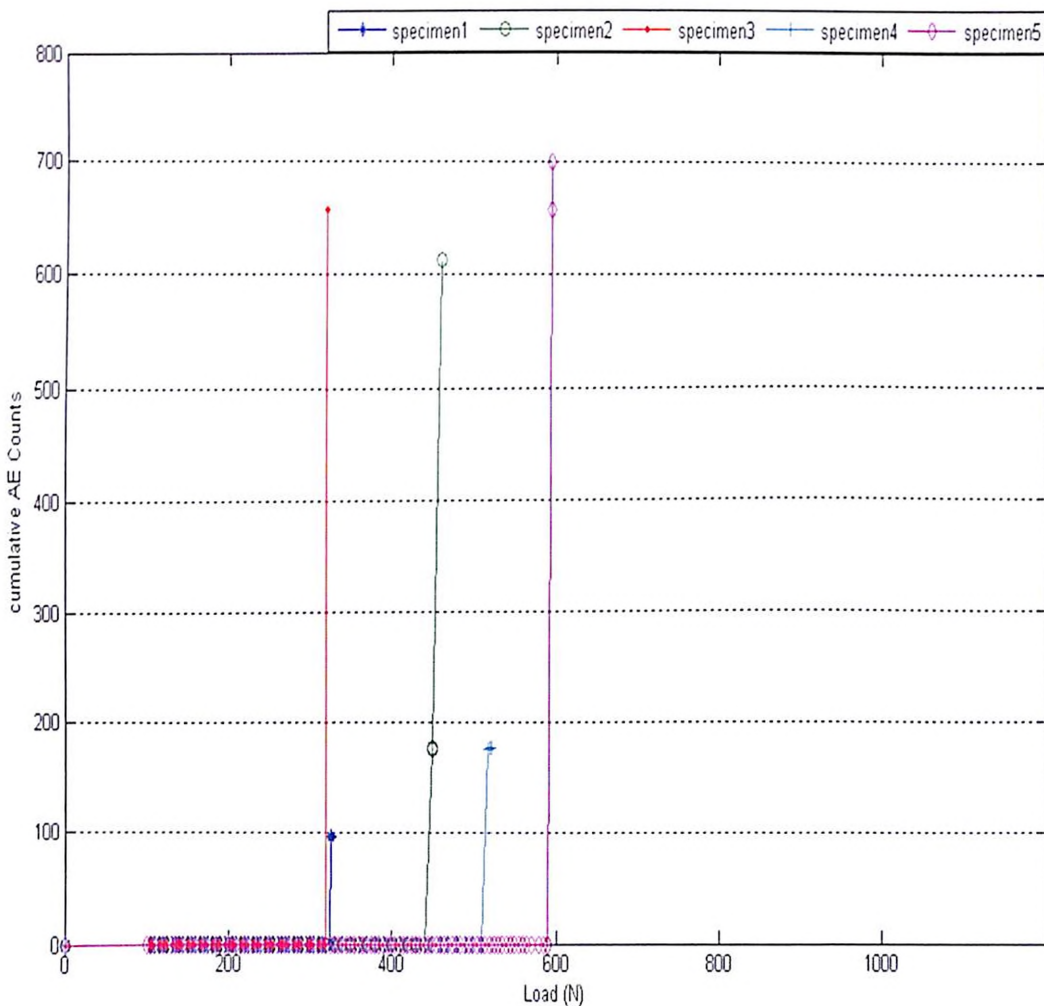


Figure 3.13 Acoustic Emission Response of Fresh Bones (S.R. = 5 mm/minute)

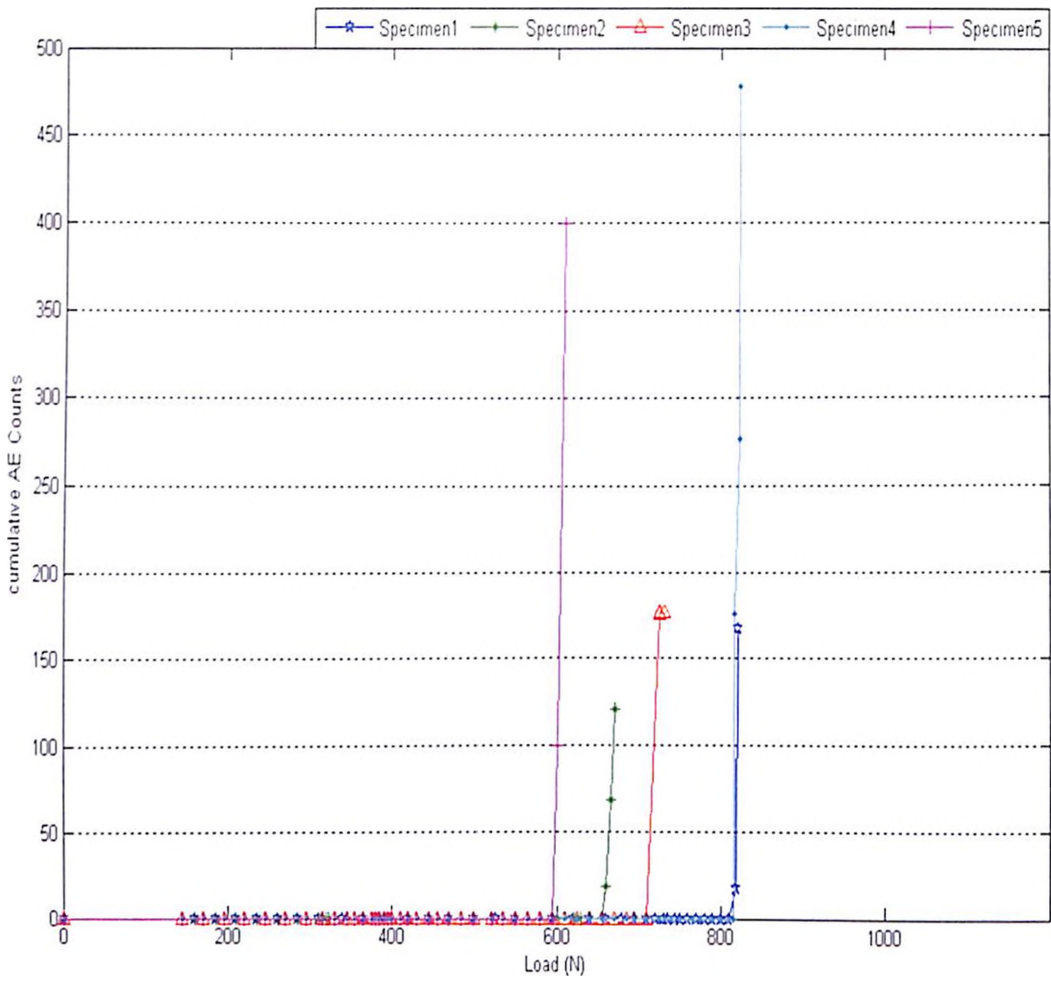


Figure 3.14 Acoustic Emission Response of Fresh Bones (S.R. = 15 mm/minute)

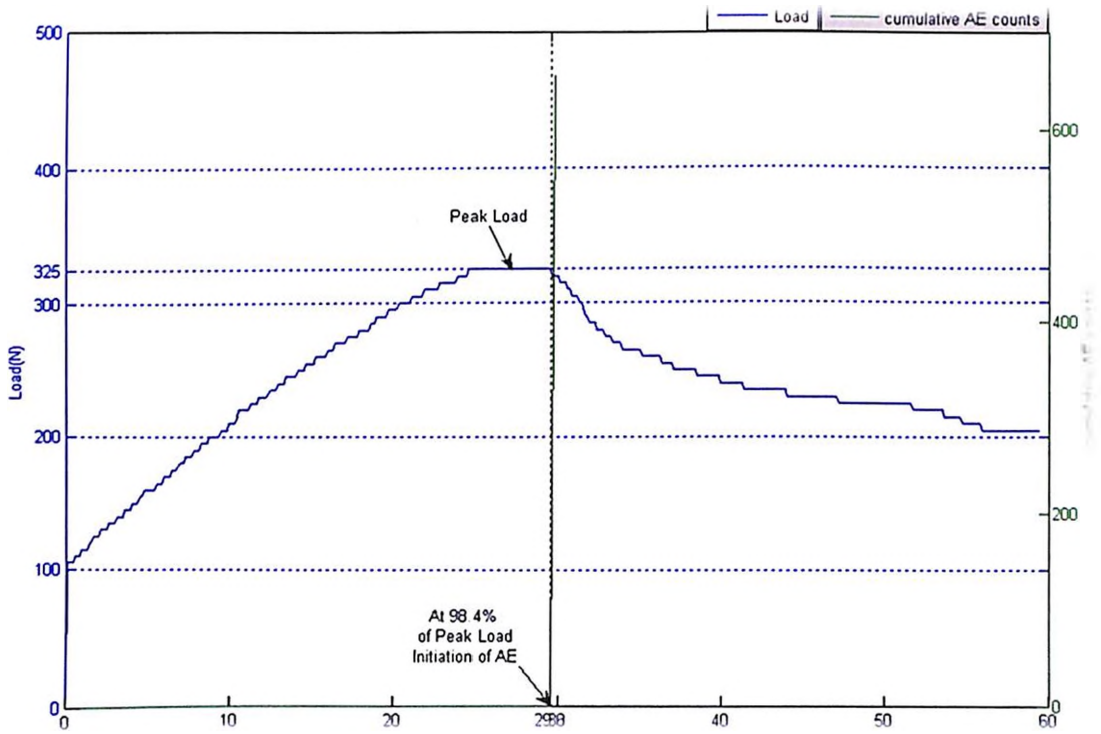


Figure 3.15 AE characteristic of fresh bone sample-1(S.R.= 5mm/minute)

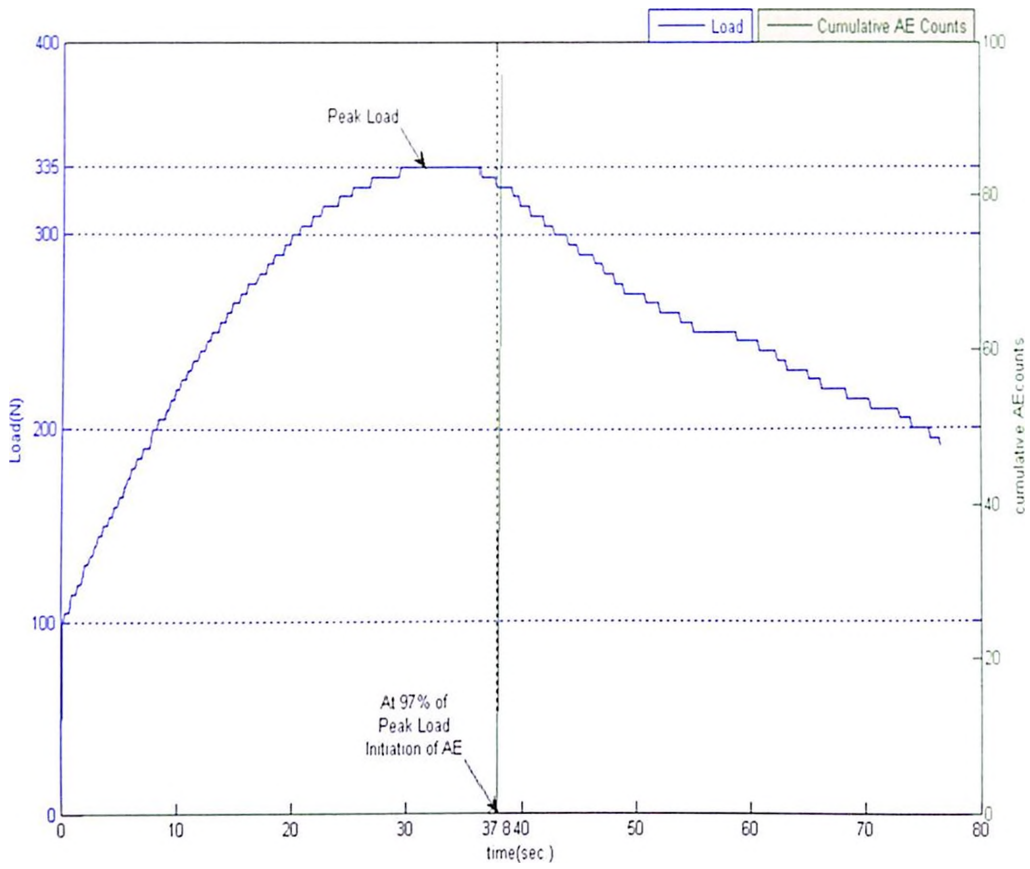


Figure 3.16 AE characteristic of fresh bone sample-2 (S.R.= 5 mm/minute)

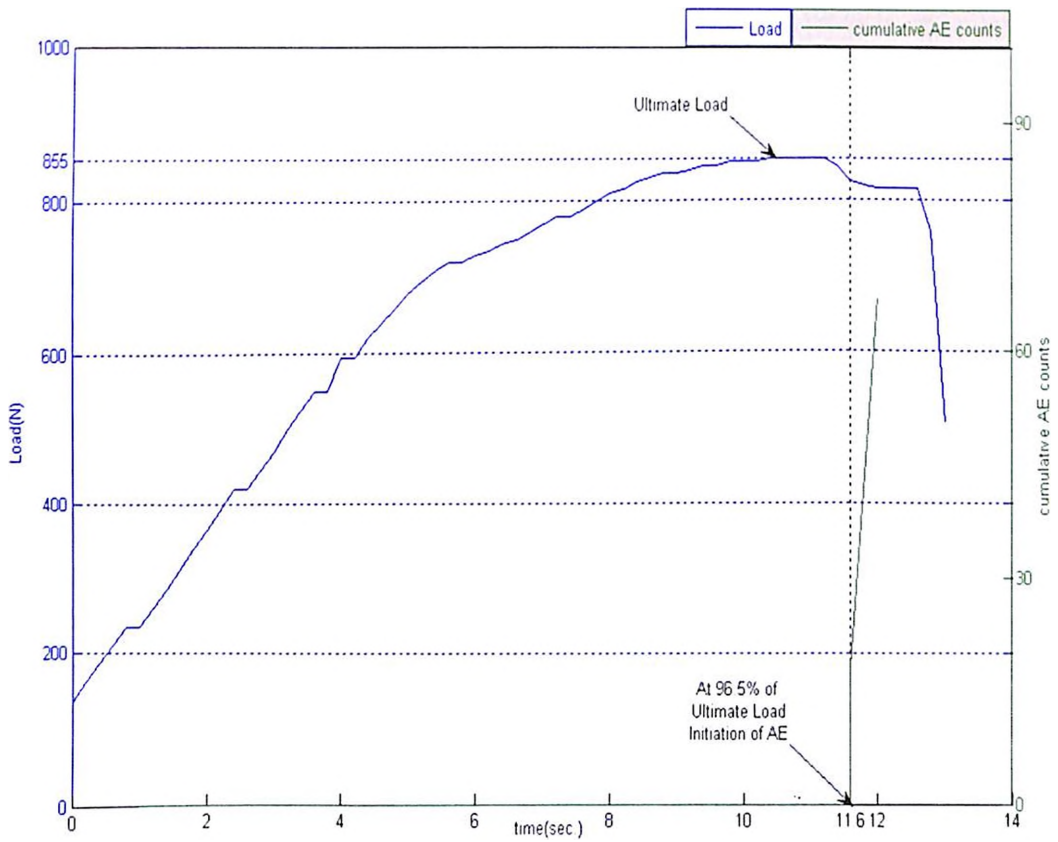


Figure 3.17 AE characteristic of fresh bone sample-5 (S.R.= 15 mm/minute)

Table 3.3 Ultimate loads of Fresh Bones under different strain rates

Failure Load (in N)	Strain Rate		p-value
	5mm/minute	15mm/minute	
Mean	415	780	p=0.0162
Standard Deviation	94.16	118.99	

No. of samples (*n*) =5

Table 3.4 Percentage of Ultimate Load at which initial AE occurred for fresh bones

Strain Rate	Mean%	Standard Deviation
5mm/minute	97.24%	0.850
15mm/minute	96.08%	2.113

No. of samples (*n*) =5

The acoustic emission response from *in vitro* studies (dry animal bones and fresh animal bones) confirms the results of previous investigators to some extent. The results differ in the context of initiation of acoustic emission in dry bone samples. The difference in the results may be probably due to the conditions of dry bone samples used for study. The flesh on the fresh bone were remove manually and then kept for drying. The first acoustic emission signal obtained was mainly due to fracture of this dried flesh left on the surface of the bones. Many other investigators ^[8, 11, 12] also reported that the AE counts not occurred before the plastic deformation. The present study also confirms that initial AE in bone occurs just before or during the failure. To clearly establish this fact a method was used in this study to simultaneously record both AE and load signals with respect to time. The results clearly indicate that initial AE occurred only in the plastic region of the stress-strain curve.

Many investigations ^[13, 14, 15] on the mechanical properties of bone proved that the ultimate stress sustained by the bone depend on the strain rate i.e. the viscoelastic nature of the bone. In this study, the acoustic emission response under two different strain rates (5 mm/minute and 15 mm/minute cross head

speed) is investigated. In both the cases initial AE occurred only during the plastic deformation or just before the failure. So the use of different strain rates doesn't have any influence on the time of occurrence of initial AE. However, the amplitude distributions of the AE counts are different for different strain rates. At higher strain rate, the high amplitude counts occurred. In the case of lower strain rate (5 mm/minute), AE counts occurred with less peak amplitude.

Though an attempt was made to test the bone under some more strain rates, due to some practical difficulties in performing tests, they were not carried out in this study. The noise coming from the testing apparatus under higher strain rates found to be a big problem. This was minimized to some extent by increasing the threshold voltage used for the AE counts processing and then selecting the floating threshold capability.

In this work, the acoustic emission characteristics were studied mainly to see the use of the same technique for the clinical applications. Though the AE technique has been established as one of the non-destructive testing technique for testing composite materials, the results from the present study indicate that it is not a safe technique (i.e. it is an almost destructive technique) for testing the bone because the initial AE occurred just before or during the permanent deformation.

3.4 CONCLUSION

The acoustic emission response of dry bovine bones and fresh bovine bones were studied. The three point bending load arrangement was used to test whole bones at two different strain rates (5 mm/minute and 15 mm/minute). The effects of strain rate on the amplitude distribution, the time of occurrence of initial AE were studied. The results from the present investigation of AE characteristics of *in vitro* bone show that the initial AE in both dry bovine bones and fresh bovine bones occurred just before or during the failure/deformation only. The strain rate value does not have any significant effect on the time of occurrence of initial AE. The acoustic emission technique cannot be used for non-destructive testing of normal bones because AE does not occur in the bone until the plastic deformation occurs.

References

1. Rubin, C. T., and Lanyon, L.E. (1982) Limb Mechanics as a Function of Speed and Gait : A Study of the Functional Strains in the radius and Tibia of Horse and Dog, *J.Exp. Biol*, 101, pp.187-211.
2. Lanyon, L.E., Hampson, W.G.J., Goodship, A.E., and Shah, J.S., (1975) Bone Deformation Recorded *In Vivo* from Strain Gauges attached to the Tibial Shaft, *Acta Orthop. Scand*, 46, pp.256-268.
3. Burr, D.B., Milgrom, C., Fyhrie, D., Forwood, M., Nyska, M., Finestone, A., Hoshaw, s., Saiag, E., and Simkin, A. (1996) *In Vivo* Measurements of Human Tibial Strains During Vigorous Activity, *Bone (N.Y)*, 18, pp. 405-410.
4. Hayes, W.C. (1978) Biomechanical Measurements of Bones, In. *CRC Handbook on Engineering in Medicine and Biology, Section B. Instruments and Measurements. Vol. I*, Feinberg, B.N. and Fleming, D.G. (eds.) pp. 333-372, CRC Press, Florida.
5. Hangud, S., Clinton, R.G. and Lopez, J.P (1973) Acoustic Emission in Bone Substance, *Proceedings of Biomechanics Symposium of the American Society of Mechanical Engineers*, pp.74, ASME, New York.
6. Wright, T.M. and Carr, J.M. (1983) Soft Tissue Attenuation of Acoustic Emission Pulses, *Trans. of ASME J. of Biomechanical Engineering*, 105:1, pp.21-23.
7. Thomas, R.A., Yoon, H.S. and Katz, J.L. (1977) Acoustic Emission from Fresh Bovine Femora, *Ultrasonic Symposium Proceedings. IEEE Cat. No. TICH12G4-ISU*, pp.237-240.
8. Netz, P. (1979) The Diaphyseal Bone under Torgue, *Acta Orthop. Scand. Suppl.*, 176, pp.1-31.
9. Fischer, R.A., Arms, S.W., Pope, M.H. and Seligson, D.(1986) Analysis of the Effect of Using Two Different Strain Rates on the Acoustic Emission in Bones, *J. Biomechanics*, 19:2, pp.416-418.
10. Burstein, A.H., Frankel, V.H. (1971) A Standard Test for Laboratory Animal Bone, *J. Biomechanics*, 4:2, pp.155-158.

11. Yoon, H.S. Caraco, B.R. and Katz, J.L. (1980) Further studies on the Acoustic Emission of Fresh Animal Bone, IEEE Trans. Sonics. Ultrasonics, SU-27, pp.160.
12. Wright, T.M., Booburgh, F. and Burstein, A.H. (1981) Permanent Deformation of Compact Bone Monitored by Acoustic Emission, J. Biomechanics, 14, pp.405-409.
13. Mc Elhaney, J.H. (1966) Dynamic Response of Bone and muscle Tissue, J. Appl. Physiol., 21, pp.1231-1236.
14. Panjabi, M.M., White, A.A., and Southwick, W.O. (1973) Mechanical Properties of Bone as a Function of Rate of Deformation, J. Bone. J. Surg., 55(A), pp.322-330.
15. Hansen, U., Zioupos, P., Simpson, R., Currey, J.D., Hynd, D. (2008) The Effect of strain rate on the mechanical properties of Human Cortical Bone, J.Biomech. Engg., 130, pp. (011011-1)-(011011-8).

CHAPTER 4

LOCATION OF FRACTURE BY ACOUSTIC EMISSION TECHNIQUE

4.1 INTRODUCTION

Acoustic emission (AE) technique is used successfully in a wide range of applications including: detecting and locating faults in pressure vessels or leakage in storage tanks or piping systems, monitoring welding and other processes, machinery monitoring, corrosion and erosion process monitoring, and analysis of partial discharges from components subjected to high voltage. As such, one of the main advantages of AE is its relative sensitivity to a range of phenomena leading to degradation, or at least those indicative of mechanical, electrical, or fluid mechanical processes.

Most currently available commercial AE systems give only a qualitative indication of the monitoring target, whether it is the presence of defects or the state of a machine or process. Quantitative or semi-quantitative approaches require the resolution of a number of key technical issues, one of which is how a signal generated from a source changes as it travels to the sensor or sensor array. This propagative nature of AE can be an advantage, because it permits location of non-continuous sources, but can also be a disadvantage if there is a source of AE 'noise' in the vicinity of the sensor array, the more so if this is continuous since it will be difficult to reject by source location. Nevertheless, there are many applications where this disadvantage can be overcome. In large structures and for most sources, AE waves propagate in more than one mode, travelling at different speeds so, for pipe applications, it is important to determine arrival times for different components of the wave and also their relative rates of attenuation. Knowledge of these two factors permits spatial reconstitution, a term used to describe the attribution of a signal recorded at a sensor array as time series at various source locations^[1-3].

AE event source location is based on the arrival times of transient signals measured at a number of transducers. If the propagation velocity is known, the

difference in arrival times for an event at sensors, a known distance apart, can be used to locate the source. There are many algorithms for source location in one, two, or three dimensions but all depend on identifying arrival time(s) and wave speed(s) of what is actually a multi-mode broadband wave in a specific material. Surgeon and Wevers^[4] noted that there are three classes of wave modes in wave theory, although only the extensional and the flexural modes can be detected in practice. Also, Inoue et. al. ^[5] showed that a three-dimensional plot of the magnitude of the wavelet transform (WT) in time–frequency space has peaks whose locations indicate the arrival times of each component of the wave. Most authors have observed that the velocity of propagation is frequency-dependent ^[2, 6, 7].

AE source location technique has been used successfully in large structures, but the concept in the small specimen like bones have not been much attempted. In this chapter, an attempt has been made to locate the fracture in dry bones using the linear location technique.

4.2 AE SOURCE LOCATION TECHNIQUES

There are various techniques to locate the source with acoustic emission technique. The two simplest source location techniques are linear location and Zonal location approach.

4.2.1 Linear Location Technique

This is the simplest form of source location for a point between two sensors as shown in Figure 4.1^[8]. The location of source from sensor S_2 can be expressed as.

$$x_2 = \frac{1}{2}(X + \Delta tV) \quad (4.1)$$

where Δt is the time lag between the signals recorded at each sensor, which can be determined in a number of different ways such as threshold the threshold cross-correlation, and WTs. V is the velocity and depends on the material and may also vary with frequency and/or mode. When the source is located at the midpoint, the time of arrival difference for the wave at the two sensors is zero. If the source is closer to one of the sensors, a difference in

arrival times is measured. To calculate the distance of the source location from the midpoint, the arrival time is multiplied by the wave velocity. Whether the location lies to the right or left of the midpoint is determined by which sensor first records the hit. This is a linear relationship and applies to any event sources between the sensors. Because the above scenario implicitly assumes that the source is on a line passing through the two sensors, it is only valid for a linear problem.

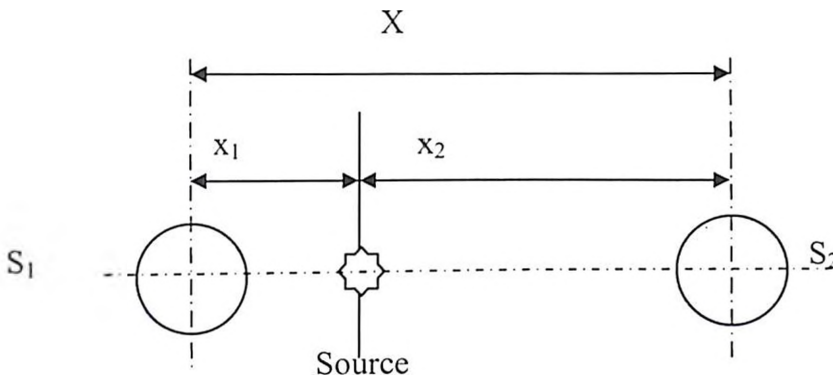


Figure 4.1 Linear source location

The principle of linear location technique is shown in Figure 4.2.

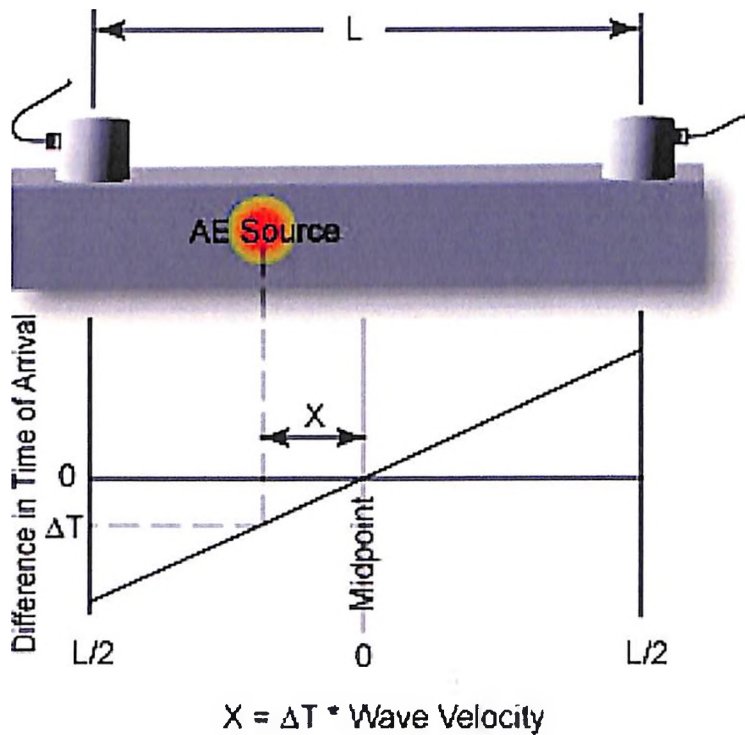


Figure 4.2 Linear Source Location measured from the mid point

When the source is at the midpoint, the wave arrives at sensors S_1 and S_2 simultaneously and the arrival of time difference is zero.

$$\Delta t = 0 \quad (4.2)$$

The greater the distance between the source from the midpoint, the greater the Δt .

The relationship is linear:

$$\Delta t = \frac{2X}{V} \quad (4.3)$$

Where X is the distance of the source from the midpoint, and V is the velocity of the sound. This relationship holds so long as the source is between the sensors. The accurate calculation of the source location requires both an accurate measurement of Δt , and an accurate calculation of velocity V .

4.2.2 Zonal Location Technique

Another approach is the zonal location approach. Zonal location is a mode where the first hit sensor of an event group is identified. This first hit sensor defines a source zone or area where that AE event emanated from.

In this chapter, an attempt has been made to locate the fracture in dry bones by linear location technique. GUI based software was developed to calculate the distance of the source from the two sensors, based on the time arrival of the signal at two sensors. The results were compared with the results obtained from the acoustic emission equipment. The equipment used has the facility of performing the linear location test.

4.3 MATERIALS AND METHODS

Dry bovine bones were obtained from the slaughter house and kept for drying in the electric oven at the temperature of 40°C - 50°C for 3-4 days, the facility available in the central animal house of Birla Institute of Technology and Science, Pilani. The Schematic diagram for AE set up used for this study is shown in Figure 4.3.

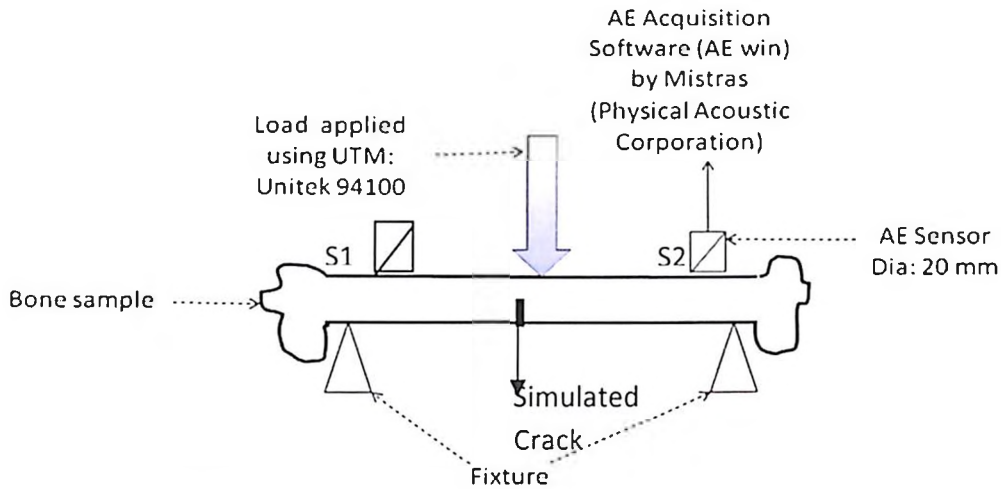


Figure 4.3 Schematic diagram for acoustic emission set up

4.3.1 Calculation of Wave Velocity

The first step in source location is to calculate the wave velocity. This was calculated with the help of timing feature available within the PAC AE equipment. The timing feature used is the first threshold crossing. In order to calculate the velocity, the procedure recommended in the instruction manual of PAC AE was adopted ^[9]. The crack was simulated in the bone in the form of cut of 2mm. Three samples were taken with the same simulated fracture, and the distance between the two sensors was varied during each experiment. As the crack was a dead defect all the natural emissions have already been emitted from it. To activate this crack, we placed the bone having the simulated crack on the bending fixture in unitek electronic UTM. Two AE sensors R15D-AA51 of Diameter: 20 mm, and frequency response of 3kHz -3 MHz was placed on the opposite surface of bone to the surface where the crack was simulated. The sensor was attached to the specimen with the help of adhesive tape. The high vacuum grease was used as a couplant between sensor and the specimen.

The distance between the two sensors was measured. Then the very small amount of bending /compression load was applied with the help of Electronic UTM for less than a second. As the source was already present the counts were obtained immediately. After receiving the first hit on both the sensors the experiment was stopped. Acoustic emission preamplifier (1220A, Physical Acoustics Corporation, U.S.A.) with the frequency response of 20-1200 KHz and

gain of 40dB/60dB was used to amplify the AE signals picked up from the specimen. The preamplifier was powered by the AE-1A Acoustic emission amplifier (PAC, USA). Preamplifier (1220A, Physical Acoustics Corporation, U.S.A.) with the frequency response of 20-1200 KHz and gain of 40 dB was used to amplify the AE signals picked up from the specimen. The results from the AE equipment were converted to ASCII files, for further processing. The actual transmit time to traverse between the two sensors was calculated (Δt), by recording the time when the first counts were obtained at the two sensors respectively. If t_1 and t_2 are the times at which the two sensors were first hit respectively then,

$$\Delta t = t_1 - t_2 \quad (4.4)$$

Then the velocity was calculated using the formula,

$$v = \frac{x}{\Delta t} \quad (4.5)$$

The same procedure was used for the other two samples, and the velocity was calculated. It was found that hardly any change in the value of Δt was there, as the distance between the two sensors could not be varied by many amounts. The length of the bone was only 110 mm. The velocity obtained was equal to 3169.48 m/s. This wave velocity was then further used to calculate the source location using the facility available with the AE equipment and also the GUI software specially (Appendix A) for linear location of fracture.

4.3.2 Linear Location of Fracture Using GUI Software

The same procedure as used in calculating the wave velocity was used in calculating the difference in the time arrival of the signal to the two sensors. The fracture/crack was simulated on the bottom surface of dry bones in the form of cut (2-2.5 mm). Then the two sensors separated at a known distance on the top surface were kept on the either side of crack as shown in Figure 4.3. The load was applied to activate the crack, and the signal was received by the two acoustic emission sensors having the frequency response of 3 kHz -3 MHz. The first signal arrival time at the two sensors was recorded. Let t_1 and t_2 are the

arrival time of first count recorded at the two sensors, then using the linear relationship as, the difference in the time arrival of the signals were calculated.

$$t_1 = \frac{x_1}{V} \quad (4.6)$$

$$t_2 = \frac{x_2}{V} \quad (4.7)$$

Subtracting equation 4.7 from equation 4.6 we get,

$$\Delta t = t_1 - t_2 = \frac{(x_1 - x_2)}{V} \quad (4.8)$$

where, x_1 and x_2 are the distance of the two sensors from the crack respectively and V is the wave velocity as calculated above. Also let the distance between the two sensors be X and

$$X = (x_1 + x_2) \quad (4.9)$$

The distance between the sensors is known to us, and in equation 4.8 t_1 and t_2 are known from the results obtained from the AE equipment. Solving equations 4.8 and equation 4.9 we can calculate the desired results as x_1 and x_2 . The GUI software specially designed for this linear location requires the input as velocity and the values of t_1 and t_2 .

4.3.3 Linear Location of Fracture using AE 2-Channel Set Up

The two sensors attached to two channels were set at known distances and entered in the general setup menu of the location mode. The location group was selected in the group section of the analysis. Then in the timing mode the primary timing feature of threshold crossing was selected. The wave velocity calculated above was entered for the further calculation. After these steps, the sensor's placements were defined in the window popped. The location of two sensors was mentioned as (0, 0) and (X, 0), where X is the distance between the two sensors in the x-direction. Then the above steps of applying the load were carried out and the results could be seen on the linear location graph.

4.4 RESULTS AND DISCUSSION

Figure 4.4 gives the linear location of the crack recorded by the AE set up. The two sensors are clearly been shown separated by 5 cm. The first sensor is positioned at (0, 0) distance, whereas the second sensor is positioned at the distance of (5, 0). Figure 4.4 shows that there is a location of source occurring between the two sensors. The location of source is nearly at the centre of the two sensors i.e. at the distance of 2.5 cm from either sensor. The result obtained from the GUI software in Figure 4.5 also confirms the result of Figure 4.4.

Figure 4.6 and Figure 4.7 give the location of the crack when it is situated somewhere between the sensors which are separated by the distance 6.5cm from each other.

The results obtained through the AE instrument in Figure 4.6 clearly shows that majority of the events has occurred at a distance of approx 3.2 cm from the first sensor , which contradicts the results to some extent obtained from the GUI software. The reason behind would be that initially the signals to the two sensors reached at the same time. As the load was increased the difference in the time arrival of the signals were noticed. As the load was increased the crack might have propagated in some direction away from one of the sensors. Thereafter the difference in time arrival of the signals at the two sensors were obtained, which were used for the calculation of source location. If the first arrival time would be chosen, which was same, we would have obtained the same results as obtained from the AE instrument.

Table 4.1 summaries the results obtained from the software for three separation distance of the two sensors.

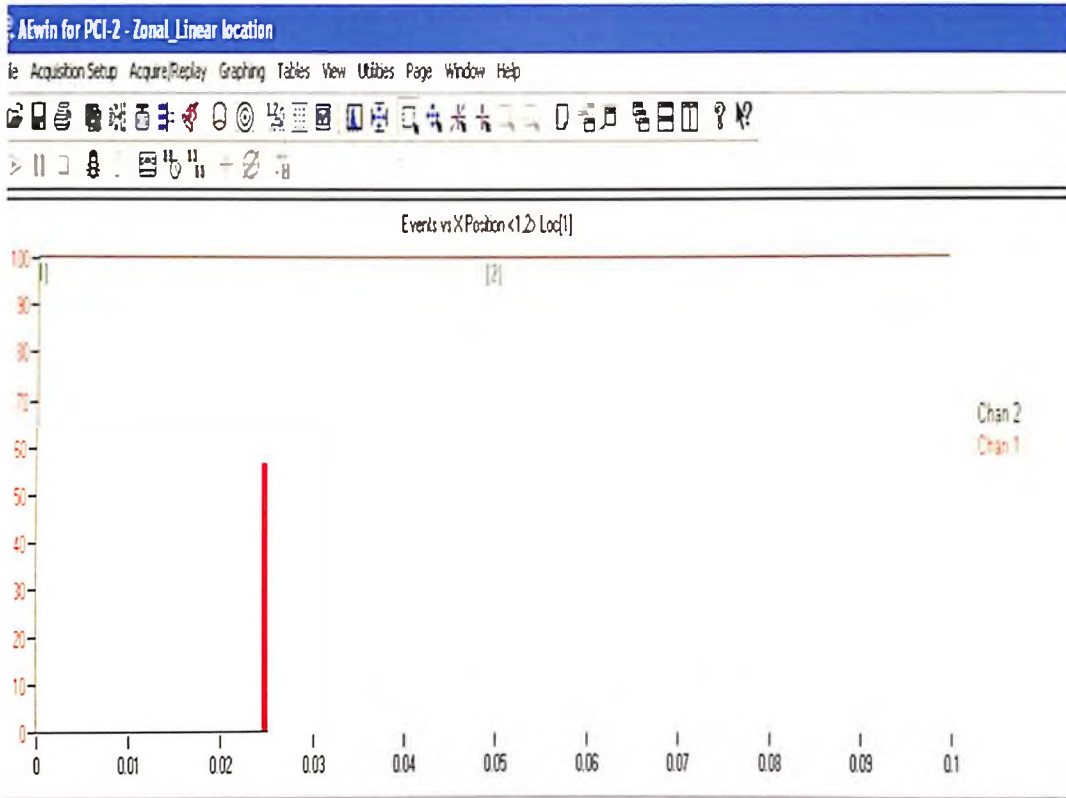


Figure 4.4 Linear location of fracture by AE-2 Channel set up
(Distance between sensors = 5 cm)



Figure 4.5 Linear location of fracture by GUI software
(Distance between sensors = 5 cm)

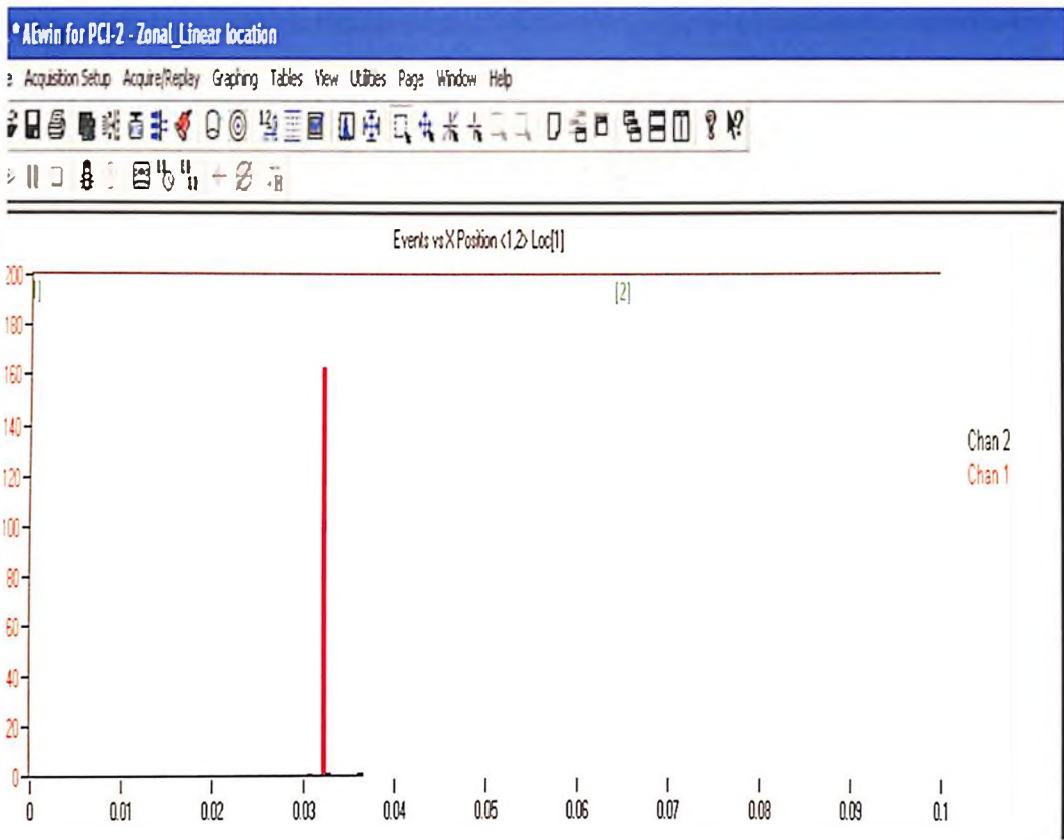


Figure 4.6 Linear location of fracture by AE-2 Channel set up
(Distance between sensors = 6.5 cm)

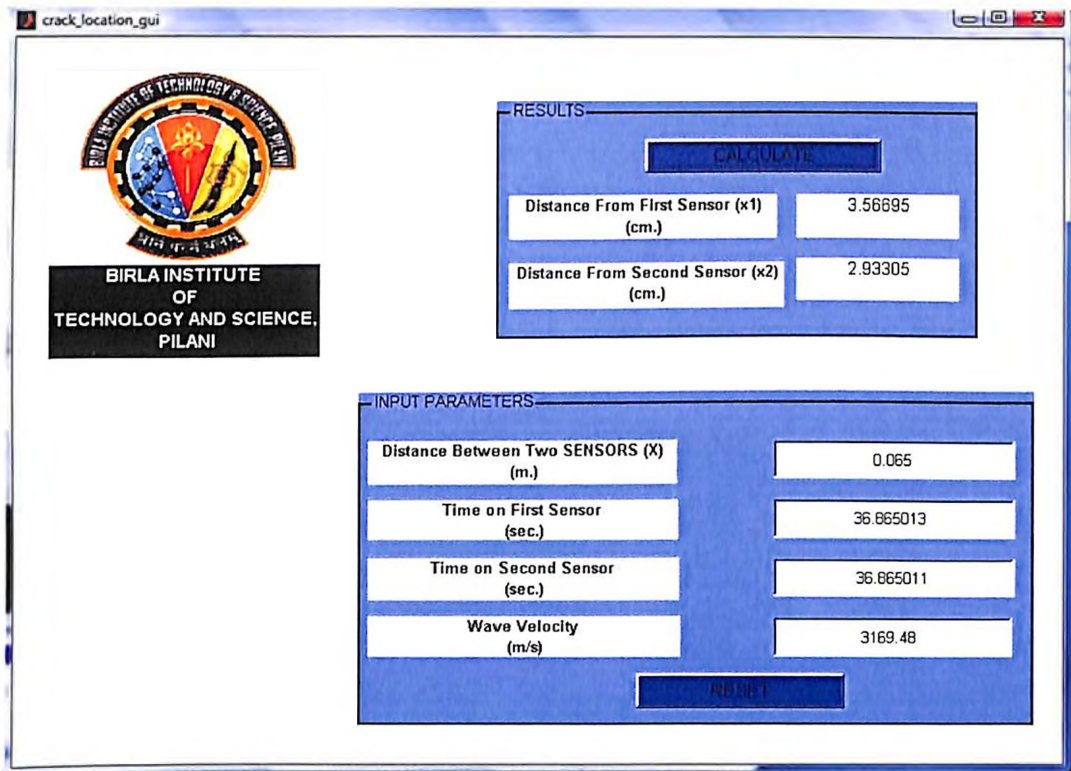


Figure 4.7 Linear location of fracture by GUI software
(Distance between sensors = 6.5 cm)

Table 4.1 Summary of results obtained from the software

Distance between sensors(cm)	Signal Arrival time at the first sensor (t_1)	Signal Arrival time at the first sensor (t_2)	Difference in time arrival $\Delta t (t_1-t_2)$	Distance of the source from the first sensor x_1 (cm)	Distance of the source from the first sensor x_2 (cm)
5	0.2382823	0.2382823	3E-06	2.5	2.5
6	51.9291948	51.9291945	0.0000003	3.047	2.9524
6.5	36.865013	36.865011	2.8E-06	3.56695	2.93305

4.5 CONCLUSION

Acoustic emission technique which has been used successfully for locating defects in large structures can also be used for locating fracture in bones. The software based linear location technique could easily be developed for locating the fracture in bones. The limitation of the acoustic emission in locating the fracture in bones clinically lies in the design of appropriate loading conditions to activate the inactive or passive defect. The linear location technique could be useful only when the source lies between the sensors. Secondly, the results would be more accurate at the long bones in comparison to the smaller bones because in case of longer bones, the wave velocity could be calculated more accurately by trial and error method i.e. measuring the velocity with different spacing between the sensors. The accuracy of the technique lies in the accuracy of the calculation of the wave velocity and the accurate measurement of arrival time of the signals. In our case, the length of the bone was only 11cm and therefore while calculating the velocity, it was found that the initial hit at the two sensors took place more or less at the same time. The difference in the arrival times of the signal was found to be zero in most of the cases. However, if a proper method of calculating the velocity could be developed, this technique could be very useful in locating the fracture in bones. The present software calculates only the difference in arrival time of the AE signals to the sensors and the location of the fracture by assuming the linear relationship between the velocity and the difference in the arrival time of the signals. If this software can slightly be modified and made more accurate in terms of higher accuracy in

calculating the arrival time of signals to the respective sensors, better discrimination would be achieved. Here in this work, the calculation of the arrival time of the AE signals to the sensors fully depends on the hardware settings. Software can be developed to minimize the effect of hardware settings on the calculation of arrival time of the signals to the respective sensors. Finally, it may be concluded that the present research does demonstrate the feasibility of fracture location in bones using acoustic emission technique. Further improvements are possible using better time interval discrimination techniques.

References

1. Nivesrangsan, P., Cochrane, C., Steel, J. A., and Reuben, R. L. (2002) AE mapping of engines for spatially located time series, 25th European Conference on AE Testing, Prague, 2, pp. 1151-1158.
2. Pollock, A. A. (1986) Classical wave theory in practical AE testing, Progress in acoustic emission III, Japanese Society of Non-Destructive Testing, pp. 708-721.
3. Holford, K. M. and Carter, D. C. (1999) Acoustic emission source location, Key Eng. Mater, pp. 167-168, 162-171.
4. Surgeon, M. and Wevers, M. (1999) One sensor linear location of acoustic emission events using plate wave theories, Mater. Sci. Eng. A, 265, pp. 254-261.
5. Inoue, H., Kishimoto, K., and Shibuya, T. (1996) Experimental wavelet analysis of flexural waves in beams. Exp. Mech., 36:3, pp. 212-217.
6. Maji, A. K., Satpathi, D., and Kratochvil, T. (1997) Acoustic emission source location using Lamb wave modes, J. Eng. Mech., 123: 2, pp.154-161.
7. Ding, Y., Reuben, R. L., and Steel, J. A. (2004) A new method for waveform analysis for estimating AE wave arrival times using wavelet decomposition, NDT&E Int., 37: 4, pp.279-290.
8. Miller, R. K. and McIntire, P. (1987) Non-destructive testing handbook. Acoustic emission testing, 2nd edition, 5 (American Society for Non-destructive Testing, New York).
9. Physical Acoustic Corporation (2003) PCI-2 based AE system user's manual, Princeton Junction, NJ, pp.23-31.

CHAPTER 5

ASSESSMENT OF *IN VITRO* BONE CONDITION BY ACOUSTO- ULTRASONIC TECHNIQUE

5.1 INTRODUCTION

The basic idea for Acousto-ultrasonic (AU) approach came in the year 1976 from the work of Egle and Brown ^[1] who investigated stress wave simulation by using various excitation methods. Vary and his colleagues ^[2-4] advanced the technique by using ultrasonically simulated stress waves and acoustic emission analysis method to evaluate defect states and mechanical properties ^[2-3]. Acousto-ultrasonic technique is still in developmental stage. Though initial work was done in late seventies, major improvements and applications of advanced digital signal processing technique were made only in the last few years. Acousto-Ultrasonic technique denotes the combination of certain aspects of acoustic emission (AE) and ultrasonic materials characterization methodology ^[5]. Unlike AE, Acousto-Ultrasonic technique is not concerned with flaw location and characterization; instead it deals primarily with the assessment of integrated effect of diffused defect states and population of sub critical flaws. In this technique discrete ultrasonic pulses are injected in to the material using an ultrasonic pulser and the ultrasound is allowed to interact with the material. Due to this interaction of ultrasound with the internal features of the material, the resultant waveform provides a modulated signal characterizing the material quality. An acoustic emission sensor is then used to pick up this resultant waveform. The signal thus obtained is suitably processed to provide the measure of quality of the material under test. Unlike the acoustic emission technique, this technique is truly non-destructive, wherein only application of low intensively pulses are made and that too only for few seconds to get proper evaluation of the specimen. Due to its truly non-destructive nature and also its ability to evaluate the mechanical performance of materials under test, makes this technique far more suitable for the non-invasive assessment of bone condition.

In the present study the acousto-ultrasonic technique's clinical applications are investigated. But for any technique which is going to be used for clinical applications, the first and most important requirement is good reproducibility. The good sensitivity is also another important requirement for any clinical tool. So a study was undertaken to see the factors affecting the reproducibility and the sensitivity of the AU technique and also to find the ways to improve them.

5.2 A CRITICAL ASSESSMENT OF ACOUSTO-ULTRASONIC TECHNIQUE

Acousto-ultrasonic technique is one of the promising non-destructive testing techniques which found its applications mainly in the field of composite materials. Many researchers reported the close correlation between acousto-ultrasonic measurements and the mechanical properties of the materials^[6-9]. But the use of the same technique outside the laboratory, by actual users didn't meet with success due to poor reproducibility problem^[10]. Also the instrument settings have to be selected very carefully to get better sensitivity from this technique. These problems were studied previously by researchers^[11] but still nothing fruitful has been done to minimize the errors and to increase the sensitivity.

5.2.1 Modified Acousto-Ultrasonic Technique

In the conventional acousto-ultrasonic technique, the stress wave factor is measured by the formula $g \times r \times n$ ^[11], where g is gain setting, r is repetition rate and n represents no. of counts. This method of calculating the SWF is arbitrary and depends on the instrument settings. To make the AU measurements more accurate and also to make it free from most of the instruments settings, here a new and modified AUT is developed. Here, instead of ringdown counts, and the peak voltage of waveform, the energy content of the acousto-ultrasonic signal is used for the better estimation of the signal.

Energy Measurement of AU Signal

The stress wave factor for the research work carried out using AU technique is taken as the energy content of AU signals. The energy content is given by formula^[12]

$$\text{Energy integral} = \text{SWF} = \int_{t_1}^{t_2} [v(t)]^2 dt \quad (5.1)$$

where $v(t)$ is the amplitude distribution with respect to time.

To calculate the energy a MATLAB coding was developed [Appendix B]. The big advantage of using this method is that there is no need to specify the threshold voltage for calculating the SWF. However it is necessary to specify the time intervals of the integrals, which correlate best with the particular flaw states or material properties of the interest. The modified AUT developed here for AU signal processing could be used to check the sensitivity of the instrument by varying the gate width values. Hence it makes the instrument less dependent on hardware settings specially in choosing the gate width values. Although the energy integral method for calculating the SWF doesn't need the threshold voltage to be specified but the selection of proper threshold is necessary to eliminate noises and henceforth to receive the signal of interest. The change of threshold would definitely change the energy content of the recieved signal.

5.2.2 Reproducibility of the Acousto-Ultrasonic Technique

Adequate reproducibility is particularly more important for Acousto-ultrasonic technique. This means that an Acousto-ultrasonic measurement of a test object of acceptable and uniform quality level must give consistent readings within narrow limit. The experimental set-up shown in figure 5.1 was used for entire research work carried out using acousto-ultrasonic technique.

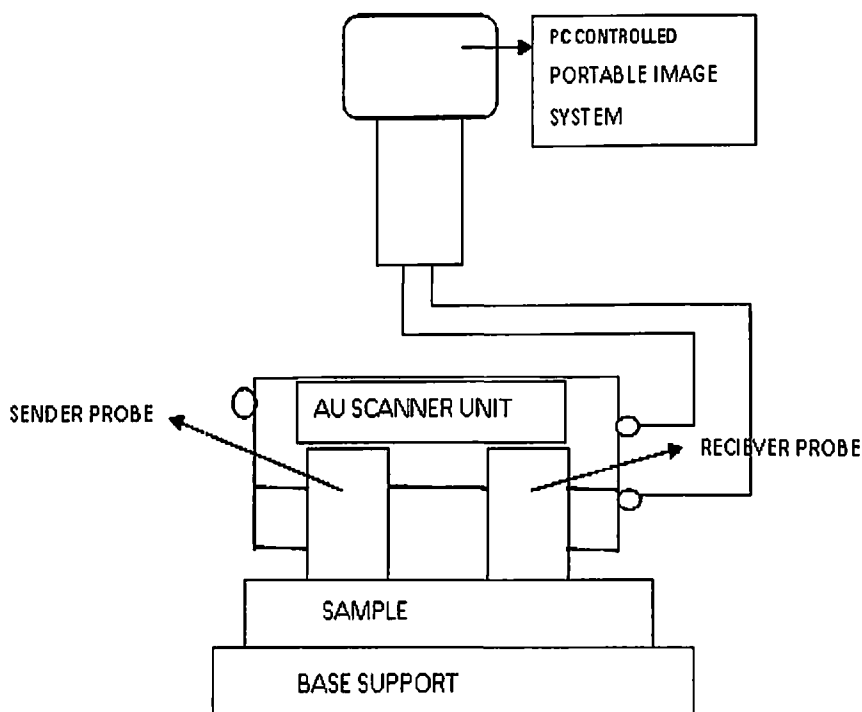


Figure 5.1 Schematic diagram of Acousto-Ultrasonic Unit

5.2.2.1 Materials and Methods

To analyze the problem of reproducibility a series of 15 tests were conducted with the same specimen (Glass Fiber Reinforce composite) by every time placing the AU sensors at the same location and removing them [figure 5.2]. The AU rolling scanner unit consists of a spring -loaded; wheeled rolling pulser transducer assembly which outputs acoustic bursts in to the structure. Meanwhile a second spring loaded wheeled rolling receiver transducer 1 inch away, detects and conditions the structure-modified signals through an on-board preamplifier (Gain: 40dB) to the pocket AU unit.

The instrument settings were kept same for all the 15 tests. The noise level was brought down to approximately 25% of the full scale with the facilities available within the unit. The input settings for all the tests are mentioned below in table 5.1.

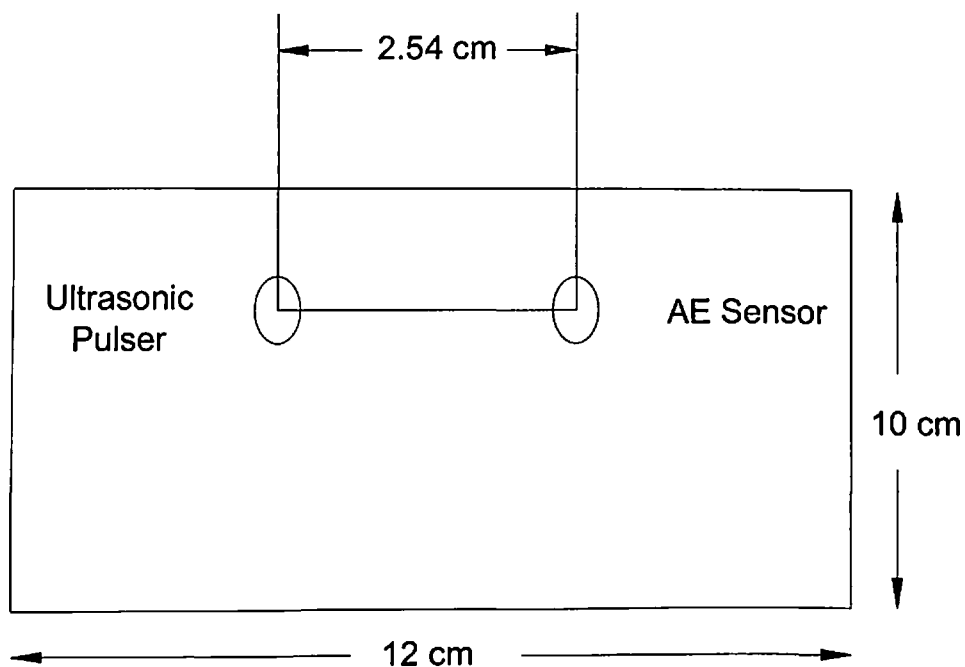


Figure 5.2 Positioning of Transducers on GFRP Specimen for AU Measurements

The A-scan data obtained for the AU unit was converted in to the ASCII code and the readings were saved in the note pad file for further processing.

Table 5.1 Input Settings for testing Reproducibility of AU measurements

Pulser mode	swept
Start frequency	100kHz
End frequency	250 kHz
Low pass filter	1000 kHz
High pass filter:	100 kHz
Window delay:	0.0 μ sec
Window length	200 μ sec
Gate start	55 μ sec
Gate length	134 μ sec
Gate threshold	120 mV

5.2.2.2 Results and Discussions

Statistical Analysis

Mean of SWF = 9.498

Standard deviation = 0.302

%Coefficient of variation in SWF = (standard deviation/mean) x 100 = 3.18%

The percentage coefficient of variation in the results of SWF was found to be 3.18%, which is found to be acceptable for clinical use [figure 5.3].

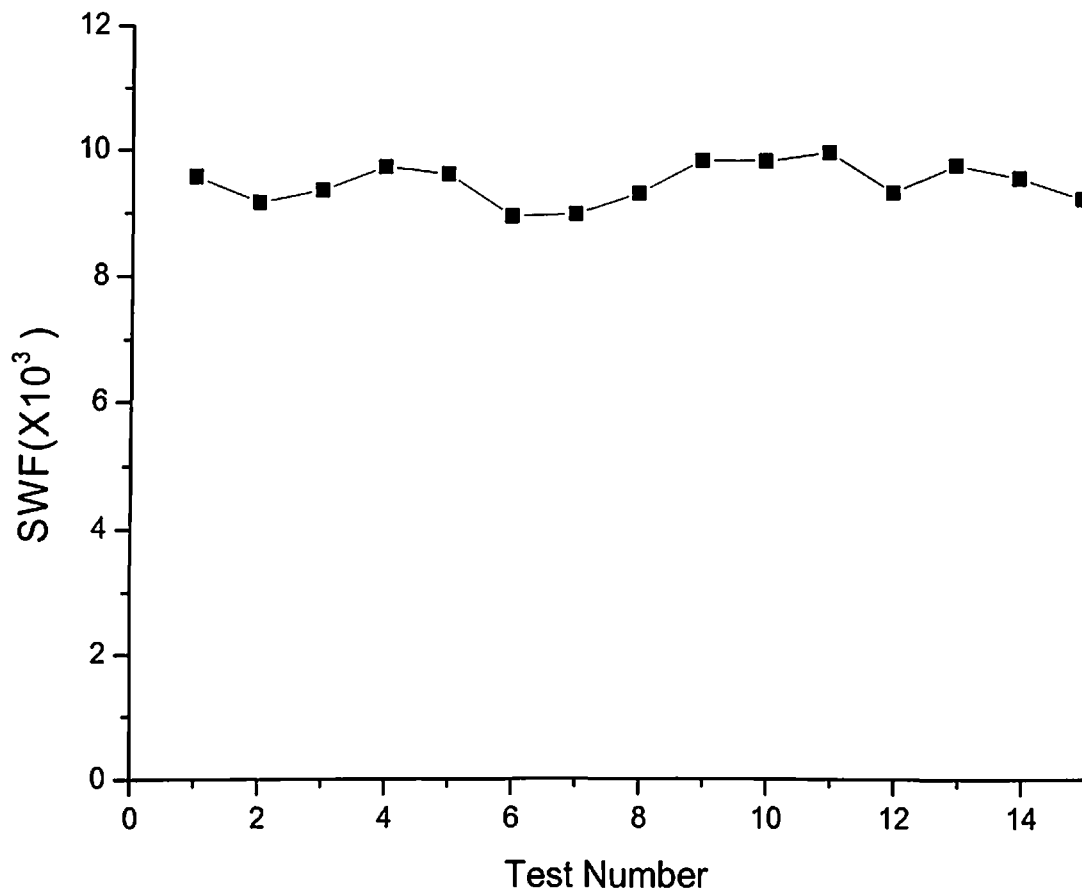


Figure 5.3 Reproducibility of SWF in Acousto-ultrasonic Measurements

5.2.2.3 Conclusions

The results of the study indicate that the better reproducibility can be achieved by maintaining proper contact between the sensors and test specimen. The proper contact can be achieved by maintaining constant contact pressure on the scanner by hand. The unit is spring loaded which assures that when the scanner is pressed against the specimen surface, the constant contact pressure is maintained. The percentage of coefficient of variation was found to be less than 5% which can be accepted for clinical application.

5.2.3 Sensitivity of the Acousto-Ultrasonic Technique

Like reproducibility, the sensitivity is also equally important for the success of Acousto-ultrasonic technique. By sensitivity we mean that the SWF value for the defective specimen must be significantly different from the "baseline" defined by the acceptable quality material.

5.2.3.1 Materials and Methods

To check the sensitivity of AUT a series of tests were conducted with GFRP composite laminate as test specimen. Defect was simulated in the very small area of laminate by subjecting them to impact damage. This was done by dropping 1 kg weight falling from 30 cm at the centre of the specimen. This was repeated 10 times producing a small indentation on the top surface [figure 5.4]. The ultrasonic pulses were injected to the specimen using ultrasonic pulser and the receiving AE sensors were used to receive the modified signals. The same input settings were used for this study as used during the test for reproducibility.

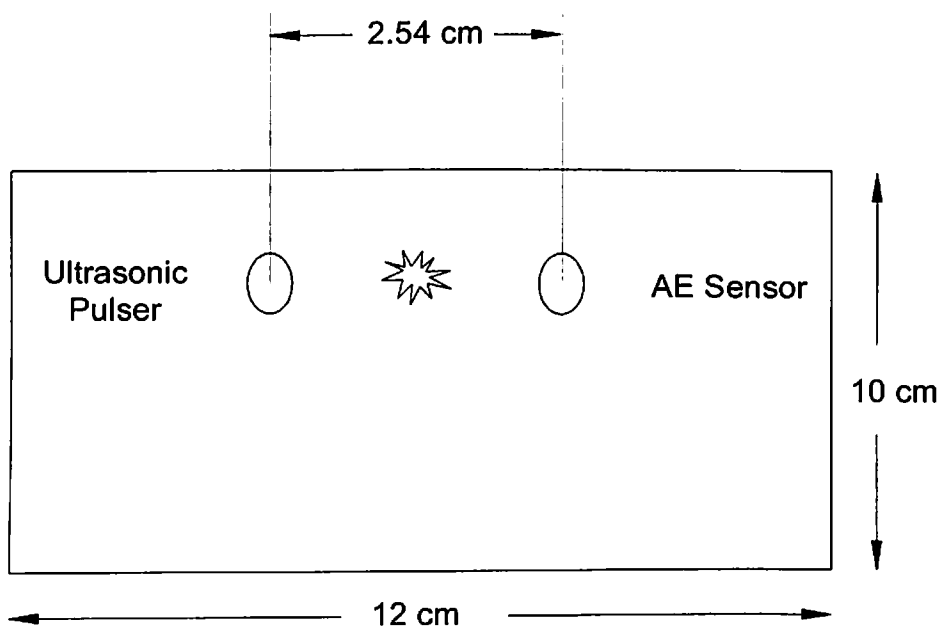


Figure 5.4 GFRP Specimen with small indentation at the centre

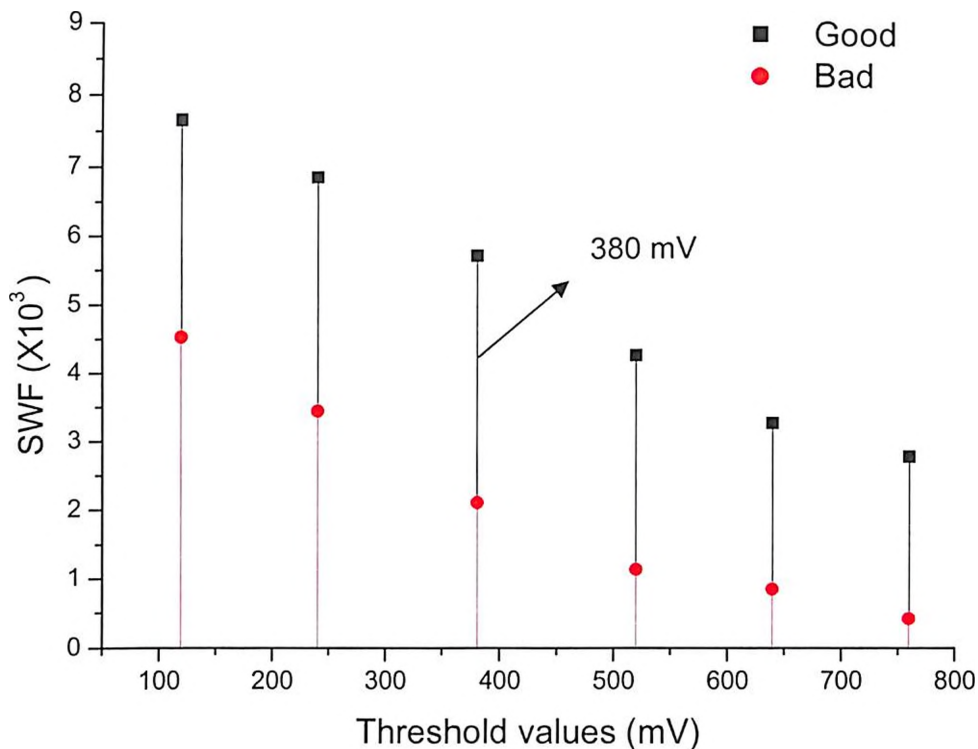
The sensitivity is mainly dependent on threshold settings and the gate width values. Hence first different threshold settings were used to find out which one gave better sensitivity for the identification of damage. Thereafter the effects of different gatewidth values were tested for the most sensitive threshold to find out which one correlates best with the damage. Table 5.2 shows the gate width values at which the specimens were tested.

Table 5.2 Gate width values for testing the sensitivity of AU measurements

First Range of Gate (t_1 micro seconds)	Second Range of Gate (t_2 micro seconds)	Gate Width ($t_2 - t_1$) micro seconds
44	196	152
30	210	190
50	265	215
60	300	240
1	400	400

5.2.3.2 Results and Discussions

The results of sensitivity dependent on threshold values are shown in Figure 5.5. It's clear that the threshold setting at 380 mV gives better sensitivity. Figure 5.6 shows the detection of damage at 380 mV threshold setting. Figure 5.7 shows the different gatewidth values chosen for the signal received at threshold of 380 mV. It was found that the gate width value of 240 microseconds gave better sensitivity.

**Figure 5.5 SWF of Good Area and Bad Area at different Threshold values**

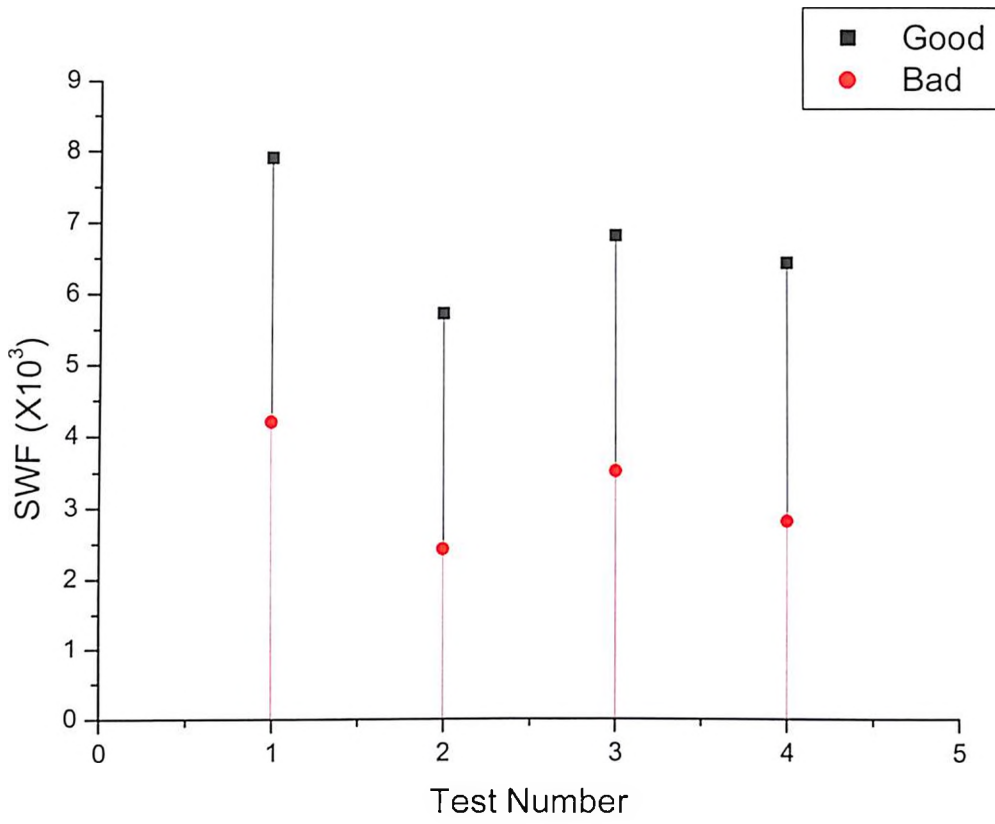


Figure 5.6 AU measurements with 380 mV threshold setting

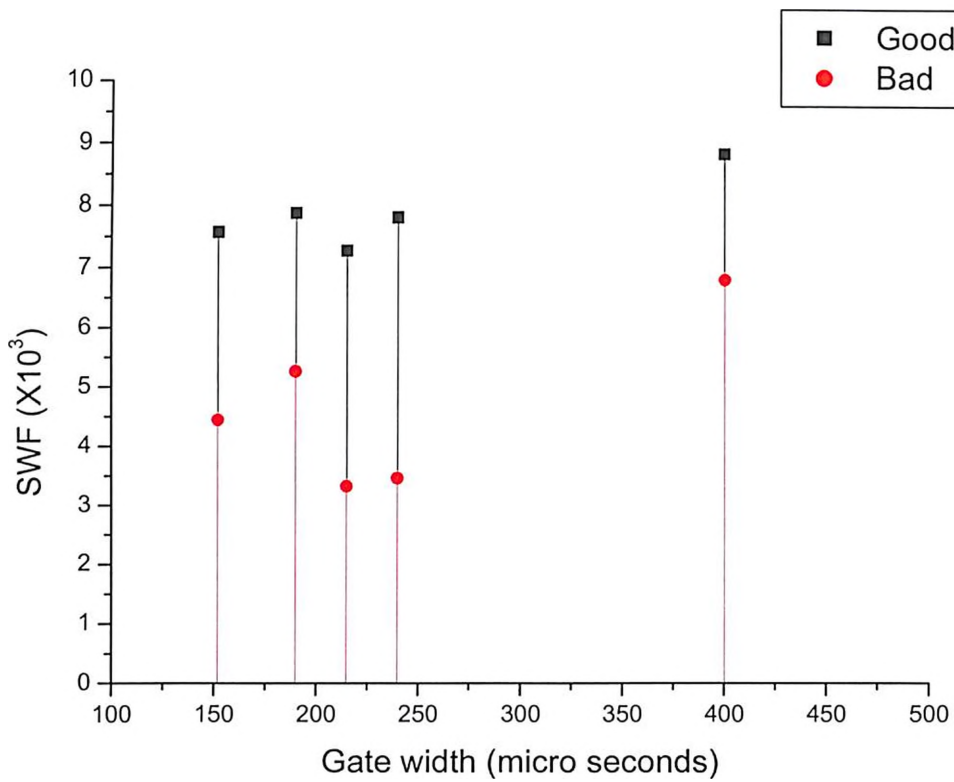


Figure 5.7 SWF of Good Area and Bad Area at different Gate width Values
(Threshold 380 mV)

5.2.3.3 Conclusions

The better sensitivity can be achieved by careful selection of the threshold setting and the gate width value used for the Acousto-ultrasonic measurements. Hence the modified Acousto-ultrasonic technique which is software based could easily be used to achieve better sensitivity by analyzing different gate width values. The importance of software based signal processing lies in that it is free of hardware dependence of the equipment in choosing the gate width values.

5.3 *IN VITRO* ANALYSIS BY ACOUSTO-ULTRASONIC TECHNIQUE

5.3.1 Materials and Methods

The structure of bone is very much similar to engineering composite materials and is therefore advantageous to use a non-destructive testing technique, which has already proved its usefulness in the field of composite materials testing. As Acousto-ultrasonic technique has already proved its usefulness for composites, the study was conducted initially by testing glass-fibre reinforced plastic composite rods (8 mm dia). The defect in these rods was made in the form of a cut. The effect with the increasing depth of cut was also studied. Thereafter the analysis was done for both dry and fresh bovine bones. The acousto-ultrasonic measurements were taken from the whole bone specimens from both categories. The Acousto-ultrasonic measurements were made before and after simulated defect in bone specimens. The defect was made in the form of cut in the bone specimens. The experimental set up shown in Figure 5.1 was used for the *in vitro* study. The signal analysis was done through a software program (developed in MATLAB 6.5). The stress wave factor was taken as the energy content of the signal as mentioned above. The baseline noise (almost 25%) was eliminated by the facility available within the instrument. The pulsar was excited at a fixed frequency of 250 kHz and the duration of the signal chosen was 100 μ s. The modulated signal after travelling through the specimen was picked up by acoustic emission sensors. The digital signals obtained were then transferred to PC for signal quantification. The dry bones were also put under bending test in an electronic UTM for studying the correlation between mechanical strength of bones and acousto-ultrasonic parameter.

5.3.2 Results and Discussions

5.3.2.1 Acousto-Ultrasonic Measurements on Composite Specimens

The fracture was made in the form of a cut in a glass-fibre reinforced plastic composite rod. Figure 5.8 shows the changes in the values of SWF for both good and bad specimens. Table 5.3 summarizes the result obtained. The T-paired test was also performed to check the probability of significance of the results obtained. The SWF was significantly reduced after the simulated fracture was introduced in the specimen. A good quality material without any major defect transmits the stress waves better than the material with defect. Since the stress wave factor is a measure of the ability of the material to transmit the stress waves, its value was reduced once a disturbance in the stress wave transmission in the form of fracture site was introduced in the composite specimen.

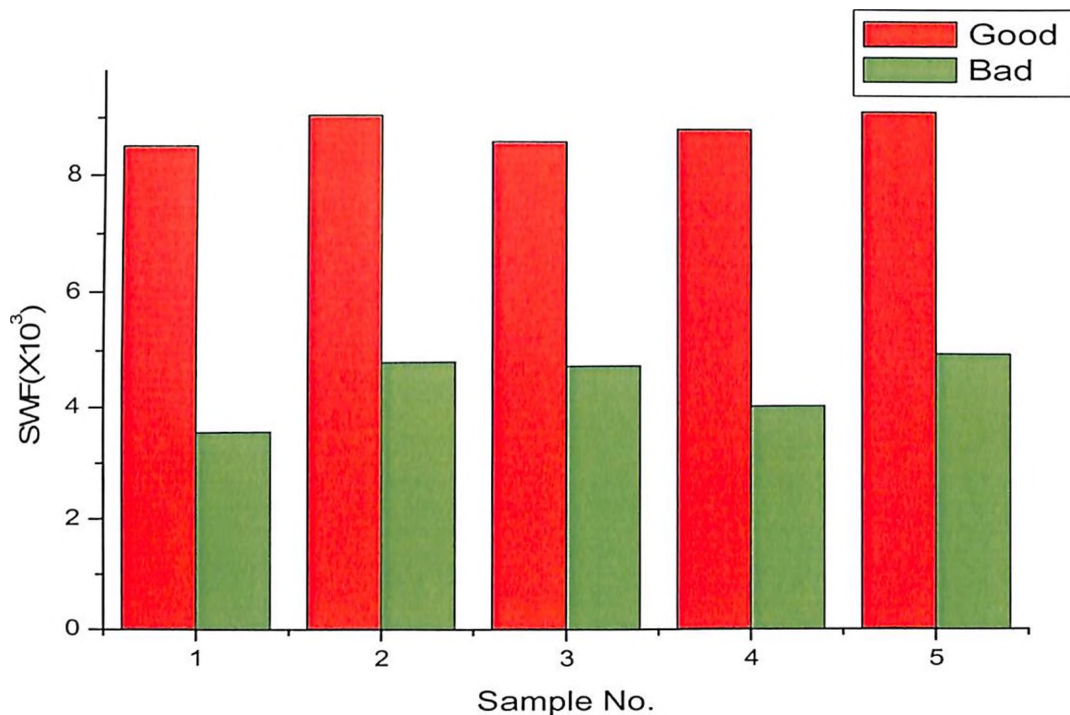


Figure 5.8 Change in the value of SWF (Composite rod specimens)

Table 5.3 Acousto-Ultrasonic measurements from Composite specimens

Material	Stress Wave Factor		
Composite rod	Good	Mean = 8878	Standard Deviation = 378.84
	Bad	Mean = 4552	Standard Deviation = 693.88
P < 0.0001, N=5			

Figure 5.9 shows how the cuts of different depths have affected the ability of material to transmit the transient waves. It shows the relation between the measured SWF and the depth of cut made in the rod. There is a good correlation ($R = -0.94$) existing between these two parameters

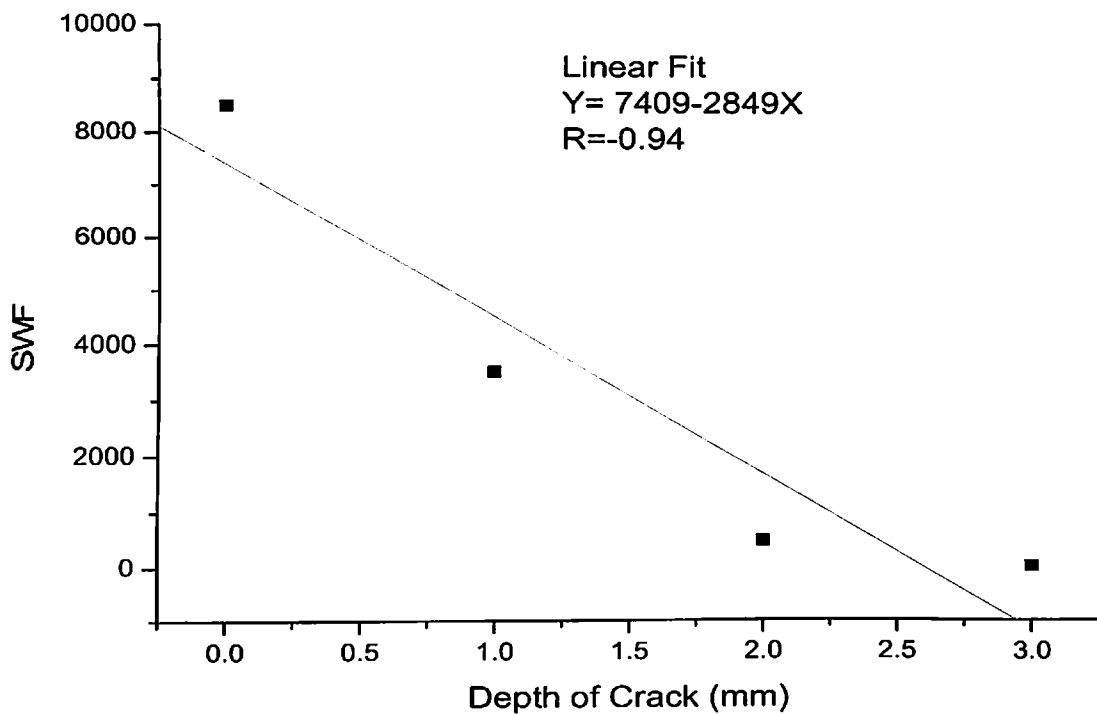


Figure 5.9 Change in the value of the SWF with the depth of cut for composite specimens

5.3.2.2 Acousto-Ultrasonic Measurements on Dry Bones

The same experimental procedures were adapted as in the case of composite materials. The bones were fractured in the form of a cut. Figure 5.10 and Figure 5.11 show the waveform for both normal and fractured bone in one of the sample.

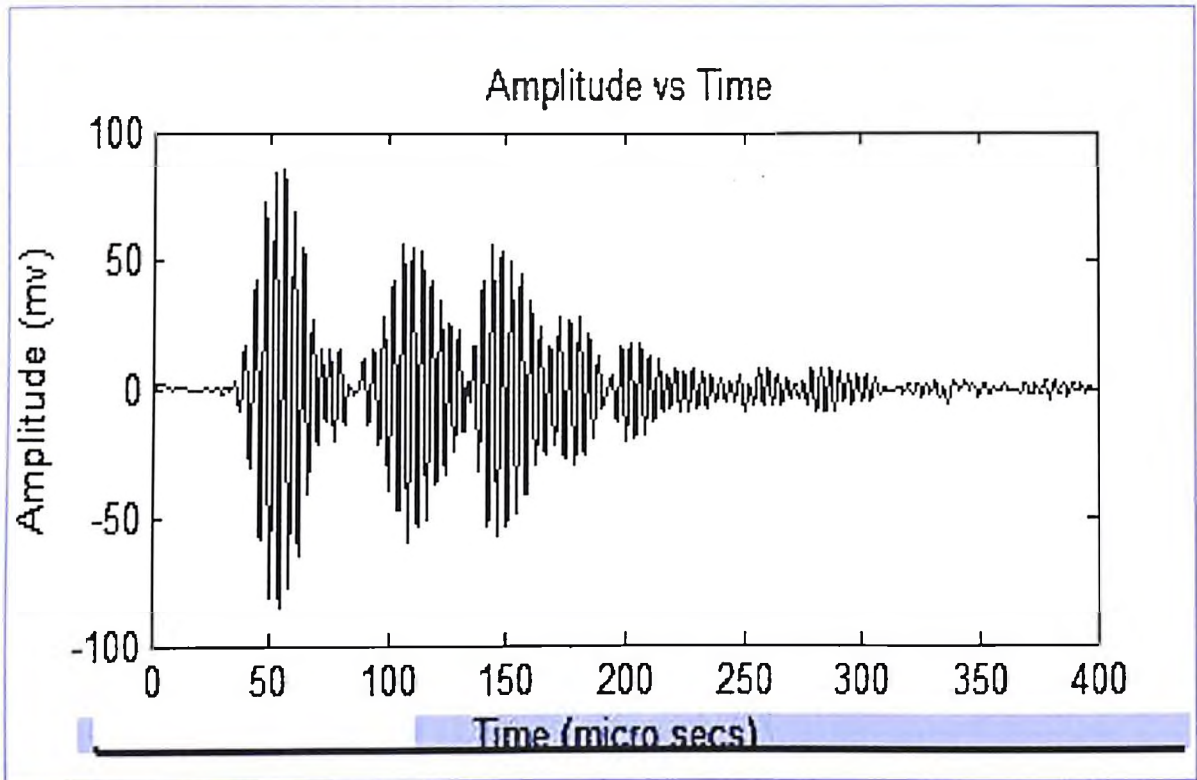


Figure 5.10 A-waveform for normal dry bone (sample1)

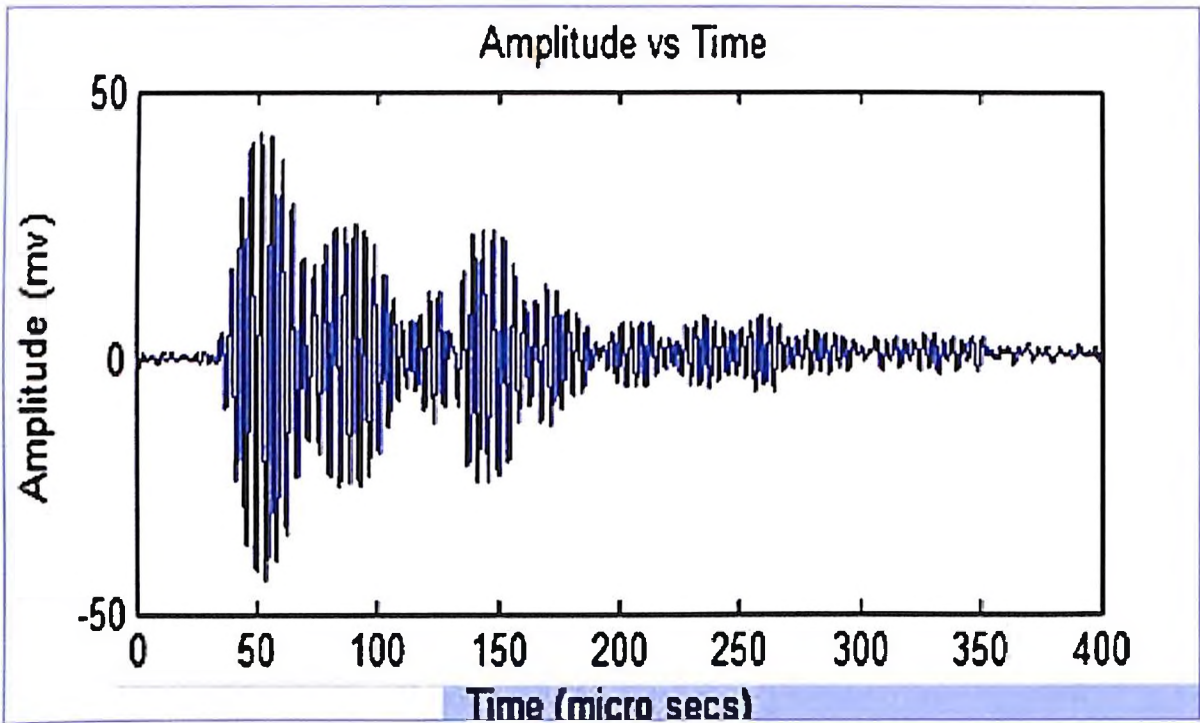


Figure 5.11 A-waveform for fractured dry bone (sample1)

Figure 5.12 shows the Acousto-ultrasonic measurements made before and after the simulated fracture were made in dry bones. Table 5.4 summarizes the result obtained from the *in vitro* study of dry bones. The T-paired test was also performed to check the probability of significance of the results obtained. The same observations were noted as in the case of composite specimens. SWF was significantly reduced after the simulated fracture was introduced in the bone specimen.

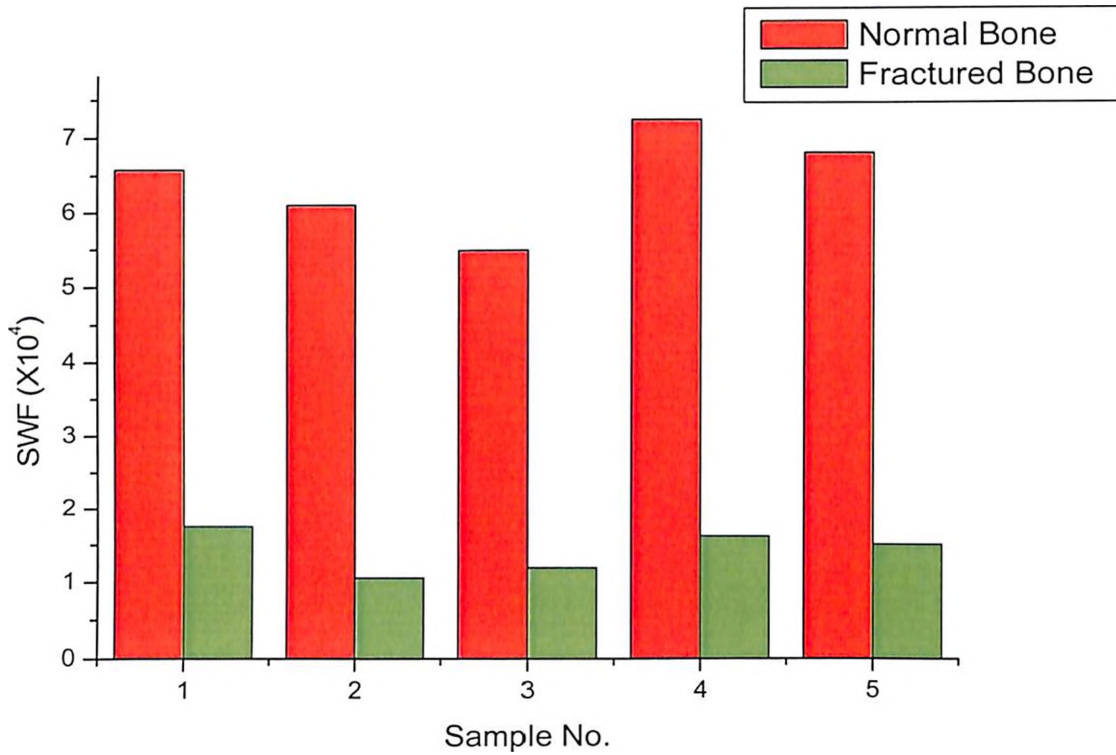


Figure 5.12 Change in the value of SWF (In Dry Bone)

Table 5.4 Acousto-Ultrasonic measurements from dry bone specimens

Material	Stress Wave Factor		
	Dry Bones	Normal	Mean= 6.9060
	Fractured	Mean= 1.3060	Standard Deviation = 0.5087
P < 0.0007, N = 5			

Figure 5.13 shows the decrease in the peak amplitude of the signal after the crack is simulated in the bones. The peak amplitude could also be used for the quantification of acousto-ultrasonic signals. The decrease in the amplitude of the

signal results due to the attenuation of the signal by the crack surface. Table 5.5 summarizes the result obtained by taking the peak amplitude as the factor for quantifying the signal. Here also the significant results are obtained.

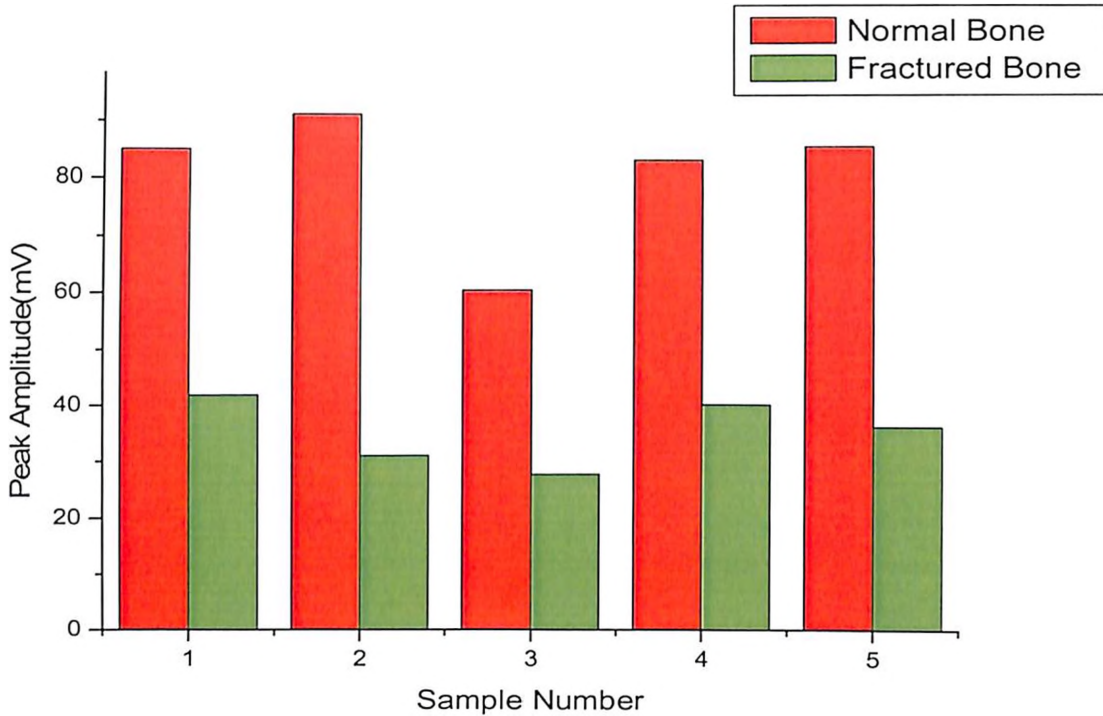


Figure 5.13 Change in the value of peak amplitude (In Dry Bone)

Table 5.5 Acousto-Ultrasonic measurements from dry bone specimens

Material	Peak Amplitude		
	Dry Bones	Normal	Mean= 81.020
Fractured		Mean= 35.120	Standard Deviation =6.026
P < 0.0005, N=5			

Figure 5.14 and Table 5.6 shows how the cuts of different depths have affected the ability of material to transmit the transient waves. It shows that both the SWF and the peak amplitude significantly decreases with increase in depth of cut made in bone.

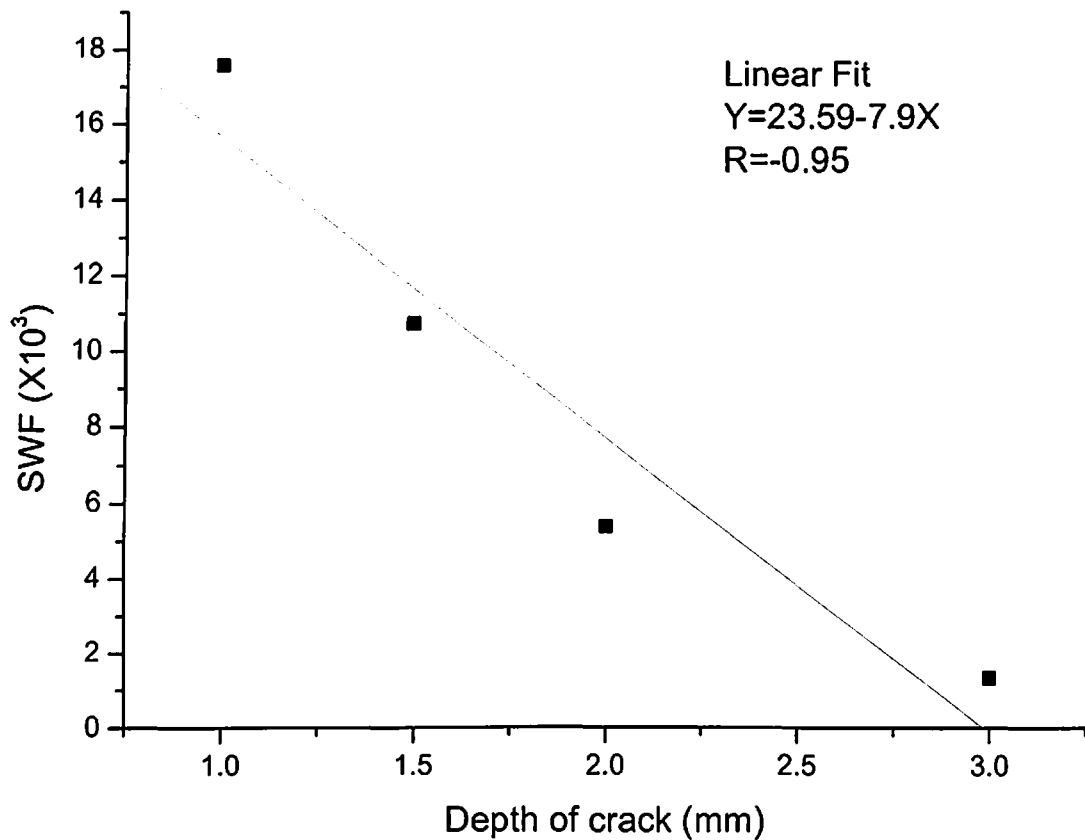


Figure 5.14 Change in the value of the SWF with the depth of crack for dry bone

Table 5.6 Change in the value of the peak amplitude with the depth of crack for dry bone

Depth of Cut (mm)	Peak Amplitude(mV)
1	27.4
1.5	19.1
2	14.9
3	10.8

The attempt was also made to correlate the flexural strength of bone with the SWF. The dry bones were tested under three point bending on an electronic universal testing machine. Before testing for flexural strength, the SWF were measured for all the samples used. Here also good correlation was found between the two measured parameters. Figure 5.15 shows the relation between the SWF and the flexural strength of specimen. Figure 5.16 also give the clear indication that peak amplitude of the signal could also be correlated with the strength of the bone.

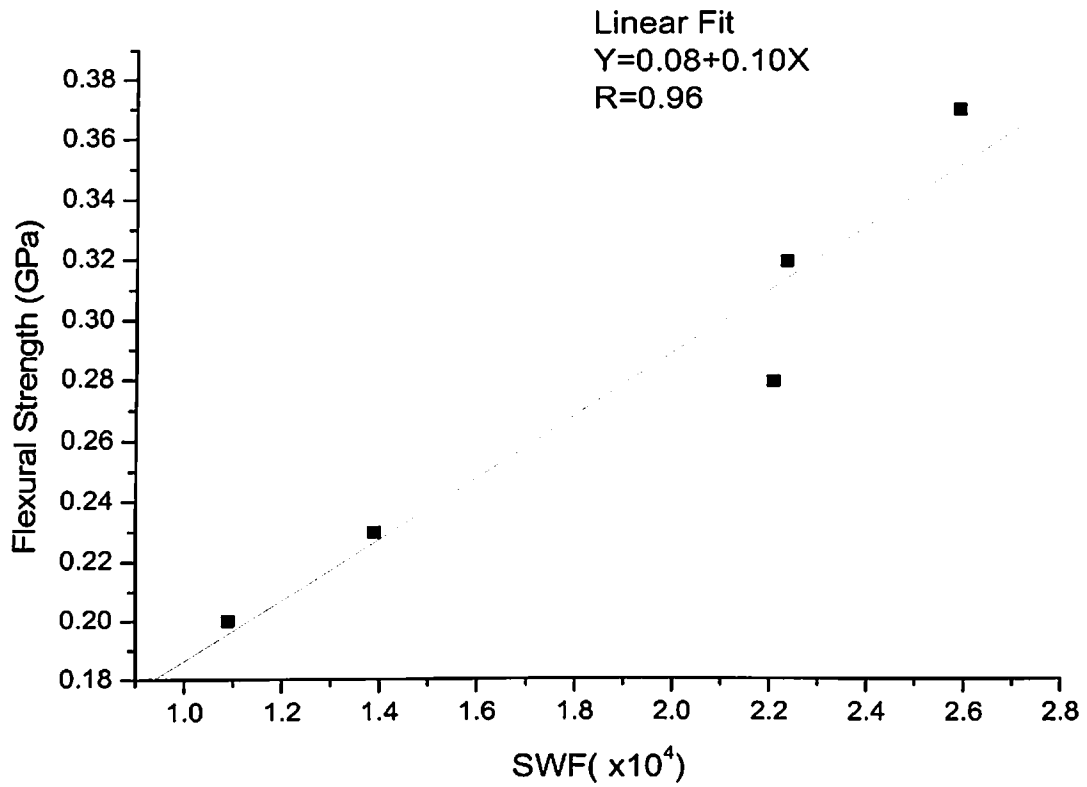


Figure 5.15 Relation between SWF and Flexural Strength of Dry Bones

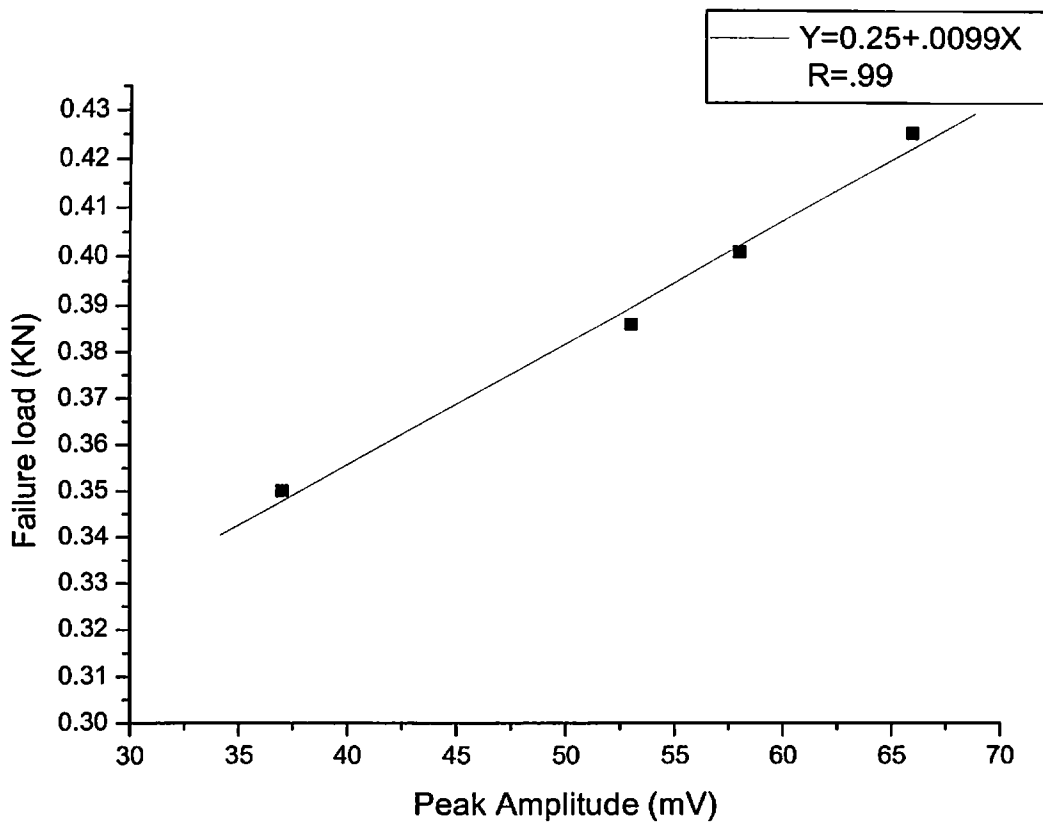


Figure 5.16 Relation between Peak amplitude and Failure Load of Dry Bones

5.3.2.3 Acousto-ultrasonic measurements on Fresh Bones

The bones were fractured in the form of a cut as given in the aforementioned study. Figure 5.17 and Figure 5.18 shows the waveform for both normal and fractured bone in one of the samples. The fresh bovine bones were directly obtained from slaughter house immediately after sacrificing the animal, were always kept in normal saline to keep the bone moistened. All the tests were carried on the same day within 2 hours. The magnitude of amplitude for good wet bone was also found considerably lower than that obtained in the case of good dry bone. The reason behind might be due to the absorption and attenuation of signals by the soft tissues, which were left intentionally on the surface of fresh bones to analyze the more realistic situation.

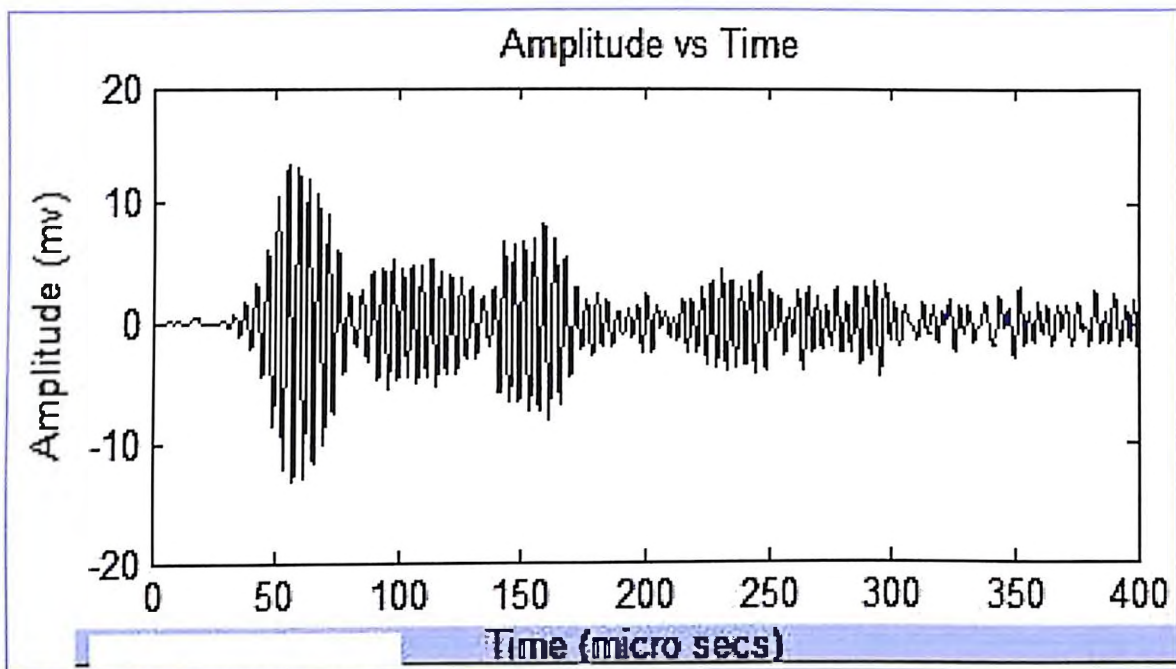


Figure 5.17 A-waveform for normal fresh bone (sample1)

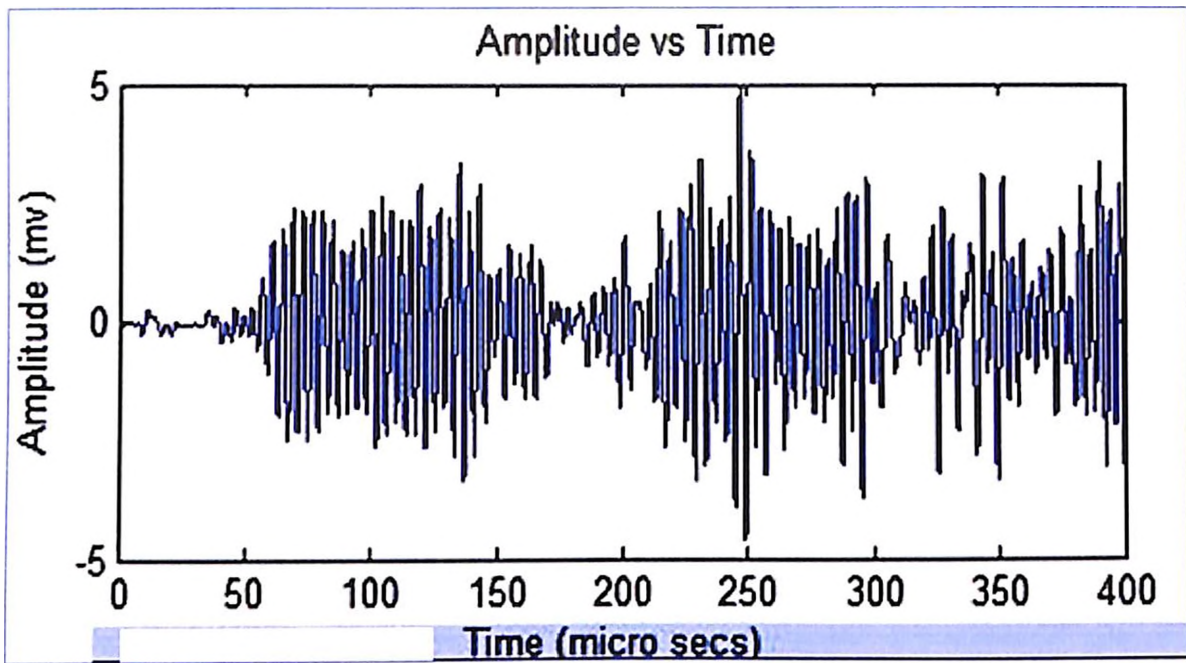


Figure 5.18 A-waveform for fractured fresh bone (sample1)

Figure 5.19 and Figure 5.20 shows the Acousto-ultrasonic measurements made before and after the simulated fracture was made in fresh bone.

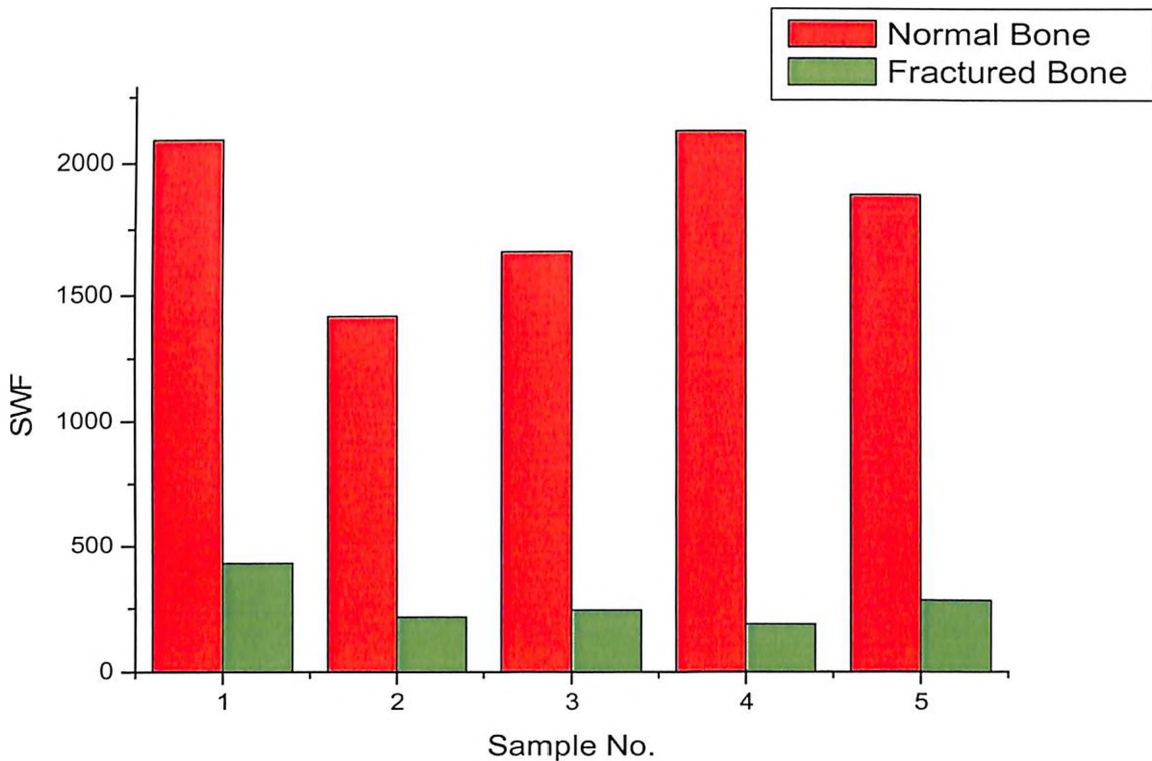


Figure 5.19 Change in the value of SWF (In Fresh Bovine Bone)

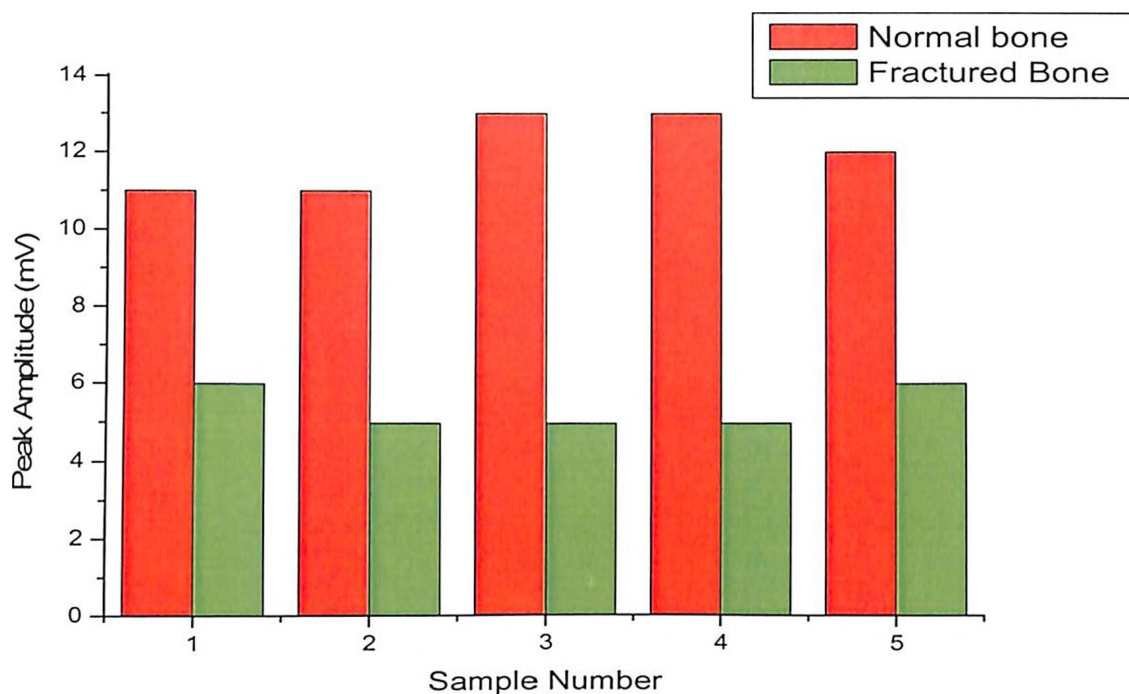


Figure 5.20 Change in the value of Peak amplitude (In Fresh Bone)

Table 5.7 and Table 5.8, Summarizes the result obtained from the in vitro study of fresh bovine bones.

Table 5.7 Acousto-Ultrasonic measurements from Fresh bone specimens

Material	Stress Wave Factor		
	Fresh Bones	Normal	Mean = 1829.00
	Fractured	Mean = 271.97	Standard Deviation = 95.701
P < 0.0002, N=5			

Table 5.8 Acousto-Ultrasonic measurements from Fresh bone specimens

Material	Peak Amplitude		
	Fresh Bones	Normal	Mean= 12
	Fractured	Mean= 5.40	Standard Deviation = 0.55
P < 0.0004, N = 5			

The T-paired test was also performed to check the probability of significance of the results obtained. Here also SWF was significantly reduced after the simulated fracture was introduced in the bone specimen.

Figure 5.21 and Table 5.9 shows the effect of increase in depth of cut on SWF and peak amplitude of AU signal.

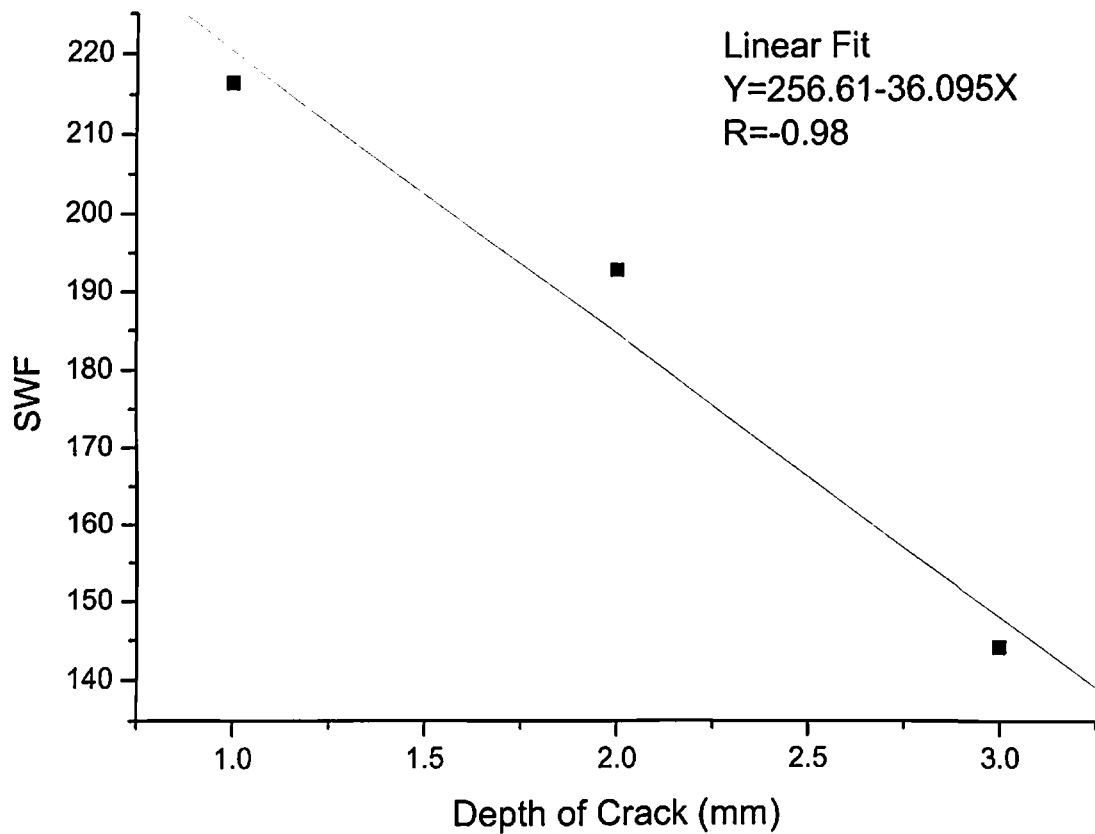


Figure 5.21 Change in the value of SWF with the depth of crack in fresh bone

Table 5.9 Change in the value of the peak amplitude with the depth of crack for fresh bone

Depth of Cut (mm)	Peak Amplitude (mV)
1	11
2	7
3	3

5.3.2.4 Conclusions

The application of Acousto-Ultrasonic technique for the assessment on *in vivo* bone condition was investigated. The significant decrease in the value of stress wave factor and the peak amplitude after the simulated fracture site was introduced indicate that the Acousto-Ultrasonic technique can be used to detect the bone abnormalities such as osteoporosis and also in monitoring the fracture healing process. The good correlation between the stress wave factor and the depth of cut and the correlation between the stress wave factor and the flexural strength of the dry bones indicate that this technique can be used to assess the mechanical integrity of bone.

References

1. Egle, D.M. and Brown, A.E. (1976) A note on Pseudo Acoustic Emission Sources, *J. Testing and Evaluation*. 4:196-199.
2. Vary, A. and Bowles, K.J. (1977) Ultrasonic Evaluation of the strength of Unidirectional Graphite-Polimide Composite, In *Proceedings of the Eleventh Symposium on Non-destructive testing*, American Society for Nondestructive Testing and Southwest Research Institute, San Antonio, Tex., pp.242-258.
3. Vary, A. and Lark, R.F. (1979) Correlation of fiber composite Tensile Strength with the Ultrasonic Stress Wave factor, *J. Testing and Evaluation* 7, pp.185-191.
4. Vary, A. (1988) The Acousto-ultrasonic approach. In *Acousto-Ultrasonics Theory and Application*, Duke J.C.Jr.(ed.). Plenum Press, New York, NY, pp.1-22.
5. ASTM. (Current edition). *Annual Book of ASTM Standards*. Philadelphia, PA: American Society for Testing and Materials.
6. ASTM E1316-99. Standard terminology for non-destructive examinations.
7. Duke, J.C. Jr., Henneke, E.G.II, and Stenchcomb, W.W. (1986) *Ultrasonic Stress Wave Characterisation of Composite Materials*, NASA CR – 3976, NASA, Cleveland.
8. Duke, J.C. Jr., Henneke, E.G.II, and Stenchcomb, W.W. and Reifsnider, K.L. (1984) *Characterisation of Composite Materials by Means of the Ultrasonic Stress Wave Factor*, In *Composite structures*, 2, Marshall, I.H.(ed.), Applied Sciences, Publishers, London.
9. Williams, J.H. Jr. and Doll, B. (1980) Ultrasonic Attenuation as an Indicator of Fatigue Life of Graphite Fiber Epoxy Composite, *Materials Evaluation*, 38:5, pp.33-37.
10. Talreja, R. (1988) Application of Acousto-Ultrasonic to Quality Control and Damage Assessment of Composites, In *Acousto-Ultrasonics Theory and Application*, Duke J.C. Jr. (ed.), Plenum Press. New York, NY, pp.177-190.

11. Russell-Floyd, R. and Philips, M.G. (1988) A Critical Assessment of Acousto-Ultrasonic Technique as a Method of Non Destructive Examination of Carbon Reinforced Thermoplastic Laminates, *NDT International*, 21:4, pp.247-257.
12. Standard Guide for Acousto-Ultrasonic assessment of composites, laminates, and bonded joints, ASTM International, Designation: E 1496-02, 100 Barr Harbor drive, west Conshohocken, PA 19428-2959, united states, pp.1-9.

CHAPTER 6

MONITORING THE FRACTURE HEALING PROCESS BY ACOUSTO-ULTRASONIC TECHNIQUE

6.1 INTRODUCTION

Bone fractures are the most common injury treated by the orthopaedic surgeons. Millions of fractures occur every year worldwide, with nearly 6.2 million fractures reported annually in the United States alone ^[1]. Fracture in bone results from two general causes, trauma or pathological conditions. A trauma induced fracture usually occurs when the normal range of loading to which a bone has adapted during growth and development is exceeded. A pathological fracture usually occurs under normal loading conditions after the bone has been weakened by diseases, such as osteoporosis or bone tumours. Bone fracture healing is a complex and dynamic regenerative process that gradually restores the structural integrity and mechanical function of bone. The healing process advances in stages of callus formation and consolidation and is eventually completed within some months. However, in about 5–10% of the millions of fractures that occur annually, impairment of the healing process may lead to delayed union or non-union requiring further conservative or even surgical procedures ^[2].

Monitoring of fracture healing refers to the evaluation of the status of the healing bone, the detection of complications in the process, and the accurate assessment of the endpoint of healing. In daily practice, evaluation of fracture healing is performed by serial clinical and radiographic examinations, both of which depend on the orthopaedic surgeon's expertise and clinical judgment ^[3]. The development of more objective and quantitative means of monitoring the healing process may assist the treating physicians to diagnose and treat delayed unions and non-unions early and also to identify the healing endpoint, thus preventing prolonged treatment or incorrect timing of the removal of an external or internal fixation device.

Several non-invasive quantitative methods for monitoring fracture healing have been reported in the literature. These include bone densitometry ^[4, 5], vibrational

analysis^[6-8], acoustic emission^[9, 10] and the attachment of strain gauges to external fixation devices^[6, 11-13]. All of these methods aim to determine the stiffness of the healing bone, either directly or indirectly. Although their ability to provide useful indications of healing has been validated through *ex vivo* and *in vivo* studies, the methods are generally influenced by extrinsic bone properties, such as bone gross geometry, fracture type, etc. In addition, most of the above-mentioned methods may take place only in a clinical setting, necessitating the intervention of a specialist to configure the measuring set-up and a number of them^[9, 10, 12, 13] require the temporary removal of the external fixation device. Ultrasonic methods have also been used for the monitoring of bone fracture healing. Although some researchers have employed ultrasonography^[14, 15] and power Doppler ultrasonography^[16] to assess the appearance and neo-vascularisation of the callus tissue during healing, the majority of the studies have utilized quantitative ultrasound techniques. The most appropriate technique to examine fractures in long bones, such as the tibia and the radius, is the axial transmission approach. Typically, a transmitter and a receiver are placed in direct contact with the skin (percutaneous application) on each side of the fracture site, as illustrated in Figure 6.1. The emitted ultrasonic waves propagate from the transmitter to the receiver along the longitudinal axis of bone. The marked differences in the properties between the callus tissue and the cortical bone bring about a change in the ultrasound velocity across the fracture when compared to a baseline measurement on an intact bone. Similar changes have been observed with regard to other propagation characteristics, such as wave attenuation and velocity dispersion.

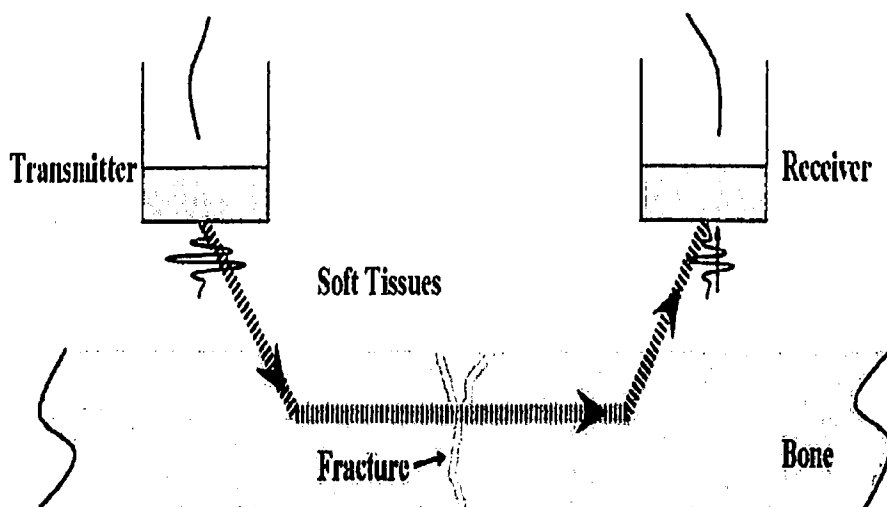


Figure 6.1 The axial transmission technique used for the ultrasonic evaluation of fracture healing in long bones

The ability of quantitative ultrasound to monitor the healing process has been investigated through animal and clinical studies over a long period. Simple experiments on bone phantoms and bone specimens have also been performed, aiming to examine the effect of the fracture characteristics (gap width, depth, etc.) on the measured quantities. The recent introduction of computational methods into bone research has extended our understanding of the underlying propagation phenomena and has helped researchers to propose new measurement techniques, such as the use of guided waves.

By considering the fact that two of the main functions of long bones are to support the body weight and locomotion it is essential that the healing of a fracture should be assessed mainly in terms of increasing mechanical strength. The application of acousto-ultrasonic technique for the assessment of *in vitro* bone condition is already studied in the previous chapter. The validity of using the same technique for assessing the *in vivo* bone condition is also proved in the *in vitro* study.

In this work an attempt has been made to use the acousto-ultrasonic technique for monitoring the fracture healing process. The animal experimentation with rabbits was conducted for this purpose and the monitoring of fracture healing process in rabbit's tibia were done with acousto-ultrasonic technique.

6.2 EXPERIMENTAL STUDY

An experimental work with rabbits was conducted in the central Animal house of Birla Institute of Technology and Science. 15 healthy rabbits of both sex were selected for the study. The average weights of the rabbits were ranging from 1.5 kg to 2.0 kg and the approximate age of the rabbits were 24 weeks. All animals were fed with standard diet during the whole experimentation period.

6.2.1 Creating Closed Fracture

Many investigators used several animal fracture models for the study of fracture healing, even with inherent advantages and disadvantages. The compromise has been made between the reproducibility of osteotomy and the realism of actual fracture. Generally, the production of real fractures increases the risk of variation in fracture site and location, which can make retesting difficult. Because

of the difficulties involved in gripping a whole bone *in vivo*, the most common fracture process has been bending^[17, 18, 19, 20], when the bone can be supported against two rests and a load can be applied from the opposite side. When a single nose is used, the location of the fracture is determined by the loading nose, and the mode is styled “three point bending”. A more even stress distribution over the tested section can be using two parallel loading points within the test span, styled “ four point bending”, but the exact location and direction of the fracture is not so well controlled. Rather the bone will fracture at the weakest section as it would in normal service^[21]. But all the methods mentioned above needed very sophisticated equipment, and apart from that the post-treatment care needed during the healing period also need a skilled person. The fracture created by any one of the method mentioned above will definitely separate the rabbit’s tibia in to two parts, which will definitely need intramedullary nailing to keep them aligned. This again would require expertise hands of surgeon. Keeping in view all this limitations, we went for creating a surgical fracture giving an oblique cut of 2-2.5 mm depth in rabbits right tibia. As this is only the first attempt of its own kind, we only wanted to investigate the application of acousto-ultrasonic technique for monitoring the fracture healing process. The type of fracture produced is not important at this point of study, but definitely it will be needed in the future study once the validity of the acousto-ultrasonic technique has been made.

6.2.2 Procedure for Creating Surgical Fracture

6.2.2.1 Pre-Requirements

The rabbits were kept nearly for 6 hours on fasting to avoid any complication due to anesthesia. The rabbits were anesthetised using a combination of xylazin (5-6 mg/Kg body weight) and ketamine hydrochloride (9-13 mg/Kg body weight)). Before starting the surgery, all surgical equipments, cottons, distill water, surgery gown, green cotton cloth were autoclaved at 121°C at 15lb pressure for 20 minutes.

6.2.2.2 Procedure

Tibia is a strong and massive long bone which extends obliquely downward and backward from stifle to hock. The bone appears twisted. Medial surface of the tibia is wider above and narrower below. Sartorius, gracilis and semimembranosus muscles are attached here. At the distal end fibula is completely fused with the distal third of the tibia. Fibula is thin and there is an elongated interosseous space between the two bones. Comparatively less musculature is present on the medial aspect of bone. This was the reason for what the rabbits tibia were chosen for the concerned study.

Hind legs of rabbit were washed with disinfectant soap (savlon) water and mopped with clean cloth. Then the hairs on the right hind legs were removed with the help of scissors and commercial hair remover. The skin was then cleaned with 70% ethyl alcohol and povidon was applied as anti bacterial reagent.

Local anaesthesia lignocane hydrochloride (aprox. 2 ml) was infiltrated at different places on the medial aspect of tibia region. The skin was removed by giving a vertical incision of 4-5 cm with the help of surgical blade. Facia were removed with the help of scalpel. The muscles were removed by giving irregular cut with the help of point to blunt scissor. At the distal end of posterior side, deep digital flexor muscle was separated from tibia by blunt incisions, at proximal third; bone was cut to the depth of 2.5-3 mm by electric saw.

The muscles were sutured by cat gut no. 2 in lock and stitch method. The facia and skin was sutured by silk no. 2 by horizontal mattress method. Figure 6.2 - Figure 6.9 clearly demonstrates all the steps performed during the surgery for creating the fracture.

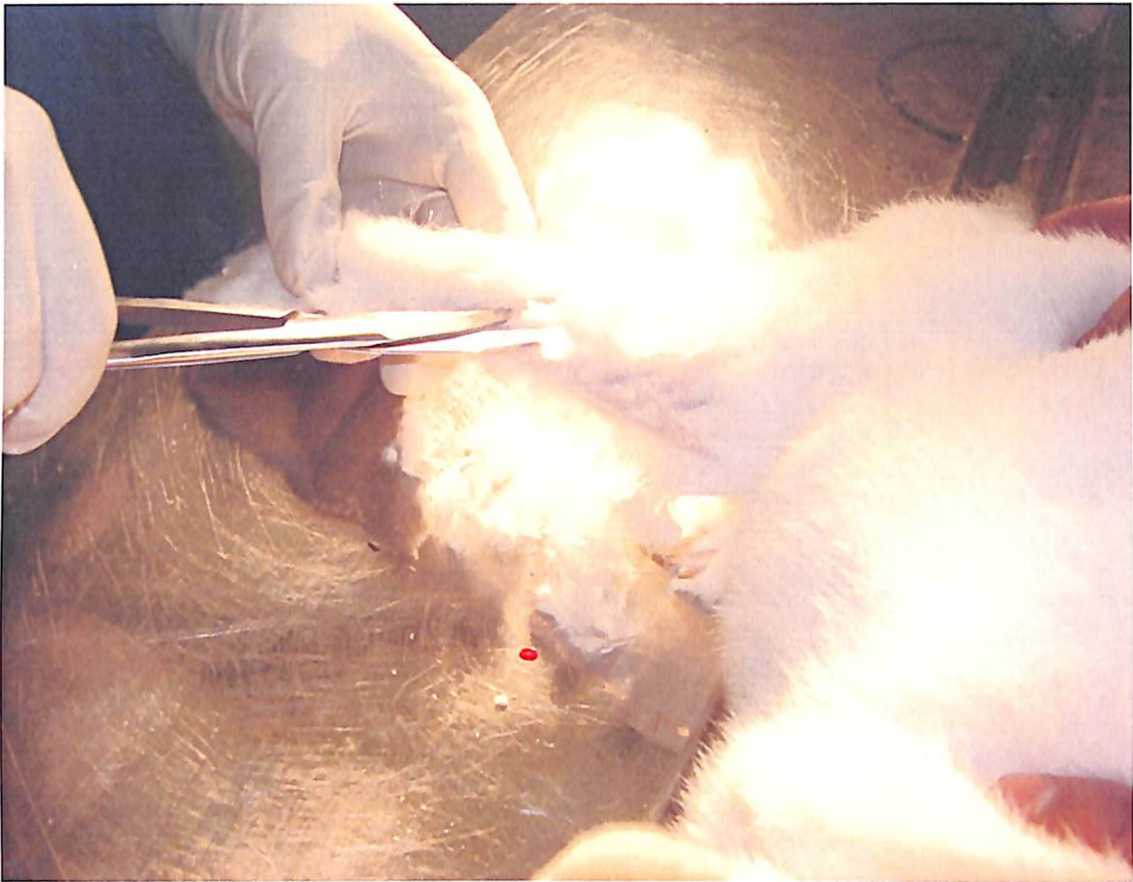


Figure 6.2 Removing of hairs form right tibia of Rabbit

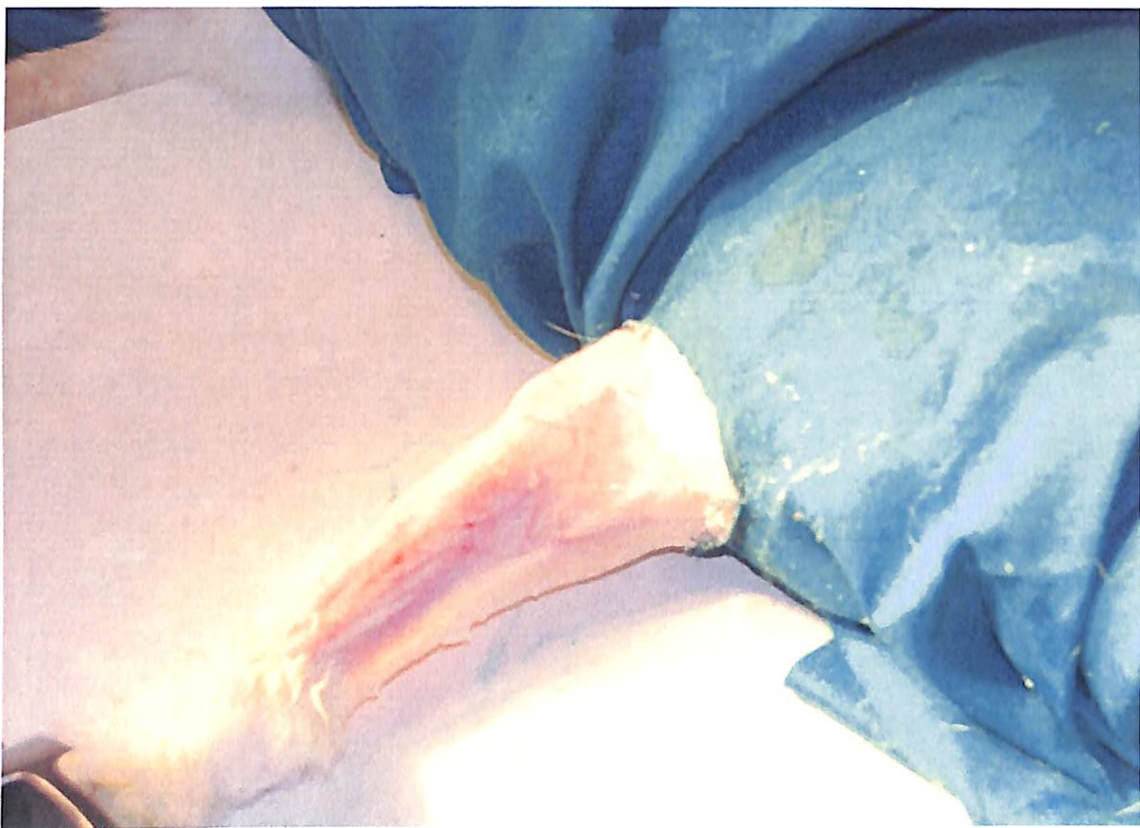


Figure 6.3 Hair removed from the rabbit right limb

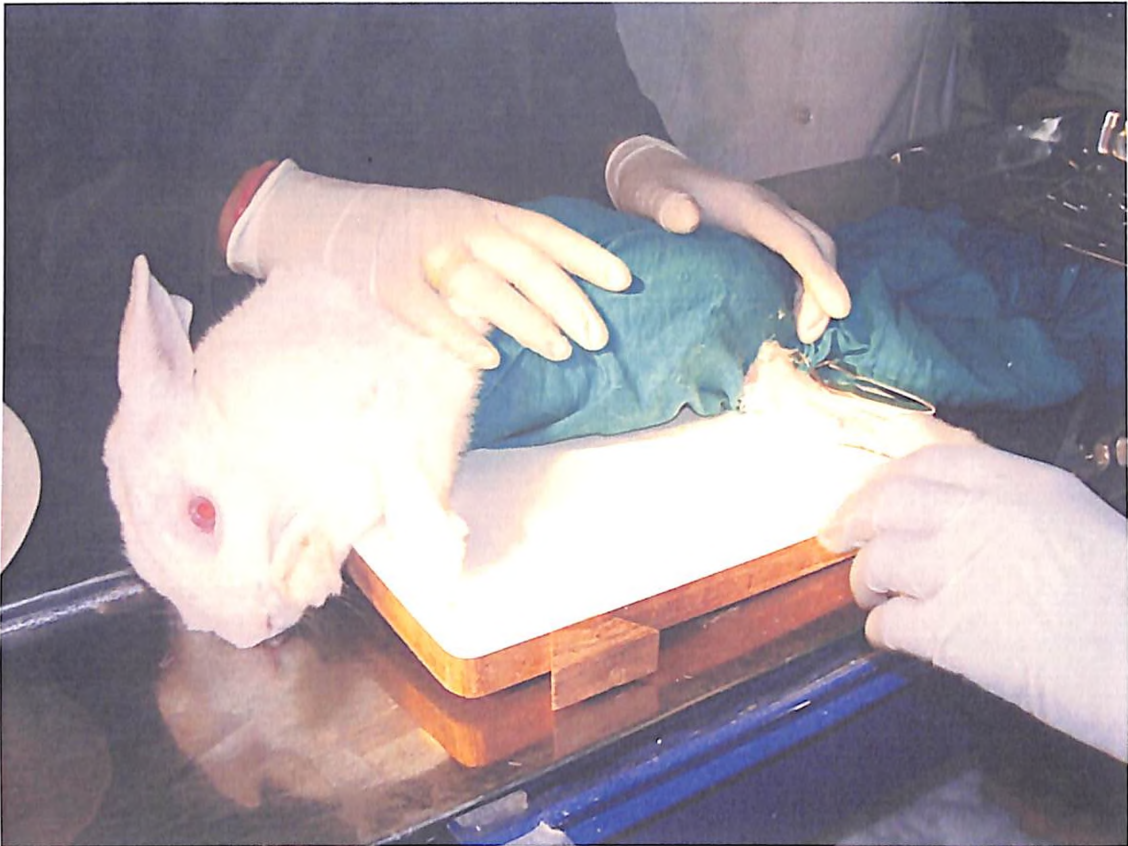


Figure 6.4 Rabbit wrapped in green cloth for surgery

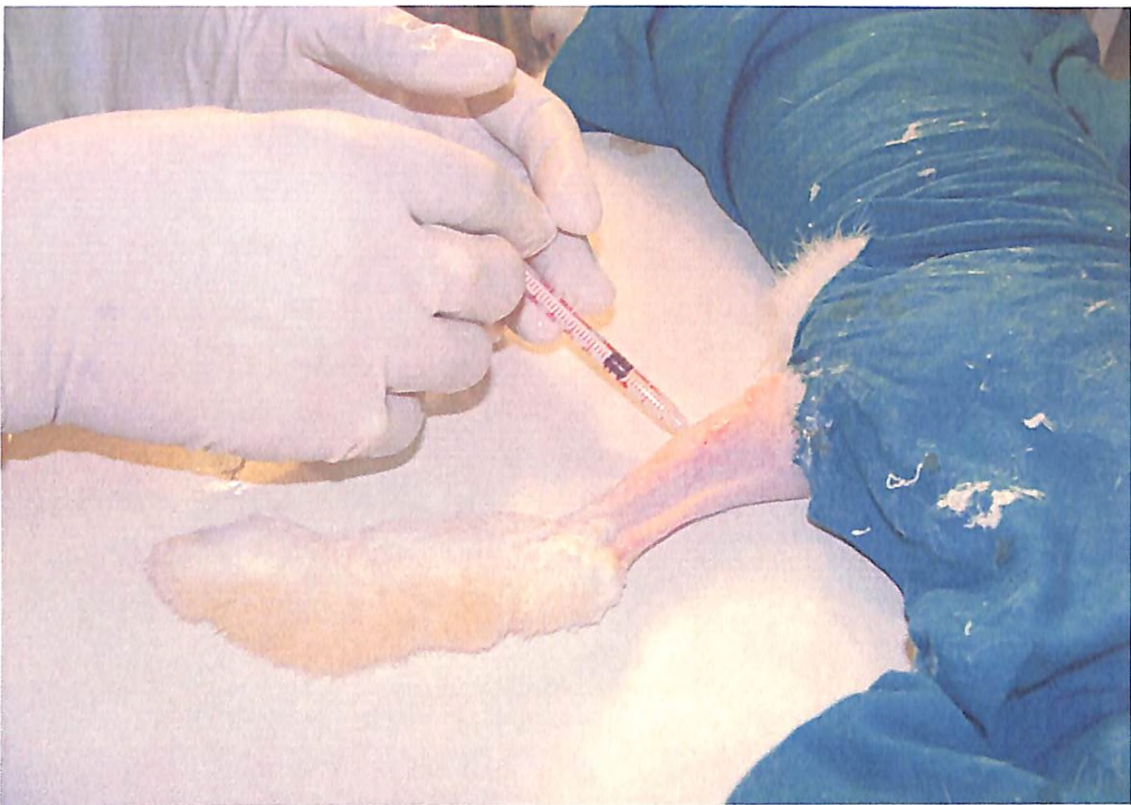


Figure 6.5 Injecting local anaesthesia on the right limb

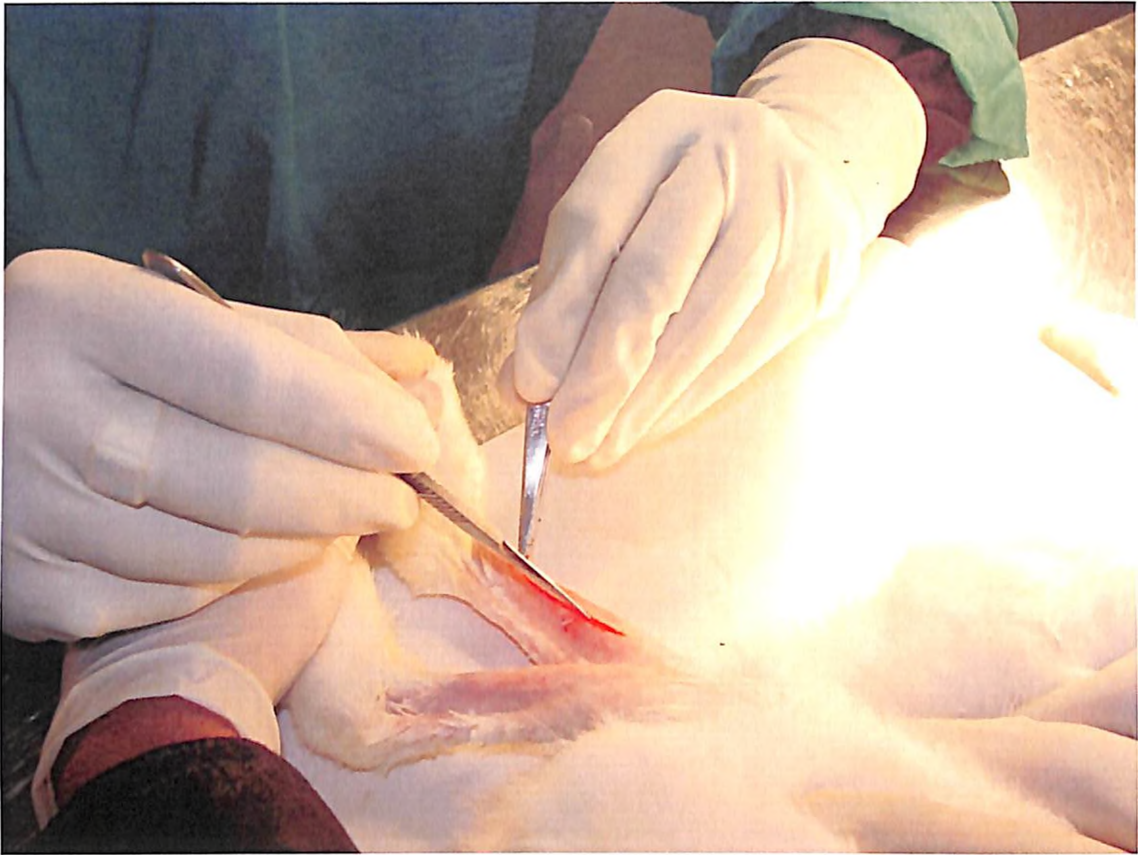


Figure 6.6 Photograph of giving vertical incision to remove the soft tissues

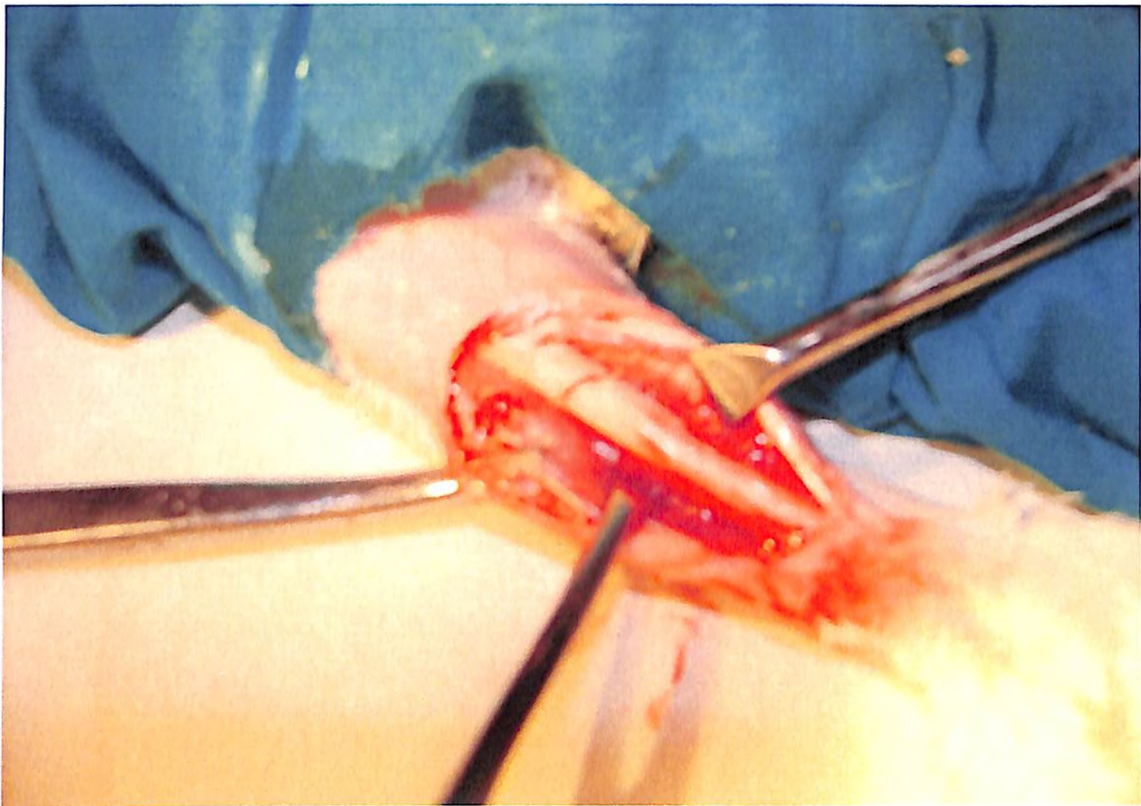


Figure 6.7 Photograph of surgical fracture

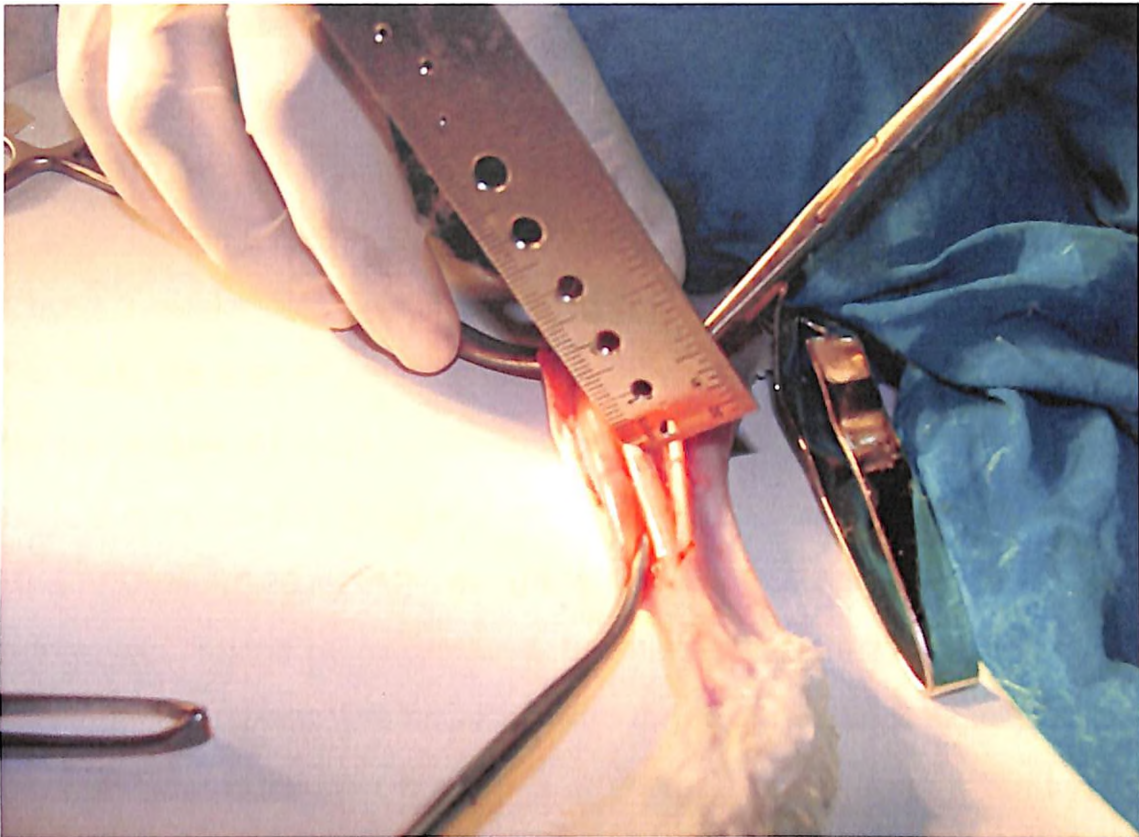


Figure 6.8 Measurement of depth of fracture



Figure 6.9 Suturing of soft tissues after surgery

6.2.2.3 Post Surgical Treatment

The rabbits hind leg were immobilised by applying Plaster of Paris cast from the stifle joint to hock joint, immobilising the ankle joint in zero position (neutral) and the knee joint in 90° of flexion [Figure 6.10]. The size of the plaster cast was reduced 3 weeks post operatively, as it was cut just distal to the knee and proximal to the ankles permitting full mobility of these joints. The very next day after the surgery 3-4 holes were drilled on the plaster of Paris near the surgical site, to provide the air passage. The antibiotic/painkiller injection fortivir (0.5 ml I/M) and Diclab (0.30 ml I/M) were given to all the rabbits for 3-4 days. As the fracture was created by electric saw, the injection T.T (0.25 ml I/M) was also given to all the rabbits. The antibiotic injection was given continuously for three days. Few rabbits showed symptoms of anorexia, which were given injection Belamyl (0.5 ml I/M) and injection cobacal D (0.75 ml I/M). All the rabbits were kept on healthy diet during the study.



Figure 6.10 Rabbit's right limb immobilised with Plaster of Paris

6.3 ACOUSTO-ULTRASONIC MEASUREMENT

Acousto-ultrasonic measurements were made from the healing limb and also from the contra lateral limb at every two week during the healing period. The contra lateral limb was used as a control for the acousto-ultrasonic measurements. The plaster cast was carefully removed during the acousto-ultrasonic measurements and if required applied again afterwards. In most of the cases the plaster cast was totally removed after 8 weeks. As the fracture was just a cut of 2-2.5 mm only, by examining the X-ray after 8 weeks, the decision was taken that whether the plaster cast should be applied again or not. The Figure 6.11 Shows the experimental set-up used for acousto-ultrasonic measurement.

The pocket hand held acousto-ultrasonic unit from NDT Automation, a member of MISTRAS group has two springs loaded, wheeled, rolling transducers attached with it. One sensor is the ultrasonic pulser and the other sensor is the acoustic emission receiver. The distance between the two sensors is one inch fixed. The instrument was mopped by 70% ethanol and the sensors were cleaned by povidon. The whole instrument was also disinfected by lorescane spray. Prior to the experimentation, the instruments were kept in operation theatre under exposure of UV light for overnight. Entire operation theatre along with the instrument was fumigated by potassium permanganate and formaldehyde in 1:3 ratio once in a week. After fumigation operation theatre was kept close for 10 hours.

Discrete ultrasonic pulses of fixed frequency 250 kHz were injected in to the rabbits tibia for the duration of 100 μ s through ultrasonic pulser. The pulser has the capability of generating the burst frequencies in the range of 50 kHz - 1 MHz, and the output voltage of 20 Volts peak to peak. The 25% of the noise signal were removed through the inbuilt system within the unit. The calibration of the amplitude height, threshold and other equipment settings were done with respect to contra lateral limb before testing the healing bone. Once the calibration was done, the entire equipment settings were kept constant during the whole monitoring process for all the rabbits. The threshold setting was done with the help of setting detection gate facility with the instruments. The stress waves after interacting within the tibia bone were picked up by the 10 kHz - 1 MHz frequency response acoustic emission

sensor. The care was taken while placing the sensors over the bone while taking the measurement. The instrument was somewhat modified, so that adequate amount of pressure is maintained so that proper sitting of the sensors could be assured. The sensor placement sites were so chosen such that the soft tissue thickness is minimum at those places. In fact the site chosen for the surgical fracture had the minimum soft tissue thickness. The received signal is then amplified by the built-in preamplifier of 40dB gain. The equipment has the facility of activating the high pass filter and low pass filter within it. The high pass filter frequency of 100 kHz and the frequency of 400 kHz for low pass filter were chosen for the *in vivo* study.

The Pocket AU has the complete working AU software program that uses A-Scan and C-Scan analysis to perform Acousto-ultrasonic inspection. Only the A-Scan analysis feature was used for this study, as the scanning of the rabbits tibia was not possible. The received signal was digitised through the dedicated feature extraction processor within the unit. The waveform parameters were then exported and converted to ASCII files and transferred to the personal computer for further signal processing.



Figure 6.11 Experimental set up for Acousto-ultrasonic measurement on rabbits

The Stress Wave factor (energy content) corresponding to both the control and healing limb were measured after every two weeks during the healing period up to 12 weeks from the date the fracture was made. A parameter called Healing Index was calculated from the stress wave measurements by taking the ratio of the SWF of the healing limb to that of control limb.

Healing was also assessed from the radiograph taken every month. The frequent X-rays were not taken due to the limited facility available near the working place.

The GUI based software was developed in MATLAB 6.05 for calculating the different parameters of the acoustic emission signal (Appendix C). The GUI based software was also developed for calculating the healing index, the term used for monitoring the healing process (Appendix D).

6.4 RESULTS AND DISCUSSION

The software specially developed for the present study takes the AU waveforms recorded during the AU measurements as input and process the signals to find different parameters such as energy content of the signal, peak amplitude, rise time, time of flight etc. The signals were also plotted directly on the screen and the calculated Healing index was also displayed. Although the tests were carried out on 15 specimens, the results of 6 representative specimens are discussed below.

Figure 6.12 gives the details of the acousto-ultrasonic measurements made in the rabbit No. 4 at the time of surgery. It clearly mentions the various parameters calculated for both the control and healing limb just after the fracture was created. The figure also mentions one of the parameters i.e power spectrum of the signal which was calculated by doing the Fast Fourier Transformation (FFT) of the received signal. The power spectrum could also be used as to quantify the signal and can be used as stress wave factor.

Figure 6.13 gives the energy content (used as SWF for the present study) for both the control and healing limb of rabbit no. 4 and the healing index at the time

of surgery. The healing index was found to be 0.003, as maximum signal got attenuated due to the presence of fracture. The X-ray picture of the limb just after the surgery clearly indicating the fracture site is shown in Figure 6.14.

Acousto-ultrasonic measurements and X-ray for rabbit No. 4 at fourth week during the healing period is shown in Figure 6.15 and Figure 6.16 respectively. The healing index calculated was 0.35, which clearly indicates that the callus formation has taken place at this time. The formation of callus is not clearly visible in the X-ray as it is just a fracture of 2-2.5 mm.

Figure 6.17, 6.18, 6.19 and 6.20 gives the value of the healing index and the X-ray photograph of rabbit 4 at the end of week eighth and week twelfth respectively. The value of the healing index clearly shows an increasing trend during the healing period. The value of the healing index after week 12 was found to nearly constant when measured at the fourteenth week. Hence the healing index value obtained after week twelfth was considered as the end point of healing process. The value of the healing index clearly indicates that it increases considerably till week eighth but after that its value increased very slowly. This was due to slow remodelling process in the final stage of fracture healing process, which continued after week 12 also.

The change in the value of healing index during the healing period and the X-ray examination for rabbit no. 6 is shown from Figure 6.21 to Figure 6.28 respectively. The healing index found at the end of twelfth week is equal to 0.79 which sets the end point of healing process, as the healing index value didn't change at the end of week fourteenth. The healing index value at the end of fourth week clearly indicates the initiation of the callus formation. The value of the healing index at the eighth week gives an idea of the full callus formation.

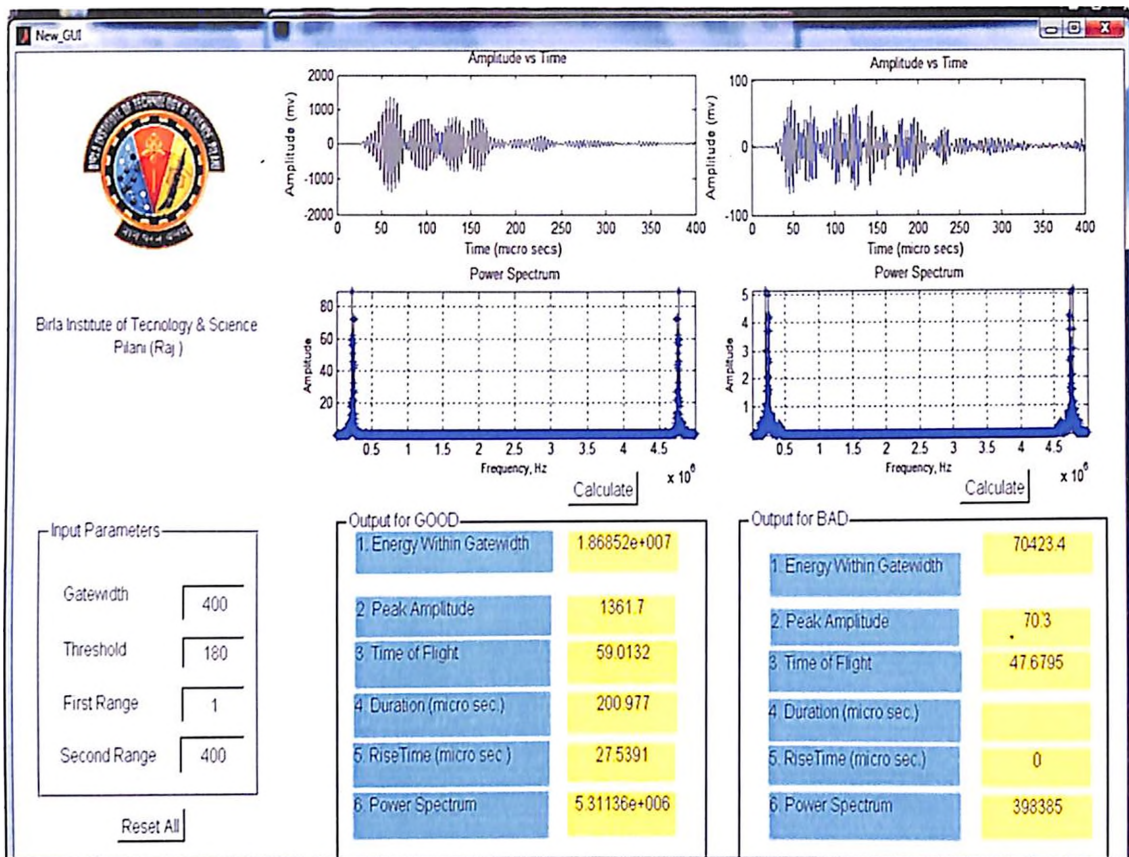


Figure 6.12 Acousto-ultrasonic parameters calculated for rabbit No. 4 just after surgery

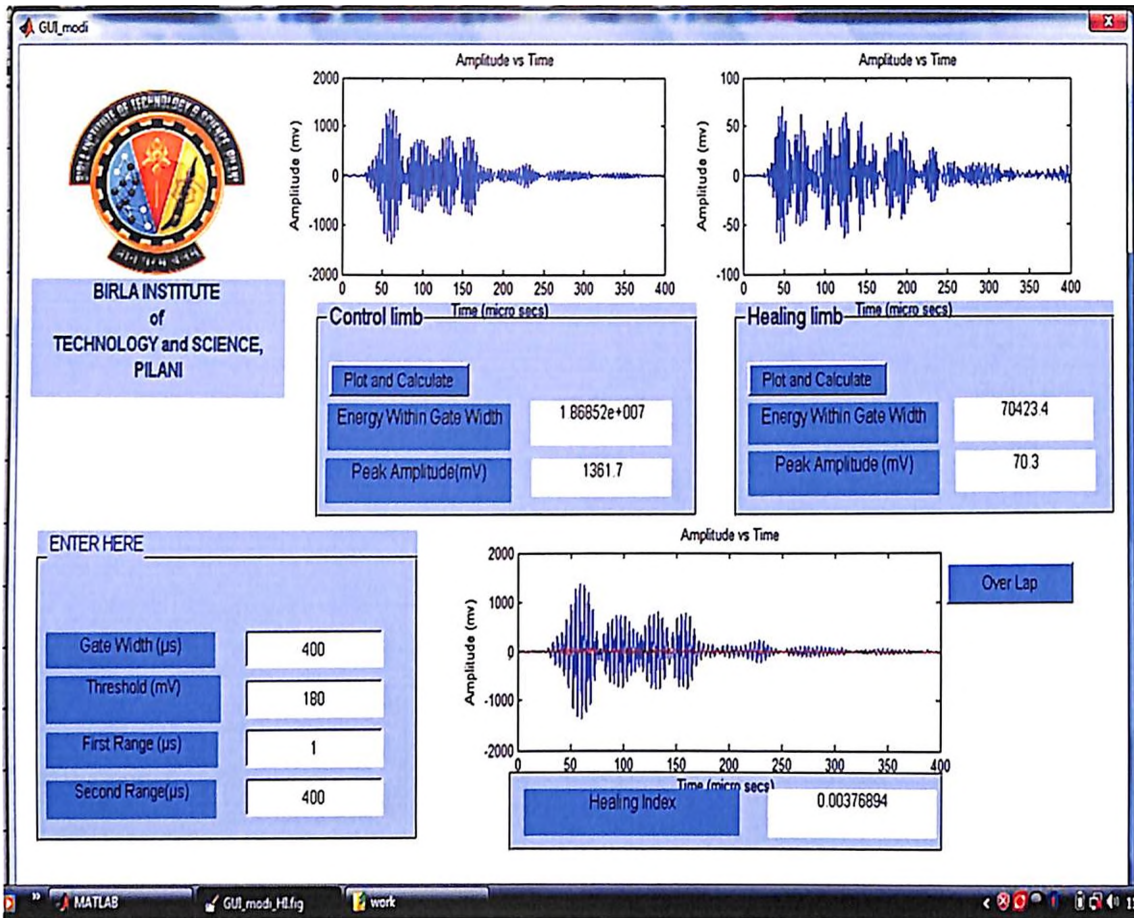


Figure 6.13 Acousto-ultrasonic measurements for rabbit No. 4 just after the surgery



Figure 6.14 X-ray of Rabbit No. 4 just after the surgery

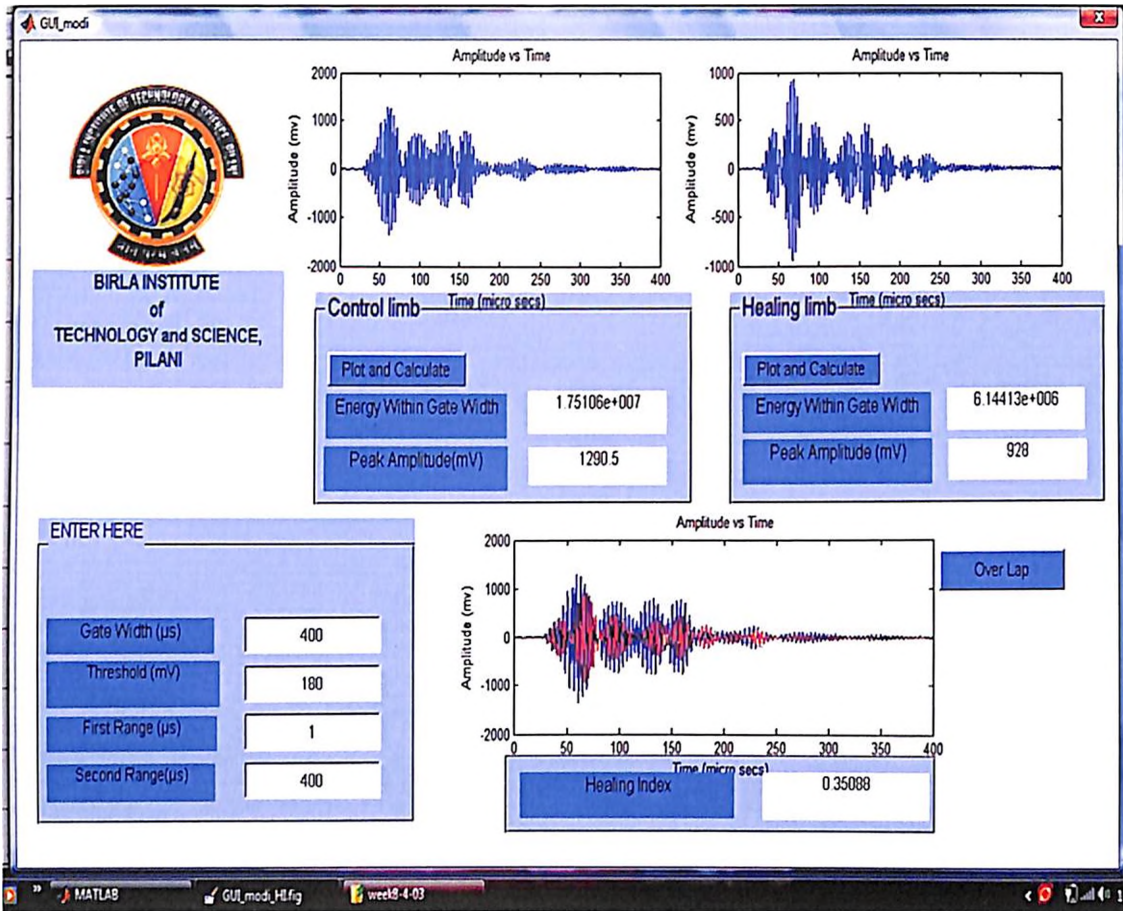


Figure 6.15 Acousto-ultrasonic measurements for rabbit No. 4 at fourth week



Figure 6.16 X-ray of rabbit No. 4 at Fourth week

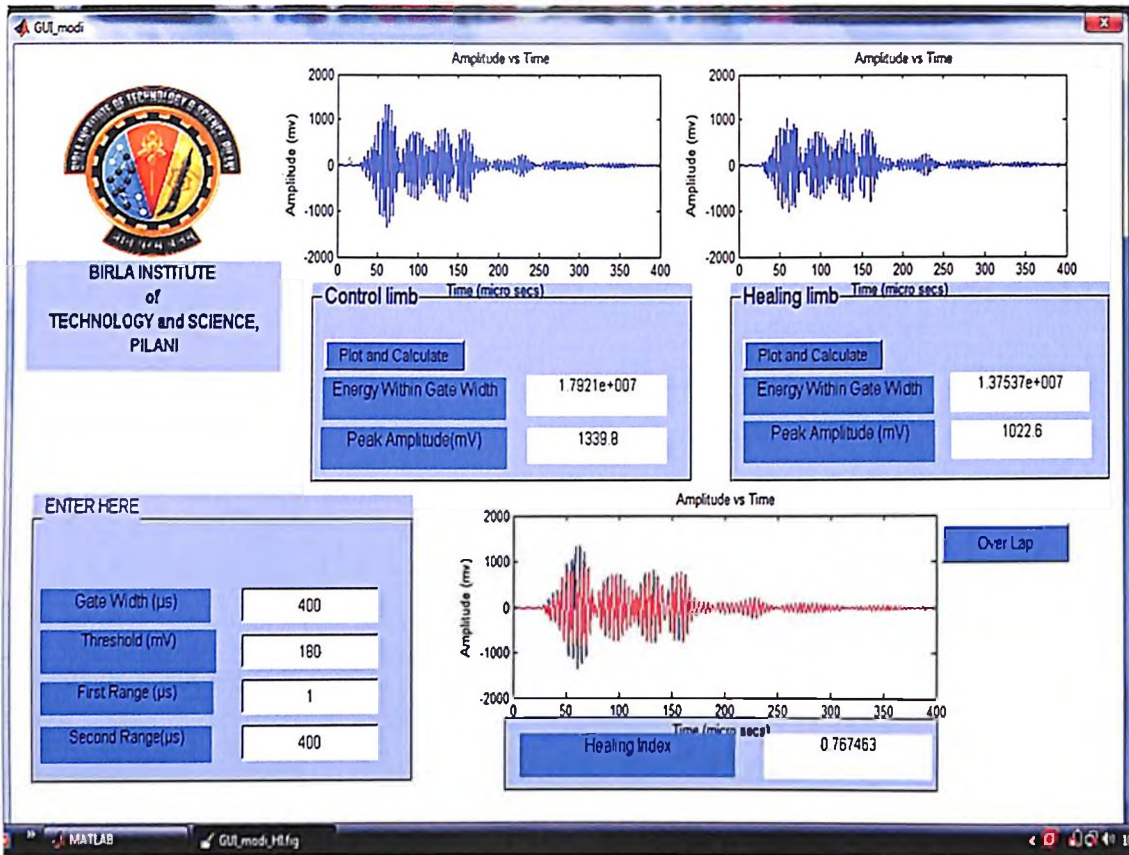


Figure 6.17 Acousto-ultrasonic measurements for rabbit No. 4 at eighth week

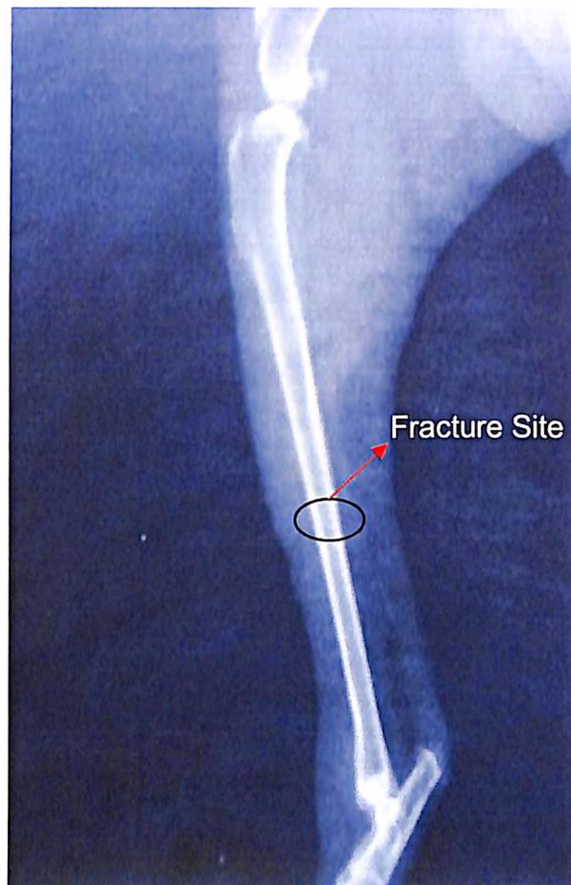


Figure 6.18 X-ray of rabbit No. 4 after eighth week

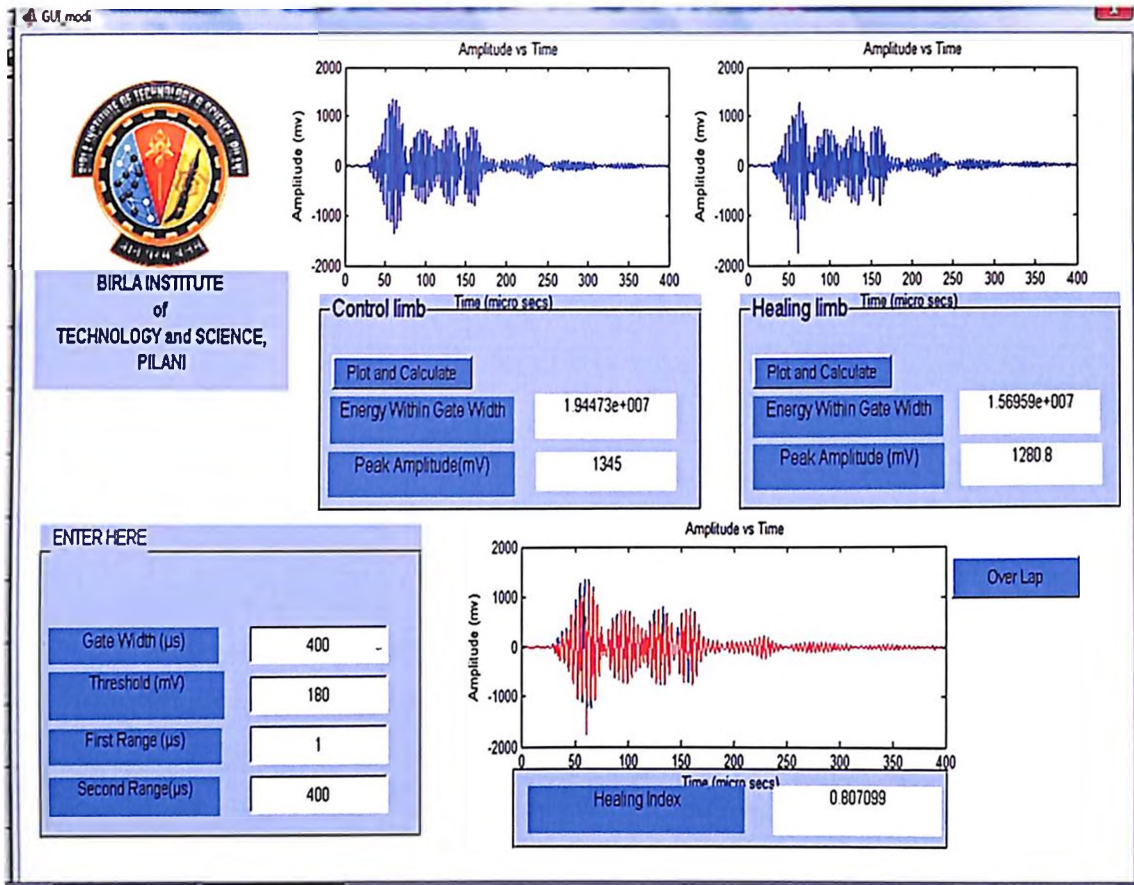


Figure 6.19 Acousto-ultrasonic measurements for rabbit No. 4 at twelfth week



Figure 6.20 X-ray of rabbit No. 4 at twelfth week

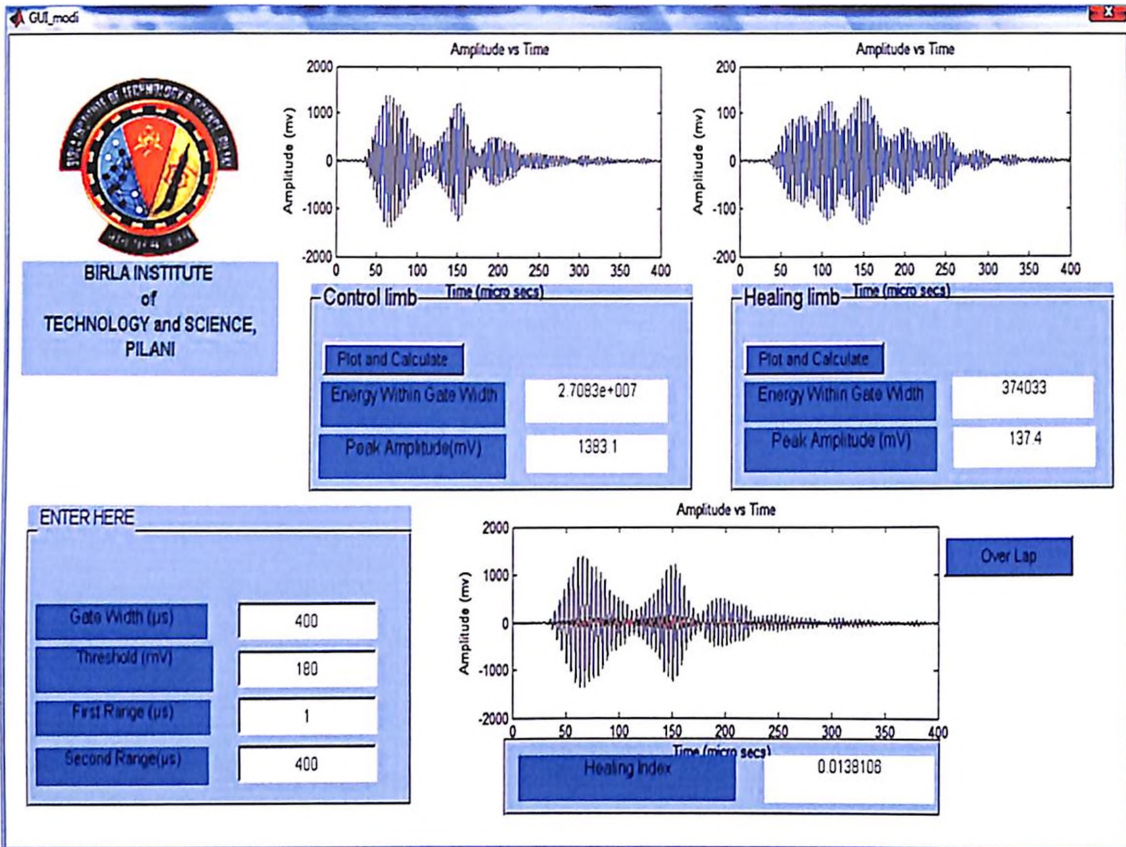


Figure 6.21 Acousto-ultrasonic measurements for rabbit No. 6 just after the surgery



Figure 6.22 X-ray of rabbit No. 6 just after the surgery

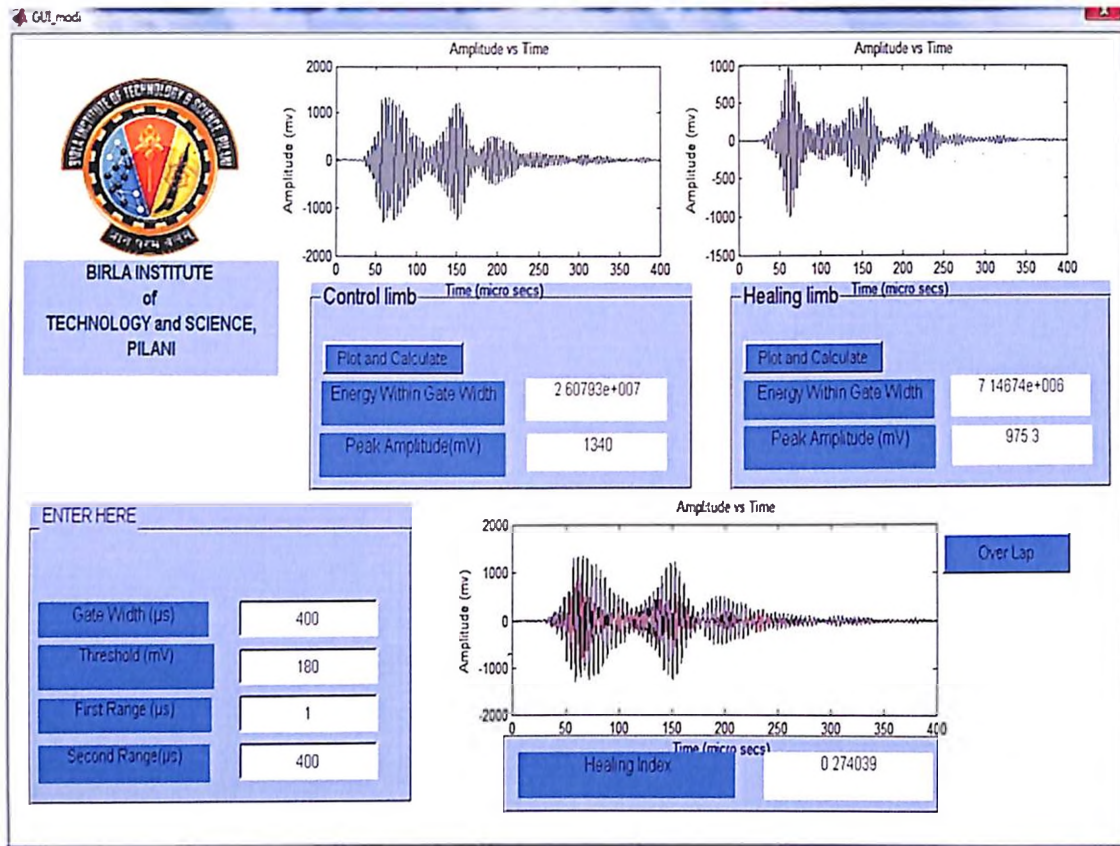


Figure 6.23 Acousto-ultrasonic measurements for rabbit No. 6 at fourth week



Figure 6.24 X-ray of rabbit No. 6 at fourth week

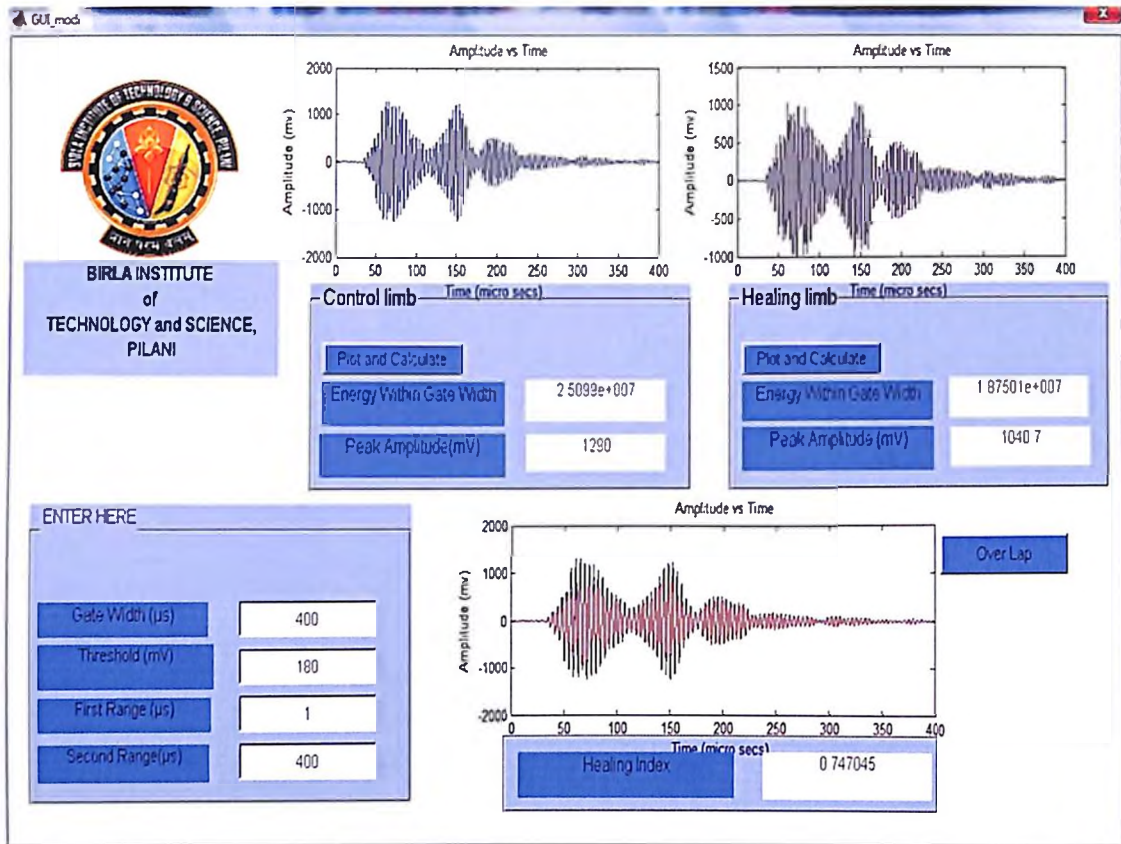


Figure 6.25 Acousto-ultrasonic measurements for rabbit No. 6 at eighth week



Figure 6.26 X-ray of rabbit No. 6 at eighth week

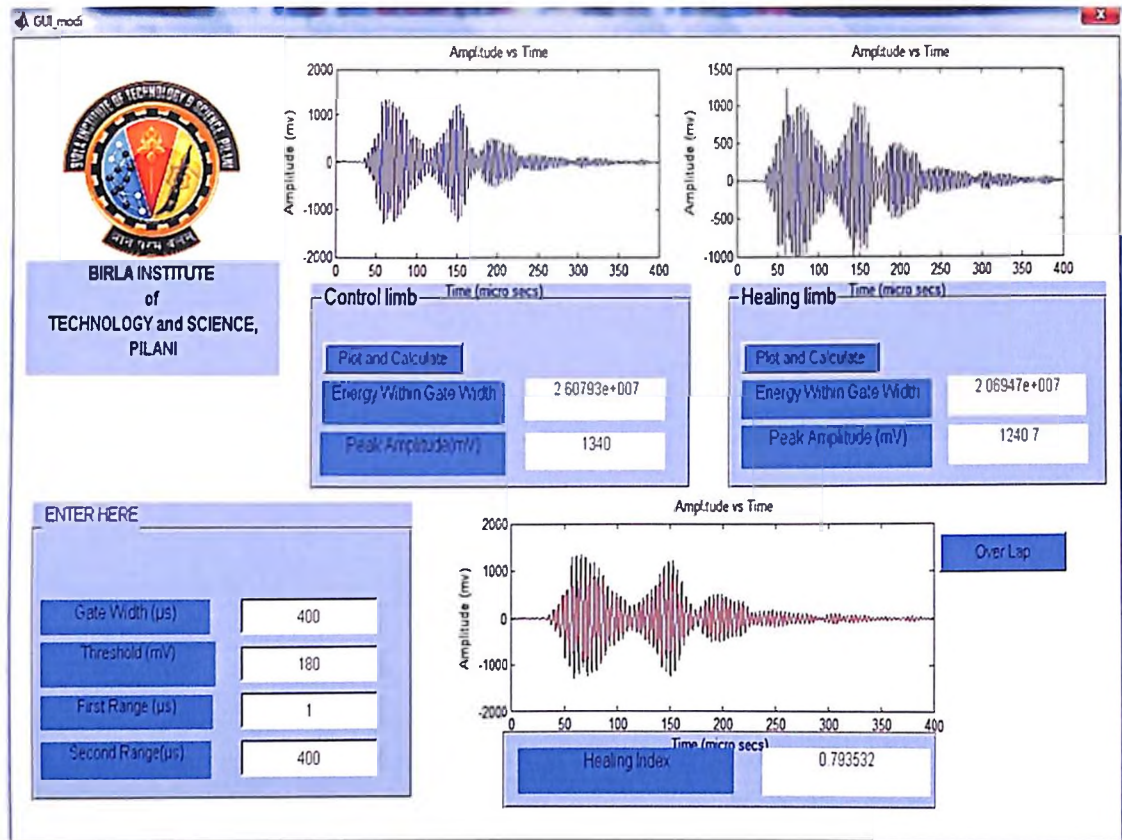


Figure 6.27 Acousto-ultrasonic measurements for rabbit No. 6 at twelfth week



Figure 6.28 X-ray of rabbit No. 6 at twelfth week

The change in the value of healing index during the healing period and the X-ray examination for rabbit no. 7 is shown from figure 6.29 to figure 6.35 respectively. Here also the value of healing index is equal to 0.42 which indicates the formation of callus at this stage. The healing index value of 0.85 at twelfth week indicates the end point of the healing process.

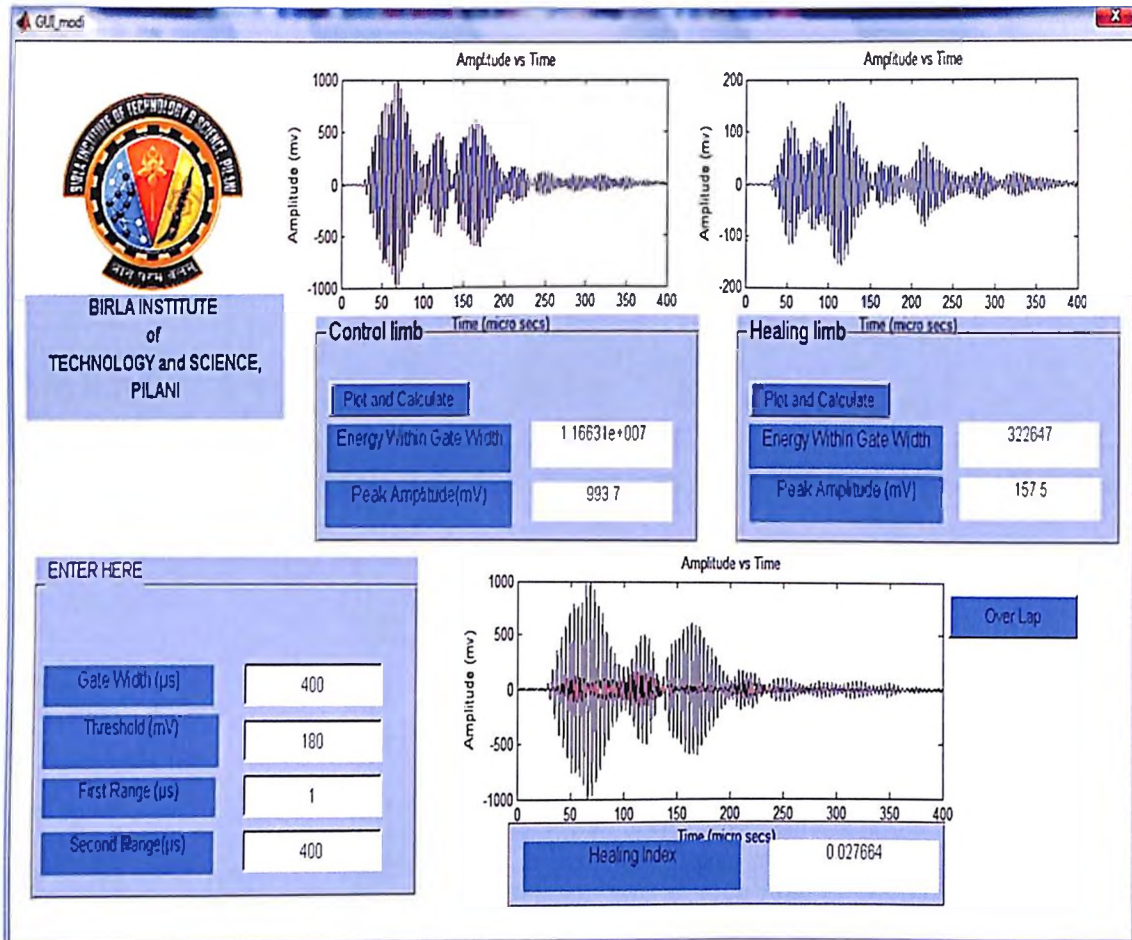


Figure 6.29 Acousto-ultrasonic measurements for rabbit No. 7 just after surgery

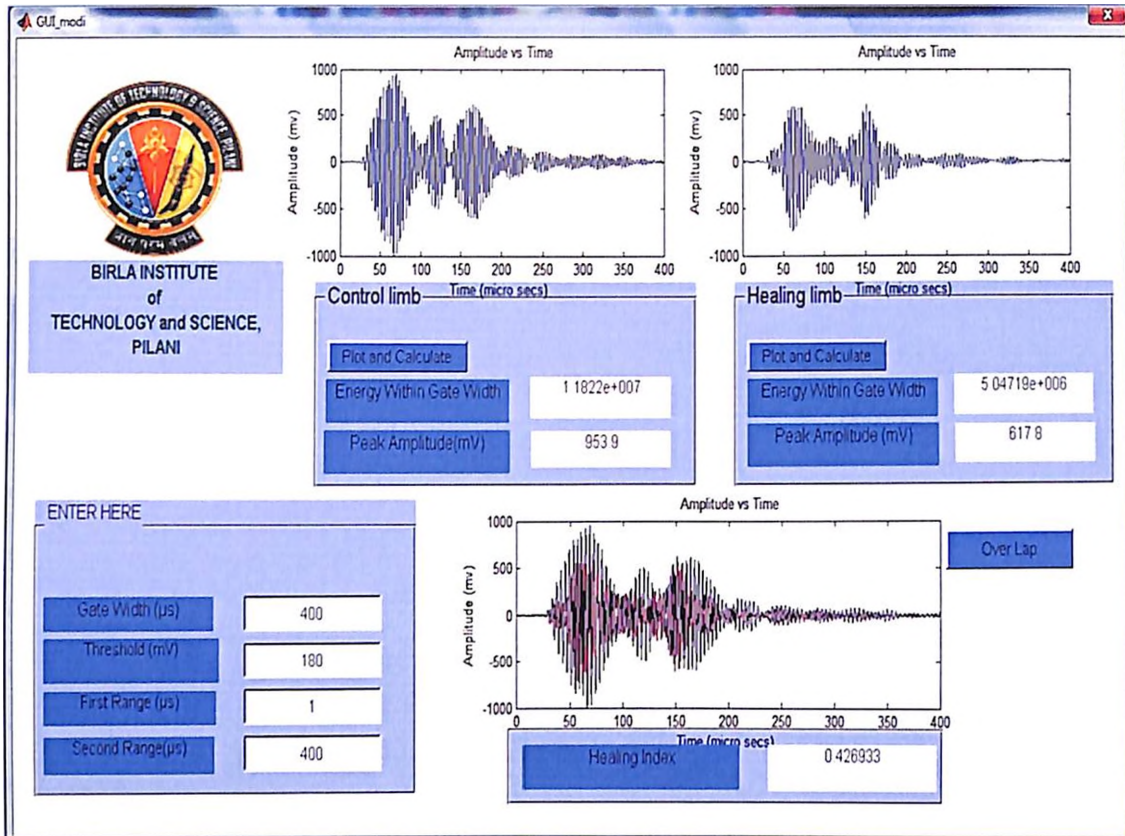


Figure 6.30 Acousto-ultrasonic measurements for rabbit No. 7 at fourth week



Figure 6.31 X-ray of rabbit No. 7 at fourth week

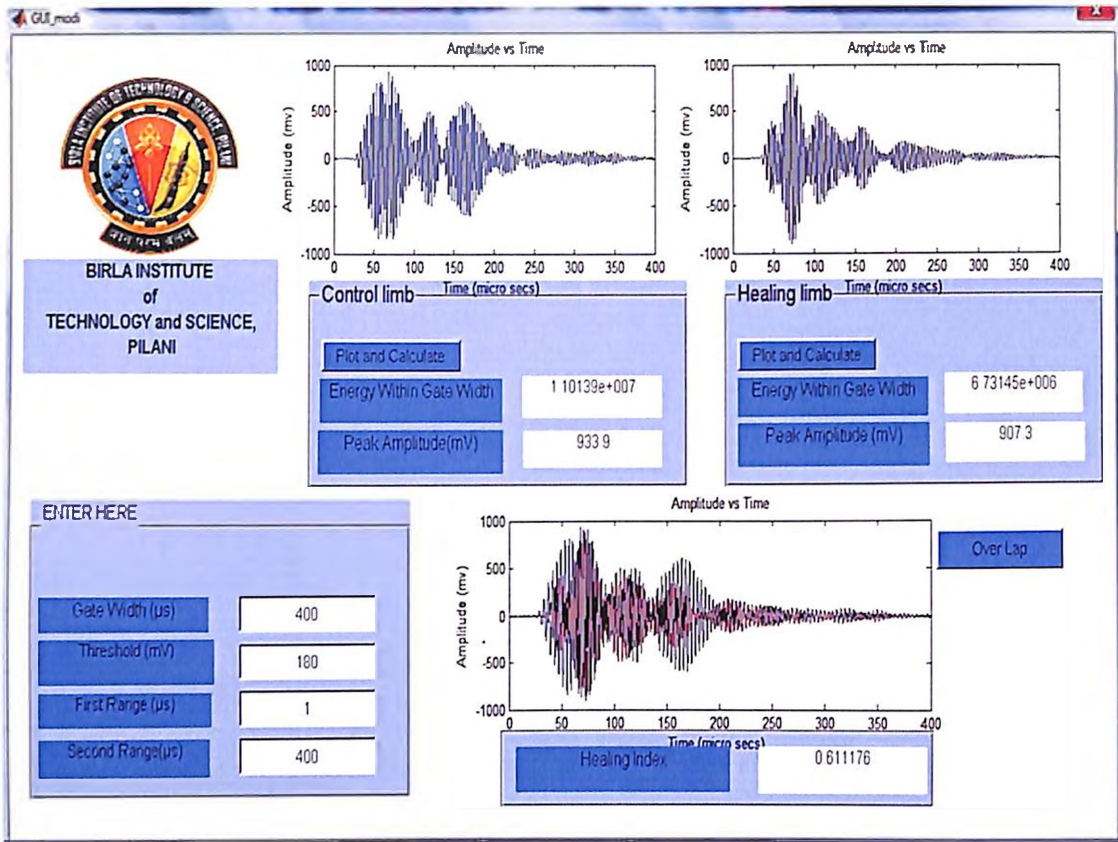


Figure 6.32 Acousto-ultrasonic measurements for rabbit No. 7 at eighth week



Figure 6.33 X-ray of rabbit No. 7 at eighth week

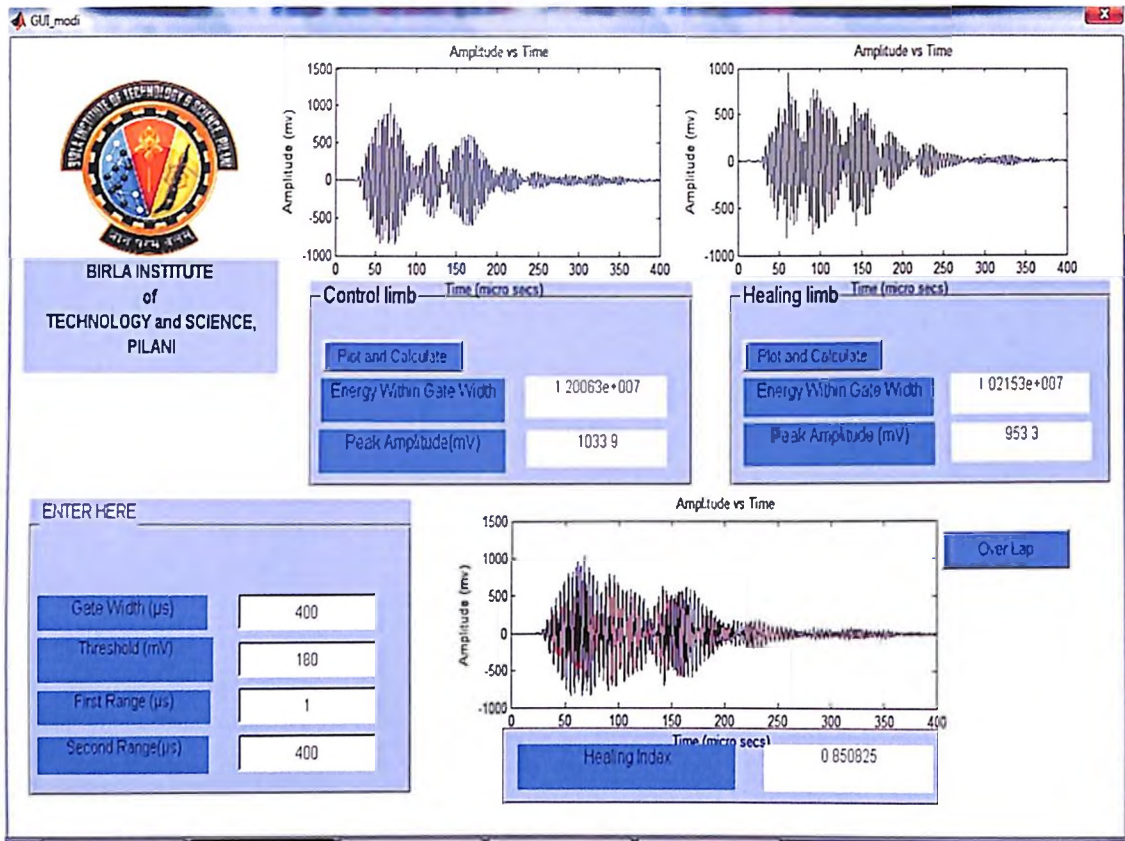


Figure 6.34 Acousto-ultrasonic measurements for rabbit No. 7 at twelfth week



Figure 6.35 X-Ray of rabbit No. 7 at twelfth week

The healing index values for rabbit No 10, 11 and 13 are shown in Figure 6.36. The sudden increase in the value can be seen at the fourth week due to the callus formation. After eighth week the increase in the value of healing index is nearly uniform at every week due to slow remodelling process at the end stage of the healing process.

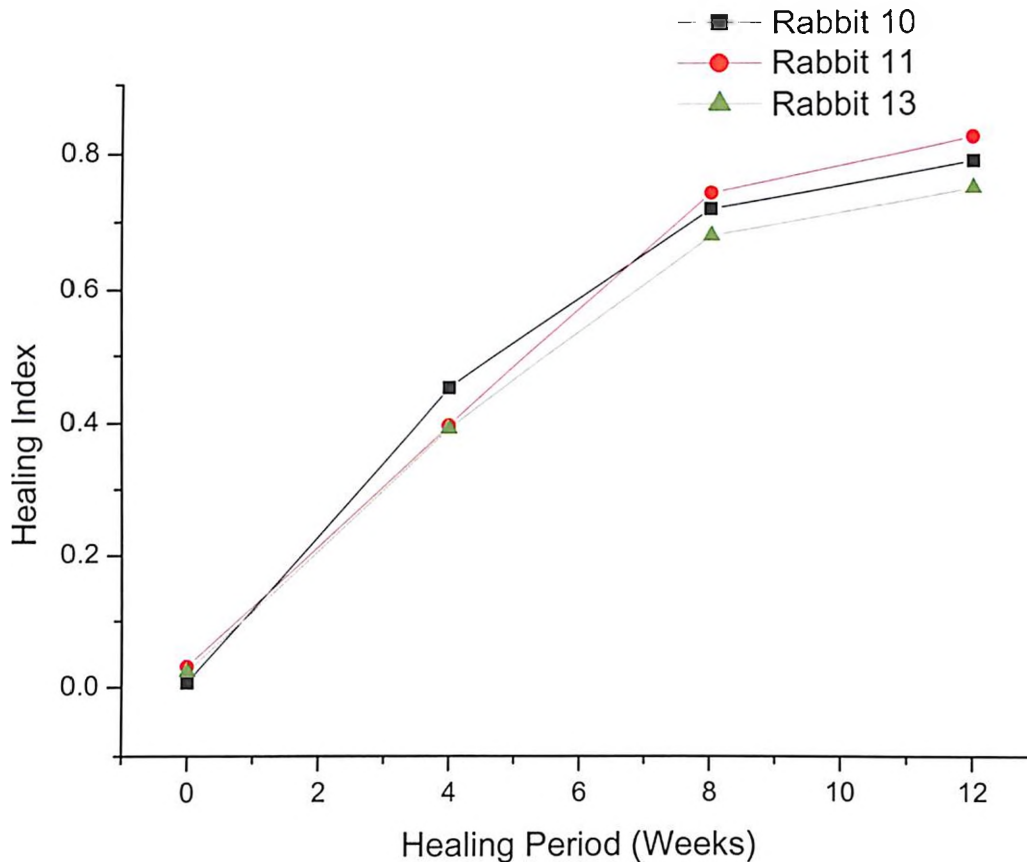


Figure 6.36 Healing Index values for Rabbit 10, 11 and 13

6.5 CONCLUSIONS

The results of the present experimental study indicate that the acousto-ultrasonic technique can be used clinically for monitoring the fracture healing process.

The calculated Healing Index from the acousto-ultrasonic measurements was found to be increasing uniformly during the healing period. The end point of the healing process was indicated by the more or less constant value of Healing Index value at 12-14 weeks of the healing period.

The X-ray examination clearly shows the healing has almost completed after the eighth week, but the Healing Index value at the same time does not confirm it. Hence it can be concluded that the healing index value which was calculated with respect to energy content of the signal, clearly assembles the strength of the bone also. Hence we conclude that the acousto-ultrasonic apart from monitoring the fracture healing process also gives the information of the strength of the bone achieved. This can be a big advantage over the X-ray technique which doesn't predict the strength of the bone. The correlation between the energy content (SWF) and the strength of the bone has already been validated in the *in vitro* study with this technique. The same study to be carried out *in vivo* on rabbits, requires skilled persons, suitable fixtures and equipment.

The above conclusions can be a big advantage for the sports person, who can really come to know what percentage of strength he has recovered during the healing fracture process, and after what time he can again restart his sports activities and up to what extent.

References

1. Praemer, A., Furner, S., Price, O. (1992) Musculoskeletal conditions in the United States, *Am. Acad. Orthop. Surg.*, pp.85-91.
2. Einhorn, T. A. (1995) Enhancement of fracture-healing, *J. Bone Joint Surg. Am.*, 77: 6, pp.940-956.
3. Blokhuis, T. J., De Bruine, J. H., Bramer, J. A., F. C., Den Boer, F. C., Bakker, F. C., Patka, P., Haarman, H. J. and Manoliu, R. A. (2001)The reliability of plain radiography in experimental fracture healing, *Skeletal Radiol*, 30:3, pp.151-156.
4. Augat, P., Merk, J., Genant, H. K., and Claes, L. (1997) Quantitative assessment of experimental fracture repair by peripheral computed tomography, *Calcif. Tissue Int*, 60:2, pp.194-199.
5. Markel, M. D., Morin, R. L., Wikenheiser, M. A., Lewallen, D. G. and Chao, E. Y. (1991) Quantitative CT for the evaluation of bone healing, *Calcif. Tissue Int*, 49:6, pp.427-432.
6. Cunningham, J. L., Kenwright, J. and Kershaw, C. J. (1990) Biomechanical measurement of fracture healing, *J. Med. Eng. Technol*, 14:3, pp.92-101.
7. Nakatsuchi, Y., Tsuchikane, A. and Nomura, A. (1996) Assessment of fracture healing in the tibia using the impulse response method, *J. Orthop. Trauma*, 10:1, pp.50-62.
8. Nikiforidis, G., Bezerianos, A., Dimarogonas, A. and Sutherland, C. (1990) Monitoring of fracture healing by lateral and axial vibration analysis, *J. Biomech*, 23:4, pp.323-330.
9. Hirasawa, Y., Takai, S., Kim, W. C., Takenaka, N., Yoshino, N. and Watanabe, Y. (2002) Biomechanical monitoring of healing bone based on acoustic emission technology, *Clin. Orthop. Relat. Res*, 402, pp.236–244,
10. Watanabe, Y., Takai, S., Arai, Y., Yoshino, N. and Hirasawa, Y. (2001) Prediction of mechanical properties of healing fractures using acoustic emission, *J. Orthop. Res*, 19: 4, pp.548-553.
11. Claes, L., Grass, R., Schmickal, T., Kisse, B., Eggers, C., Gerngross, H., Mutschler, W., Arand, M., Wintermeyer, T. and Wentzensen, A. (2002)

Monitoring and healing analysis of 100 tibial shaft fractures, *Langenbecks Arch. Surg*, 387:3-4, pp.146-152.

12. Moorcroft, C. I., Ogrodnik, P. J., Thomas, P. B. and Wade, R. H. (2001) Mechanical properties of callus in human tibial fractures: A preliminary investigation, *Clin. Biomech*, 16:9, pp.776-782.
13. Richardson, J. B., Cunningham, J. L., Goodship, A. E., O'Connor, B. T. and Kenwright, J. (1994) Measuring stiffness can define healing of tibial fractures, *J. Bone Joint Surg. Br*, 76:3, pp.389-394.
14. Maffulli N. and Thornton, A. (1995) Ultrasonographic appearance of external callus in long-bone fractures, *Injury*, 26:1, pp.5-12.
15. Moed, B. R. , Subramanian, S. , van, H. M. , Watson, J. T. , Cramer, K. E., Karges, D. E. , Craig, J. G. and Bouffard, J. A. (1998) Ultrasound for the early diagnosis of tibial fracture healing after static interlocked nailing without reaming: Clinical results, *J. Orthop. Trauma*, 12:3, pp.206-213.
16. Risselada, M., van Bree, H., Kramer, M., Chiers, K., Duchateau, L., Verleyen, P. and Saunders, J. H. (2006) Evaluation of non-union fractures in dogs by use of B-mode ultrasonography, power Doppler ultrasonography, radiography, and histologic examination, *Am. J. Vet. Res.*, 67:8, pp.1354-1361.
17. Ashhurst, D.E., Hogg, J., Perren, S.M. (1982) A Method for Making Reproducible Experimental Fractures of the Rabbit Tibia, *Injury*, 14:3, pp.236-242.
18. Davy, D.T. and Connolly, J.F. (1982) The Biomechanical Behaviour of Healing Canine Radii and Ribs, *J. Biomechanics*, 15:4, pp.235-247.
19. Macdonald, W., Skirving, A.P., Scull, ER. (1988) A Device for Producing Experimental Fractures, *Acta. Orthop. Scand*, 59:5, pp.542-544.
20. Carpenter, S.H. and Zhu, Z. (1991) Correlation of the Acoustic Emission and the Fracture Toughness of the Ductile Modular Cast Iron, *J. Material Science*, 26, pp.2057-2062.
21. Burstein, A.H. and Frankel, V.H. (1971) A Standard Test for Laboratory Animal Bone, *J. Biomechanics*, 40:2, pp.155-158.

CHAPTER 7

OVERALL CONCLUSIONS AND FUTURE SCOPE OF WORK

The assessment of bone condition using acoustic emission and acousto-ultrasonic techniques were investigated. A systematic study was carried out with both the techniques including the standardisation of the technique, modifying the instrument setups to make it suitable for the present application, *in vitro* studies to prove the validity of using the study for the current purpose, and the experimental study with rabbits to assess the *in vivo* bone condition. The important results of the present work are summarised in the following paragraphs.

7.1 ACOUSTIC EMISSION STUDY

A systematic investigation was made to see the application of the acoustic emission technique for the assessment of bone condition. The *in vitro* studies were carried out to see the effect of acoustic emission characteristic with respect to strain rate. The simultaneous recording of the load -displacement and cumulative counts- time were carried out. The load-displacement readings were converted to load-time readings with the help of strain rate. Then the simultaneous plotting of cumulative AE counts and the applied load with respect to time was done. This facilitated the accurate determination of time of occurrence of initial AE with respect to load-displacement curve. Since the mechanical properties of the bone depend on the value of the strain rate, the effect of using two different strain rates on the acoustic emission response of the bone was also studied. The acoustic emission response of dry and fresh bovine bones shows that the acoustic emission occurs in both the cases, only during the plastic deformation stage. In some cases for dry bones it occurred just during the failure.

Slower strain rates (5 mm/minute) gives rise to low amplitude events, whereas the high strain rate (15 mm/minute) produces the high amplitude events. The strain rate value does not affect the time of occurrence of initial AE. At both the

strain rates the initial AE occurred only after the plastic deformation has taken place in the bone specimen.

The linear location technique was used to locate the fracture in bones. *In vitro* studies were carried out for this with dry bovine bones. It was found that this technique could be useful in locating the fracture, provided the accurate velocity is calculated. The technique is found to be useful only when the source is present in between the sensors. Hence more number of sensors could be used along the length of bone to exactly calculate its location. This technique is based in the difference in the time arrival of the signals to the different sensors; hence it becomes necessary to accurately determine this difference in time arrival of the signals. The difference in arrival time of the signals is recorded through the AE equipment; hence care must be taken of proper hardware settings. If the technique has to be used clinically then the proper loading conditions has to be designed to activate the latent crack to emit the acoustic waves. The technique might be more useful in longer bones in comparison to short bones. The software developed requires the input of velocity and the time of arrival of the AE signals to the sensors. The coding was done to calculate the location of the fracture based on the linear relationship between the velocity and the difference in the arrival time of the signals.

7.2 ACOUSTO-ULTRASONIC STUDY

In the case of acousto-ultrasonic technique, a detailed study was made on the technique itself to see its reproducibility and sensitivity. It was found that the results were reproducible if the proper contact between the sensors and the specimen is maintained. The sensitivity of the technique was mainly dependent on the threshold settings and Gate width values; hence it is dependent on the instrument settings. To minimise the affect of instrument settings, a menu driven software was developed in the MATLAB 6.5 for acousto-ultrasonic signal processing.

To check the validity of using the acousto-ultrasonic technique for the assessment of *in vivo* bone condition, an *in vitro* study was carried out with dry and fresh animal bones with simulated fractures. Composite rods of GFRP are also used in the *in vitro* study. The relation between the SWF

measured by acousto-ultrasonic technique and the depth of crack in bone specimen and also the relation between the SWF and the flexural strength of the specimens were studied. Good correlation found between all the above parameters indicate that the acousto-ultrasonic technique can be used for the assessment of bone condition.

In the case of *in vivo* study the acousto-ultrasonic technique was used to monitor the fracture healing process in rabbit's bones. An experimental study was conducted with rabbit's. The healing index calculated from the acousto-ultrasonic measurements from the healing limb and the contra lateral control limb is found to be increasing uniformly after the eight week of the healing period during the healing process. The results from the acousto-ultrasonic measurements agree with the radiological findings to much extent. The X-ray of the rabbits indicates that the healing in most of the rabbit is complete after eight week of the healing period, but the results from the acousto-ultrasonic measurements disagree with it. According to the acousto-ultrasonic measurements the healing continued till the twelfth week of the healing period. The good correlation obtained during the *in vitro* study between the SWF and the strength of the bone indicates that the healing index value gives a clear indication of the strength of bone recovered after the completion of the healing process. These results might be very useful for the sports person who can predict about the strength of his bone after getting recovered from certain fracture. The end point of the healing process is indicated by the more or less constant value of the healing index at 12th - 14th week during the healing period.

7.3 SCOPE FOR FURTHER WORK

There is enough scope for further investigation in the area of "Assessment of Bone Condition using Acoustic Emission and acousto-ultrasonic technique". The following aspects can be studied.

1. The need to develop special type loading systems for using the acoustic emission technique in clinical situations, the external fixation devices can be modified to accommodate the loading system and the

acoustic emission sensor. More studies have to be carried out using large animals like dog, goat, and monkey for the experimental study.

2. In the present study GUI software was developed to investigate the linear location of the fracture. More modified software has to be made for calculating the wave velocity and the difference in arrival time of the signals to the sensors. The other source location techniques could also be tried for locating the fracture in bones.
3. In the present study only small oblique fracture in the medial aspect of the rabbit's tibia were investigated. But in real field clinical orthopaedicians may come across different types of fractures in all types of bones and at different places. So more work have to be done to investigate the aspects of fracture healing in other bones also. Therefore, clinical studies may be conducted to provide enough proof of usefulness of acousto-ultrasonic technique in monitoring the fracture healing process.
4. The instruments used for the present study are general purpose laboratory equipments for testing the composite materials. The special instrument should be designed for the clinical application of this technique.

APPENDIX A

Fracture location using AE technique

```
function varargout = crack_location_gui(varargin)

gui_Singleton = 1;

gui_State = struct('gui_Name',    mfilename, ...
                  'gui_Singleton', gui_Singleton, ...
                  'gui_OpeningFcn', @crack_location_gui_OpeningFcn, ...
                  'gui_OutputFcn', @crack_location_gui_OutputFcn, ...
                  'gui_LayoutFcn', [] , ...
                  'gui_Callback', []);

if nargin && ischar(varargin{1})
    gui_State.gui_Callback = str2func(varargin{1});
end

if nargin
    [varargout{1:nargout}] = gui_mainfcn(gui_State, varargin{:});
else
    gui_mainfcn(gui_State, varargin{:});
end

function crack_location_gui_OpeningFcn(hObject, eventdata, handles, varargin)

i=imread('bitslogo.jpg');

axes(handles.axes1);

image(i);

axis off;

handles.output = hObject;

guidata(hObject, handles);

function varargout = crack_location_gui_OutputFcn(hObject, eventdata, handles)
```

```

varargout{1} = handles.output;
function edit1_Callback(hObject, eventdata, handles)
function edit1_CreateFcn(hObject, eventdata, handles)
if ispc
    set(hObject,'BackgroundColor','white');
else
    set(hObject,'BackgroundColor',get(0,'defaultUicontrolBackgroundColor'));
end
function edit2_Callback(hObject, eventdata, handles)
function edit2_CreateFcn(hObject, eventdata, handles)
if ispc
    set(hObject,'BackgroundColor','white');
else
    set(hObject,'BackgroundColor',get(0,'defaultUicontrolBackgroundColor'));
end
function edit3_Callback(hObject, eventdata, handles)
function edit3_CreateFcn(hObject, eventdata, handles)
if ispc
    set(hObject,'BackgroundColor','white');
else
    set(hObject,'BackgroundColor',get(0,'defaultUicontrolBackgroundColor'));
end
function edit4_Callback(hObject, eventdata, handles)
function edit4_CreateFcn(hObject, eventdata, handles)
if ispc
    set(hObject,'BackgroundColor','white');
else
    set(hObject,'BackgroundColor',get(0,'defaultUicontrolBackgroundColor'));

```

```

end

function pushbutton1_Callback(hObject, eventdata, handles)

set(handles.text10,'String','');

set(handles.text9,'String','');

set(handles.edit1,'String','');

set(handles.edit2,'String','');

set(handles.edit3,'String','');

set(handles.edit4,'String','');

function edit6_Callback(hObject, eventdata, handles)

function edit6_CreateFcn(hObject, eventdata, handles)

if ispc

    set(hObject,'BackgroundColor','white');

else

    set(hObject,'BackgroundColor',get(0,'defaultUicontrolBackgroundColor'));

end

function edit5_Callback(hObject, eventdata, handles)

function edit5_CreateFcn(hObject, eventdata, handles)

if ispc

    set(hObject,'BackgroundColor','white');

else

    set(hObject,'BackgroundColor',get(0,'defaultUicontrolBackgroundColor'));

end

function pushbutton2_Callback(hObject, eventdata, handles)

X = str2num(get(handles.edit1,'String'));

t1=str2num(get(handles.edit2,'String'));

t2=str2num(get(handles.edit3,'String'));

v=str2num(get(handles.edit4,'String'));

clc

```



```
dt=t1-t2;
```

```
dt
```

```
x1=(X+v*dt)/2;
```

```
100*x1
```

```
x2=(X-v*dt)/2;
```

```
100*x2
```

```
set(handles.text10,'String',100*x1);
```

```
set(handles.text9,'String',100*x2);
```

APPENDIX B

Acousto-Ultrasonic Signal Processing

```
clear all

clc

disp(' Birla Institute of Engineering And Sciences ')

disp('   Acousto-Ultrasonic Emission   ')

disp(' Specimen bone')

gatewidth= input(' Gate width ')

threshold= input(' threshold ')

t1= input ('input first range')

t2= input ('input second range')

B=load('C:\MATLAB701\work\healing week1.txt')

l=length(B);

A=zeros(1,l);

for i=1:l

    A(1,i)=B(i,1);

end

for i=1:l

    C(1,i)=A(1,i);

    if(C(1,i)<0)

        C(1,i)=0;

    end

end

end

T=400;

x=linspace(0,T,l);

t11=round(t1 * 2048 /400);
```

```

t21=round(t2 * 2048 /400);
for i=1:2048
    if(i>= t11 & i<= t21)
        t(1,i)=1;t2(i)= C(i);
    else
        t(1,i)=0;t2(i)=0;
    end
end
end
energy_within_gatewidth=trapz(x, (t2 .* t2))
t1= A .* t;
anan=area(x,t1 )
plot(x,t1)
xlabel('Time (micro secs) ');
ylabel(' Amplitude (mv) ');
title(' Amplitude vs Time');
axis([0 400 -200 200])
disp(' output ')
totalenergy = trapz(x,C.*C)
disp(' peak amptiude ')
amp = max(t1)
[q,w]=max(t1);
disp(' Time to peak ')
q=x(w)
maximum=t1(1,1);
flag=0; d=0;
count=0;
for j=1:length(A)-2
    if (t1(1,j+1)>t1(1,j))&&(t1(1,j+2)<t1(1,j+1))&&(t1(1,j+1)>threshold)

```

```

        count=count+1;
    end
end
for i=1:(length(A)-2)
    if (t1(1,i+1)*t1(1,i+1))>(t1(1,i)*t1(1,i))&& (t1(1,i+2)*t1(1,i+2))<(t1(1,i+1)*t1(1,i+1))
        if abs(t1(1,i+1))>threshold && flag==0
            if d==0
                k=i+1;
            end
            flag=1;
        end
        if abs(t1(1,i+1))<threshold && flag==1
            l=i+1;
            d=d+1;
            flag=0;
        end
        if(abs(t1(1,i+1))>abs(maximum))
            maximum=t1(1,i+1);
            m=i+1;
        end
    end
end
end
disp(' Number of counts ')
disp(count);
disp(' duration (microseconds) ')
duration=(400*l/2048)-(400*k/2048)
disp(' rise time(microseconds)')
risetime= (400*m/2048)-(400*k/2048)

```

APPENDIX C

GUI Software for calculating different parameters of AU signals

```
function varargout = New_GUI(varargin)

gui_Singleton = 1;

gui_State = struct('gui_Name',    mfilename, ...
                  'gui_Singleton', gui_Singleton, ...
                  'gui_OpeningFcn', @New_GUI_OpeningFcn, ...
                  'gui_OutputFcn', @New_GUI_OutputFcn, ...
                  'gui_LayoutFcn', [] , ...
                  'gui_Callback', []);

if nargin && ischar(varargin{1})
    gui_State.gui_Callback = str2func(varargin{1});
end

if nargout
    [varargout{1:nargout}] = gui_mainfcn(gui_State, varargin{:});
else
    gui_mainfcn(gui_State, varargin{:});
end

function New_GUI_OpeningFcn(hObject, eventdata, handles, varargin)

Logolmage = importdata('bitslogo.jpg');

axes(handles.axes3);

image(Logolmage);

axis off

handles.output = hObject;

guidata(hObject, handles);

function varargout = New_GUI_OutputFcn(hObject, eventdata, handles)

varargout{1} = handles.output;
```

```

function edit4_Callback(hObject, eventdata, handles)
function edit4_CreateFcn(hObject, eventdata, handles)
if ispc && isequal(get(hObject,'BackgroundColor'),
get(0,'defaultUicontrolBackgroundColor'))
    set(hObject,'BackgroundColor','white');
end
function edit2_Callback(hObject, eventdata, handles)
function edit2_CreateFcn(hObject, eventdata, handles)
if ispc && isequal(get(hObject,'BackgroundColor'),
get(0,'defaultUicontrolBackgroundColor'))
    set(hObject,'BackgroundColor','white');
end
function edit3_Callback(hObject, eventdata, handles)
function edit3_CreateFcn(hObject, eventdata, handles)
if ispc && isequal(get(hObject,'BackgroundColor'),
get(0,'defaultUicontrolBackgroundColor'))
    set(hObject,'BackgroundColor','white');
end
function pushbutton1_Callback(hObject, eventdata, handles)
    gatewidth = str2num(get(handles.edit5,'String'));
    threshold = str2num(get(handles.edit6,'String'));
    m1 = str2num(get(handles.edit7,'String'));
    m2 = str2num(get(handles.edit8,'String'));
    clc
    file=strcat('C:\MATLAB701\work\control','.txt');
    data=load(file);
    l=length(data);
    A=zeros(1,l);
    for i=1:l

```

```

    A(1,i)=data(i,1);
end
for i=1:l
    C(1,i)=A(1,i);
    if(C(1,i)<0)
        C(1,i)=0;
    end
end
end
T=400;
x=linspace(0,T,l);
t11=round(m1 * 2048 /400);
t21=round(m2 * 2048 /400);
for i=1:2048
    if(i>= t11 & i<= t21)
        t(1,i)=1;t2(i)= C(i);
    else
        t(1,i)=0;t2(i)=0;
    end
end
end
energy_within_gatewidth=trapz(x, (t2 .* t2))
t1= A .* t;
axes(handles.axes1)
plot(x,t1)
xlabel('Time (micro secs) ');
ylabel(' Amplitude (mv) ');
title(' Amplitude vs Time');
totalenergy = trapz(x,C.*C)
disp(' peak amptiude ')

```

```

amp = max(t1);
v=int2str(amp);
t=strcat(v,' milli volts');
disp(t)
[q,w]=max(t1);
disp(' Time of Flight ')
q=x(w);
v=int2str(q);
t=strcat(v,' micro seconds');
disp(t)
s_r=5e6;
t=[0:2047]'/s_r;
[a,dummy]=size(data);k=1;
while(a>(2^k))
    k=k+1;
end
ft=abs(fft(data,(2^k)))/size(data,1);
f=(0:size(ft,1)-1)*s_r./size(ft,1);
ft1=ft(1:1:2048);
t11=round(m1 * 2048 /400);
t21=round(m2 * 2048 /400);
h_(2)=figure(2);
axes(handles.axes6)
plot(f(t11:1:t21),ft(t11:1:t21),'-*');axis tight;grid on;hold on;
xlabel('Frequency, Hz','FontSize',8)
ylabel('Amplitude','FontSize',8)
title('Power Spectrum','FontSize',10)
fft_area=trapz(f(t11:t21,1),ft(t11:t21,1))

```



```

maximum=t1(1,1);
flag=0; d=0;
count=0;
for j=1:length(A)-2
    if (t1(1,j+1)>t1(1,j))&&(t1(1,j+2)<t1(1,j+1))&&(t1(1,j+1)>threshold)
        count=count+1;
    end
end
for i=1:(length(A)-2)
    if (t1(1,i+1)*t1(1,i+1))>(t1(1,i)*t1(1,i))&& (t1(1,i+2)*t1(1,i+2))<(t1(1,i+1)*t1(1,i+1))
        if abs(t1(1,i+1))>threshold && flag==0
            if d==0
                k=i+1;
            end
            flag=1;
        end
        if abs(t1(1,i+1))<threshold && flag==1
            l=i+1;
            d=d+1;
            flag=0;
        end
        if(abs(t1(1,i+1))>abs(maximum))
            maximum=t1(1,i+1);
            m=i+1;
        end
    end
end
for i=1:(length(A)-2)

```

```

if(t1(1,i+1)*t1(1,i+1))<(t1(1,i)*t1(1,i))
    if abs(t1(1,i+1)<threshold) && (t1(1,i)>threshold)
        n=i+1;
    end
end
end
end
disp(' Number of counts ')
disp(count);
if(amp>threshold)
    disp(' duration (microseconds) ')
    duration= (400*l/2048)-(400*k/2048)
    disp(' rise time(microseconds)')
    risetime= (400*m/2048)-(400*k/2048)
else
    duration=0
    risetime=0
end
set(handles.text13,'String',energy_within_gatewidth);
set(handles.text14,'String',amp);
set(handles.text15,'String',q);
set(handles.text17,'String',risetime);
set(handles.text29,'String',fft_area);
set(handles.text16,'String',duration);
function pushbutton2_Callback(hObject, eventdata, handles)
gatewidth = str2num(get(handles.edit5,'String'));
threshold = str2num(get(handles.edit6,'String'));
m1 = str2num(get(handles.edit7,'String'));
m2 = str2num(get(handles.edit8,'String'));

```

```

clc
file=strcat('C:\MATLAB701\work\h1','.txt');
data=load(file);
l=length(data);
A=zeros(1,l);
for i=1:l
    A(1,i)=data(i,1);
end
for i=1:l
    C(1,i)=A(1,i);
    if(C(1,i)<0)
        C(1,i)=0;
    end
end
end
T=400;
x=linspace(0,T,l);
t11=round(m1 * 2048 /400);
t21=round(m2 * 2048 /400);
for i=1:2048
    if(i>= t11 & i<= t21)
        t(1,i)=1;t2(i)= C(i);
    else
        t(1,i)=0;t2(i)=0;
    end
end
end
energy_within_gatewidth=trapz(x, (t2 .* t2))
t1= A .* t;
axes(handles.axes2)

```

```

plot(x,t1)
Xlabel('Time (micro secs) ');
Ylabel(' Amplitude (mv) ');
Title(' Amplitude vs Time');
totalenergy = trapz(x,C.*C)
disp(' peak amptiude ')
amp = max(t1);
v=int2str(amp);
t=strcat(v,' milli volts');
disp(t)
[q,w]=max(t1);
disp(' Time of Flight ')
q=x(w);
v=int2str(q);
t=strcat(v,' micro seconds');
disp(t)
s_r=5e6;
t=[0:2047]'./s_r;
[a,dummy]=size(data);k=1;
while(a>(2^k))
    k=k+1;
end
ft=abs(fft(data,(2^k)))./size(data,1);
f=( [0:size(ft,1)-1] *s_r)./size(ft,1);
ft1=ft(1:1:2048);
t11=round(m1 * 2048 /400);
t21=round(m2 * 2048 /400);
h_(2)=figure(2);

```

```

axes(handles.axes7)
plot(f(t11:1:t21),ft(t11:1:t21),'-*');axis tight;grid on;hold on;
xlabel('Frequency, Hz','FontSize',8)
ylabel('Amplitude','FontSize',8)
title('Power Spectrum','FontSize',10)
fft_area=trapz(f(t11:t21,1),ft(t11:t21,1))
maximum=t1(1,1);
flag=0; d=0;
count=0;
for j=1:length(A)-2
    if (t1(1,j+1)>t1(1,j))&&(t1(1,j+2)<t1(1,j+1))&&(t1(1,j+1)>threshold)
        count=count+1;
    end
end
for i=1:(length(A)-2)
    if (t1(1,i+1)*t1(1,i+1))>(t1(1,i)*t1(1,i))&& (t1(1,i+2)*t1(1,i+2))<(t1(1,i+1)*t1(1,i+1))
        if abs(t1(1,i+1))>threshold && flag==0
            if d==0
                k=i+1;
            end
            flag=1;
        end
        if abs(t1(1,i+1))<threshold && flag==1
            l=i+1;
            d=d+1;
            flag=0;
        end
    end
    if(abs(t1(1,i+1))>abs(maximum))

```

```

        maximum=t1(1,i+1);
        m=i+1;
    end
end
end
for i=1:(length(A)-2)
    if(t1(1,i+1)*t1(1,i+1))<(t1(1,i)*t1(1,i))
        if abs(t1(1,i+1)<threshold) && (t1(1,i)>threshold)
            n=i+1;
        end
    end
end
end
disp(' Number of counts ')
disp(count);
if(amp>threshold)
    disp(' duration (microseconds) ')
    duration= (400*l/2048)-(400*k/2048)
    disp(' rise time(microseconds)')
    risetime= (400*m/2048)-(400*k/2048)
else
    duration=0
    risetime=0
end
set(handles.text23,'String',energy_within_gatewidth);
set(handles.text24,'String',amp);
set(handles.text25,'String',q);
set(handles.text27,'String',risetime);
set(handles.text31,'String',fft_area);

```

```

duration= (400*n/2048)-(400*k/2048)
set(handles.text26,'String',duration);
function pushbutton3_Callback(hObject, eventdata, handles)
set(handles.text13,'String','');
set(handles.text14,'String','');
set(handles.text15,'String','');
set(handles.text16,'String','');
set(handles.text17,'String','');
set(handles.text23,'String','');
set(handles.text24,'String','');
set(handles.text25,'String','');
set(handles.text26,'String','');
set(handles.text27,'String','');
set(handles.edit5,'String','');
set(handles.edit6,'String','');
set(handles.edit7,'String','');
set(handles.edit8,'String','');
cla(handles.axes1,'reset');
cla(handles.axes2,'reset');
cla(handles.axes6,'reset');
cla(handles.axes7,'reset');
set(handles.text29,'String','');
set(handles.text31,'String','');
function edit1_Callback(hObject, eventdata, handles)
function edit1_CreateFcn(hObject, eventdata, handles)
if ispc && isequal(get(hObject,'BackgroundColor'),
get(0,'defaultUicontrolBackgroundColor'))
    set(hObject,'BackgroundColor','white');

```

```

end

function edit5_Callback(hObject, eventdata, handles)
function edit5_CreateFcn(hObject, eventdata, handles)
if ispc && isequal(get(hObject,'BackgroundColor'),
get(0,'defaultUicontrolBackgroundColor'))
    set(hObject,'BackgroundColor','white');
end

function edit6_Callback(hObject, eventdata, handles)
function edit6_CreateFcn(hObject, eventdata, handles)
if ispc && isequal(get(hObject,'BackgroundColor'),
get(0,'defaultUicontrolBackgroundColor'))
    set(hObject,'BackgroundColor','white');
end

function edit7_Callback(hObject, eventdata, handles)
function edit7_CreateFcn(hObject, eventdata, handles)
if ispc && isequal(get(hObject,'BackgroundColor'),
get(0,'defaultUicontrolBackgroundColor'))
    set(hObject,'BackgroundColor','white');
end

function edit8_Callback(hObject, eventdata, handles)
function edit8_CreateFcn(hObject, eventdata, handles)
if ispc && isequal(get(hObject,'BackgroundColor'),
get(0,'defaultUicontrolBackgroundColor'))
    set(hObject,'BackgroundColor','white');
end

function pushbutton1_KeyPressFcn(hObject, eventdata, handles)

```


APPENDIX D

GUI Software for monitoring the fracture healing process

```
function varargout = GUI_modi(varargin)

gui_Singleton = 1;

gui_State = struct('gui_Name',    mfilename, ...
                  'gui_Singleton', gui_Singleton, ...
                  'gui_OpeningFcn', @GUI_modi_OpeningFcn, ...
                  'gui_OutputFcn', @GUI_modi_OutputFcn, ...
                  'gui_LayoutFcn', [] , ...
                  'gui_Callback', []);

if nargin && ischar(varargin{1})
    gui_State.gui_Callback = str2func(varargin{1});
end

if nargout
    [varargout{1:nargout}] = gui_mainfcn(gui_State, varargin{:});
else
    gui_mainfcn(gui_State, varargin{:});
end

function GUI_modi_OpeningFcn(hObject, eventdata, handles, varargin)

i=imread('bitslogo.jpg');

axes(handles.logo);

image(i);

axis off;

handles.output = hObject;

guidata(hObject, handles);

function varargout = GUI_modi_OutputFcn(hObject, eventdata, handles)
```

```

varargout{1} = handles.output;
function figure1_ResizeFcn(hObject, eventdata, handles)
function popupmenu1_Callback(hObject, eventdata, handles)
function popupmenu1_CreateFcn(hObject, eventdata, handles)
if ispc
    set(hObject,'BackgroundColor','white');
else
    set(hObject,'BackgroundColor',get(0,'defaultUicontrolBackgroundColor'));
end
function pushbutton1_Callback(hObject, eventdata, handles)
gatewidth = str2num(get(handles.edit3,'String'));
threshold = str2num(get(handles.edit5,'String'));
m1 = str2num(get(handles.edit6,'String'));
m2 = str2num(get(handles.edit7,'String'));
clc
file=strcat('C:\MATLAB701\work\RFW0g','.txt');
data=load(file);
l=length(data);
l=length(data);
A=zeros(1,l);
for i=1:l
    A(1,i)=data(i,1);
end
for i=1:l
    C(1,i)=A(1,i);
if(C(1,i)<0)
    C(1,i)=0;
end
end

```

```

end
T=400;
x=linspace(0,T,l);
t11=round(m1 * 2048 /400);
t21=round(m2 * 2048 /400);
for i=1:2048
    if(i>= t11 & i<= t21)
        t(1,i)=1;t2(i)= C(i);
    else
        t(1,i)=0;t2(i)=0;
    end
end
end
energy_within_gatewidth=trapz(x, (t2 .* t2))
t1= A .* t;
axes(handles.axes1)
plot(x,t1)
xlabel('Time (micro secs) ');
ylabel(' Amplitude (mv) ');
title(' Amplitude vs Time');
disp(' output ')
totalenergy = trapz(x,C.*C)
disp(' peak amptiude ')
amp = max(t1)
v=int2str(amp);
t=strcat(v,' milli volts');
disp(t)
[q,w]=max(t1);
disp(' Time to peak ')

```

```

q=x(w)
v=int2str(q);
t=strcat(v,' micro seconds');
disp(t)
s_r=5e6;
t=[0:2047]'/s_r;
[a,dummy]=size(data);k=1;
while(a>(2^k))
    k=k+1;
end
ft=abs(fft(data,(2^k)))./size(data,1);
f=(0:size(ft,1)-1)*s_r./size(ft,1);
ft1=ft(1:1:2048);
t11=round(m1 * 2048 /400);
t21=round(m2 * 2048 /400);
fft_area=trapz(f(t11:t21,1),ft(t11:t21,1))
maximum=t1(1,1);
flag=0; d=0;
count=0;
for j=1:length(A)-2
    if (t1(1,j+1)>t1(1,j))&&(t1(1,j+2)<t1(1,j+1))&&(t1(1,j+1)>threshold)
        count=count+1;
    end
end
end
for i=1:(length(A)-2)
    if (t1(1,i+1)*t1(1,i+1))>(t1(1,i)*t1(1,i))&& (t1(1,i+2)*t1(1,i+2))<(t1(1,i+1)*t1(1,i+1))
        if abs(t1(1,i+1))>threshold && flag==0
            if d==0

```

```

        k=i+1;
    end
    flag=1;
end
if abs(t1(1,i+1))<threshold && flag==1
    l=i+1;
    d=d+1;
    flag=0;
end
if(abs(t1(1,i+1))>abs(maximum))
    maximum=t1(1,i+1);
    m=i+1;
end
end
end
for i=1:(length(A)-2)
    if(t1(1,i+1)*t1(1,i+1))<(t1(1,i)*t1(1,i))
        if abs(t1(1,i+1)<threshold) && (t1(1,i)>threshold)
            n=i+1;
        end
    end
end
end
disp(' Number of counts ')
disp(count);
if(amp>threshold)
    disp(' duration (microseconds) ')
    duration= (400*l/2048)-(400*k/2048)
    disp(' rise time(microseconds)')

```

```

    risetime= (400*m/2048)-(400*k/2048)
else
    duration=0
    risetime=0
end
set(handles.text5,'String',energy_within_gatewidth);
set(handles.text6,'String',amp);
function pushbutton3_Callback(hObject, eventdata, handles)
gatewidth = str2num(get(handles.edit3,'String'));
threshold = str2num(get(handles.edit5,'String'));
m1 = str2num(get(handles.edit6,'String'));
m2 = str2num(get(handles.edit7,'String'));
clc
file=strcat('C:\MATLAB701\work\RFW001','.txt');
data=load(file);
l=length(data);
l=length(data);
A=zeros(1,l);
for i=1:l
    A(1,i)=data(i,1);
end
for i=1:l
    C(1,i)=A(1,i);
    if(C(1,i)<0)
        C(1,i)=0;
    end
end
end
T=400;

```

```

x=linspace(0,T,l);
t1=round(m1 * 2048 /400);
t2=round(m2 * 2048 /400);

for i=1:2048
    if(i>= t11 & i<= t21)
        t(1,i)=1;t2(i)= C(i);
    else
        t(1,i)=0;t2(i)=0;
    end
end

energy_within_gatewidth=trapz(x, (t2 .* t2));
format bank
Eb=energy_within_gatewidth;
t1= A .* t;
axes(handles.overlap)
plot(x,t1,'b')
xlabel('Time (micro secs) ');
ylabel(' Amplitude (mv) ');
title(' Amplitude vs Time');
hold on
gatewidth = str2num(get(handles.edit3,'String'));
threshold = str2num(get(handles.edit5,'String'));
m1 = str2num(get(handles.edit6,'String'));
m2 = str2num(get(handles.edit7,'String'));
clc
file=strcat('C:\MATLAB701\work\1','.txt');
data=load(file);

```

```

l=length(data);
l=length(data);
A=zeros(1,l);
for i=1:l
    A(1,i)=data(i,1);
end
for i=1:l
    C(1,i)=A(1,i);
if(C(1,i)<0)
    C(1,i)=0;
end
end
T=400;
x=linspace(0,T,l);
t11=round(m1 * 2048 /400);
t21=round(m2 * 2048 /400);
for i=1:2048
    if(i>= t11 & i<= t21)
        t(1,i)=1;t2(i)= C(i);
    else
        t(1,i)=0;t2(i)=0;
    end
end
energy_within_gatewidth=trapz(x, (t2 .* t2));
format bank
Eg=energy_within_gatewidth;
t1= A .* t;
axes(handles.overlap)

```



```

plot(x,t1,'r')
xlabel('Time (micro secs) ');
ylabel(' Amplitude (mv) ');
title(' Amplitude vs Time');

format bank

Eb

Eg

healing_index= Eg/Eb

set(handles.text11,'String',healing_index);

function edit3_Callback(hObject, eventdata, handles)
function edit3_CreateFcn(hObject, eventdata, handles)
if ispc
    set(hObject,'BackgroundColor','white');
else
    set(hObject,'BackgroundColor',get(0,'defaultUicontrolBackgroundColor'));
end

function edit4_Callback(hObject, eventdata, handles)
function edit4_CreateFcn(hObject, eventdata, handles)
if ispc
    set(hObject,'BackgroundColor','white');
else
    set(hObject,'BackgroundColor',get(0,'defaultUicontrolBackgroundColor'));
end

function edit5_Callback(hObject, eventdata, handles)
function edit5_CreateFcn(hObject, eventdata, handles)
if ispc
    set(hObject,'BackgroundColor','white');
else

```

```

    set(hObject,'BackgroundColor',get(0,'defaultUicontrolBackgroundColor'));
end
function edit6_Callback(hObject, eventdata, handles)
function edit6_CreateFcn(hObject, eventdata, handles)
if ispc
    set(hObject,'BackgroundColor','white');
else
    set(hObject,'BackgroundColor',get(0,'defaultUicontrolBackgroundColor'));
end
function edit7_Callback(hObject, eventdata, handles)
function edit7_CreateFcn(hObject, eventdata, handles)
if ispc
    set(hObject,'BackgroundColor','white');
else
    set(hObject,'BackgroundColor',get(0,'defaultUicontrolBackgroundColor'));
end
function pushbutton4_Callback(hObject, eventdata, handles)
gatewidth = str2num(get(handles.edit3,'String'));
threshold = str2num(get(handles.edit5,'String'));
m1 = str2num(get(handles.edit6,'String'));
m2 = str2num(get(handles.edit7,'String'));
clc
file=strcat('C:\MATLAB701\work\RFW0b','.txt');
data=load(file);
l=length(data);
l=length(data);
A=zeros(1,l);
for i=1:l

```

```

    A(1,i)=data(i,1);
end
for i=1:l
    C(1,i)=A(1,i);
    if(C(1,i)<0)
        C(1,i)=0;
    end
end
end
T=400;
x=linspace(0,T,l);
t11=round(m1 * 2048 /400);
t21=round(m2 * 2048 /400);
for i=1:2048
    if(i>= t11 & i<= t21)
        t(1,i)=1;t2(i)= C(i);
    else
        t(1,i)=0;t2(i)=0;
    end
end
end
energy_within_gatewidth=trapz(x, (t2 .* t2))
t1= A .* t;
axes(handles.axes2)
plot(x,t1)
xlabel('Time (micro secs) ');
ylabel(' Amplitude (mv) ');
title(' Amplitude vs Time');
disp(' output ')
totalenergy = trapz(x,C.*C)

```

```

disp(' peak amptiude ')
amp = max(t1)
v=int2str(amp);
t=strcat(v,' milli volts');
disp(t)
[q,w]=max(t1);
disp(' Time to peak ')
q=x(w)
v=int2str(q);
t=strcat(v,' micro seconds');
disp(t)
s_r=5e6;
t=[0:2047]'/s_r;
[a,dummy]=size(data);k=1;
while(a>(2^k))
    k=k+1;
end
ft=abs(fft(data,(2^k)))/size(data,1);
f=(0:size(ft,1)-1]*s_r)/size(ft,1);
ft1=ft(1:1:2048);
t11=round(m1 * 2048 /400);
t21=round(m2 * 2048 /400);
fft_area=trapz(f(t11:t21,1),ft(t11:t21,1))
maximum=t1(1,1);
flag=0; d=0;
count=0;
for j=1:length(A)-2
    if (t1(1,j+1)>t1(1,j))&&(t1(1,j+2)<t1(1,j+1))&&(t1(1,j+1)>threshold)

```

```

        count=count+1;
    end
end
for i=1:(length(A)-2)
    if (t1(1,i+1)*t1(1,i+1))>(t1(1,i)*t1(1,i))&& (t1(1,i+2)*t1(1,i+2))<(t1(1,i+1)*t1(1,i+1))
        if abs(t1(1,i+1))>threshold && flag==0
            if d==0
                k=i+1;
            end
            flag=1;
        end
        if abs(t1(1,i+1))<threshold && flag==1
            l=i+1;
            d=d+1;
            flag=0;
        end
        if(abs(t1(1,i+1))>abs(maximum))
            maximum=t1(1,i+1);
            m=i+1;
        end
    end
end
end
for i=1:(length(A)-2)
    if(t1(1,i+1)*t1(1,i+1))<(t1(1,i)*t1(1,i))
        if abs(t1(1,i+1))<threshold && (t1(1,i))>threshold
            n=i+1;
        end
    end
end
end

```

```

end
disp(' Number of counts ')
disp(count);
if(amp>threshold)
    disp(' duration (microseconds) ')
    duration= (400*I/2048)-(400*k/2048)
    disp(' rise time(microseconds)')
    risetime= (400*m/2048)-(400*k/2048)
else
    duration=0
    risetime=0
end
disp(' duration (microseconds) ')
duration=(400*I/2048)-(400*k/2048)
disp(' rise time(microseconds)')
risetime= (400*m/2048)-(400*k/2048)
set(handles.text17,'String',energy_within_gatewidth);
set(handles.text16,'String',amp);
function text10_CreateFcn(hObject, eventdata, handles)

```

List of Publications in International/National Journals/Conference

1. **Sharad Shrivastava** and Ravi Prakash (2009) *Assessment of bone condition by acoustic emission technique: A review. J. Biomedical Science and Engineering*. Vol. 2, pp.144-154.
2. **Sharad Shrivastava** and Ravi Prakash (2010) *Assessment of Bone condition by Acousto-Ultrasonic Technique: an in vitro Study*. Health Positive. Vol. 1:12, pp.30-37.
3. **Sharad Shrivastava** and Ravi Prakash (2010) *In vitro Study of Bone Condition using Acousto-Ultrasonic Technique*. Int. J. Biomedical Engineering and Technology. (Accepted in press)
4. **Sharad Shrivastava** and Ravi Prakash (2010) *Future research directions with Acoustic Emission and Acousto-Ultrasonic technique*. Int. J. Biomedical Engineering and Technology. (Accepted in press)
5. **Sharad Shrivastava** and Ravi Prakash (2010) *Monitoring the fracture healing process by Acousto-Ultrasonic technique*. (communicated)
6. Avijit Suman, Baldev Raj, B.P.C. Rao, C.K. Mukopadhyay, **Sharad Shrivastava**, T.K. Haneef, C. Babu Rao, T. Jayakumar *A Study on Transfer Function Characteristics during Tensile Deformation of Aluminium*. Souvenirs of National seminar NDE 2009, Indian Society for NDT (ISNT), December 10-12, pp. 50. (Not related to thesis)

Brief Biography of the Supervisor

Prof. Ravi Prakash holds a Ph D degree from Cranfield University, U.K. and a Masters degree from Salford University, U.K. He was at Bath University, U.K. as Post Doctoral Research Officer and as a Visiting Professor at Hartshill Medical Institute at Stroke-on-Trent, U.K. He has more than 35 years of teaching and research experience. He is presently Vice Chancellor at JUIT, Wagnaghat, Himachal Pradesh and prior to that he was at BITS, Pilani for 15years and was Dean, Research and Consultancy Division at BITS, Pilani from 2000 to 2010. Prior to joining BITS, Pilani, he was Science Counsellor, Embassy of India, Washington D.C., USA and was also at Institute of Technology, Banaras Hindu University for 20 years. He has more than 120 research publications in the field of Materials, Non-destructive techniques and Biomedical engineering. He is members of a number of professional societies and has delivered a large number of invited lectures both in India and abroad.

Brief Biography of the Candidate

Mr. Sharad Shrivastava did his M.Tech from IIT Kharagpur. He has 10 years of teaching experience. He is presently pursuing Ph.D. from BITS, Pilani and working as a Lecturer with Mechanical Engineering Group, **BITS, Pilani**. His areas of research interest are Biomedical engineering, non-destructive testing techniques, composite materials etc.